ISTANBUL TECHNICAL UNIVERSITY ★ GRADUATE SCHOOL OF SCIENCE ENGINEERING AND TECHNOLOGY

STRENGTH AND STABILITY OF THIN WALLED STEEL COLUMNS IN STORAGE RACK STRUCTURES

M.Sc. THESIS

Atakan MANGIR

Department of Civil Engineering

Structural Engineering Programme

MAY 2014

ISTANBUL TECHNICAL UNIVERSITY ★ GRADUATE SCHOOL OF SCIENCE ENGINEERING AND TECHNOLOGY

STRENGTH AND STABILITY OF THIN WALLED STEEL COLUMNS IN STORAGE RACK STRUCTURES

M.Sc. THESIS

Atakan MANGIR
(501111007)

Department of Civil Engineering

Structural Engineering Programme

Thesis Advisor: Prof. Dr. Ünal ALDEMİR

MAY 2014

İSTANBUL TEKNİK ÜNİVERSİTESİ ★ FEN BİLİMLERİ ENSTİTÜSÜ

İNCE CİDARLI ÇELİK DEPO RAF SİSTEMLERİ KOLONLARININ DAYANIM VE STABİLİTESİ

YÜKSEK LİSANS TEZİ

Atakan MANGIR
(501111007)

İnşaat Mühendisliği Anabilim Dalı

Yapı Mühendisliği Programı

Tez Danışmanı: Prof. Dr. Ünal ALDEMİR

MAY 2014

Atakan MANGIR, a **M.Sc.** student of ITU **Institute of Science Engineering and Technology** student ID **501111007** successfully defended the **thesis/dissertation** entitled " **STRENGTH AND STABILITY OF THIN WALLED STEEL COLUMNS IN STORAGE RACK STRUCTURES** ", which he prepared after fulfilling the requirements specified in the associated legislations, before the jury whose signatures are below.

Thesis Advisor :	**Prof. Dr. Ünal ALDEMİR** Istanbul Technical University	.....
Co-advisor :	**Assoc. Prof. Dr. Güven KIYMAZ** Fatih University	.....
Jury Members :	**Prof. Dr. Abdül HAYIR** Istanbul Technical University	.....
	Prof. Dr. Bülent AKBAŞ Gebze Institute of Technology	.....
	Assis. Prof. Dr. Cüneyt VATANSEVER Istanbul Technical University	.....

Date of Submission : 5 May 2014
Date of Defense : 29 May 2014

In memory of my grandfather, to my family

FOREWORD

I would like to express my deepest gratitudes and thanks to my supervisors Prof. Dr. Ünal ALDEMİR and Assoc. Prof. Dr. Güven KIYMAZ who gave me their suggestions, supports and encouragements which made it possible for me to accomplish this dissertation. This dissertation could not have been completed without their guidance.

During the construction and completion of this thesis, my family has also a major role. I believe that any appreciation word won't be enough for their presence and support. Their help to me to get over my medical inabilities during this study is inestimable.

Specially, my sincere appreciations and gratitudes go to my collegues Ertuğrul Emre ÇALIK and Nilgün Merve ÇAĞLAR for their supports during the construction of this study.

I would like to thank Prof. Dr. Teoman PEKÖZ who is emeritus professor of Cornell University and author of major portions of the specifications and recommendations on cold-formed steel and rack structures for his precious suggestions.

May 2014

Atakan MANGIR
(Civil Engineer)

TABLE OF CONTENTS

Page

FOREWORD ..... **ix**
TABLE OF CONTENTS ..... **xi**
ABBREVIATIONS ..... **xiii**
NOTATIONS ..... **xv**
LIST OF TABLES ..... **xix**
LIST OF FIGURES ..... **xxi**
SUMMARY ..... **xxv**
ÖZET ..... **xxvii**
1. INTRODUCTION **1**
1.1 Overview of Cold Formed Steel 1
1.1.1 Production 2
1.1.2 Structural applications 3
1.1.3 Advantages and disadvantages of cold formed steel 10
1.2 Aim and Layout of the Thesis 11
2. LITERATURE REVIEW ON COLD FORMED STEEL COLUMNS **13**
2.1 General Remarks on Cold Formed Steel Column Behaviour 13
2.1.1 Yielding 14
2.1.2 Global (overall) column buckling 14
2.1.2.1 Flexural column buckling 15
Elastic buckling 15
Inelastic buckling 15
2.1.2.2 Torsional buckling and flexural-torsional buckling 17
2.1.3 Local buckling 20
2.1.4 Distortional buckling 26
2.2 Studies on Direct Strength Method 27
2.3 Studies on Perforated Cold Formed Steel Storage Rack Columns 36
3. CODIFIED DESIGN OF COLD FORMED STEEL COLUMNS UNDER PURE COMPRESSION **45**
3.1 Review of American Iron and Steel Institute S100-2007 Standart 45
3.1.1 Effective width method for concentric axially loaded compression members 45
3.1.1.1 The nominal axial strength calculations 46
3.1.1.2 Effective area calculations 48
3.1.1.3 Distortional buckling strength calculations 52
3.1.2 Example solution of a c-channel column with a simple lip edge stiffener via effective width method 54
3.1.3 Direct strength method for concentric axially loaded compression members 61
3.1.3.1 Determination of elastic buckling loads 63
3.1.3.2 Column analysis 63

Flexural, torsional, or flexural-torsional buckling 63
Local buckling 64
Distortional buckling 64
3.1.3.3. Summary and design curves of direct strength method 65
3.1.4 Example solution of a c-channel column with a simple lip edge stiffener via direct strength method 67

4. INVESTIGATION OF RACK COLUMN BEHAVIOUR THROUGH DIRECT STRENGTH METHOD 75
4.1 Analysis of Unperforated Column Models 77
4.1.1 Analytical study on unperforated members using direct strength method 79
4.1.2 Nominal strength - lip length relationships of unperforated column models 84
4.1.2.1 General comparison of results for unperforated column models 88
4.2 Analysis of Perforated Specimens 92
4.2.1 Analytical study on perforated members using direct strength method 95
4.2.2. Nominal strength - lip length relationships of perforated column models 102
4.2.2.1 General comparison of results for perforated column models 106
4.3 Comparison Between the Strength of Unperforated Rack Column Models with Perforated Rack Column Models 111

5. CONCLUSION 117
REFERENCES 119
CURRICULUM VITAE 125

ABBREVIATIONS

AISI : American Iron and Steel Institute
AS/NZS : The Australian/New Zealand Standard
ASD : Allowable Stress Design
CFS : Cold Formed Steel
CUFSM : Cornell University Finite Strip Method
D : Distortional Controlling Buckling Mode
DSM : Direct Strength Method
EC : Eurocode
EN : European Standart
EWM : Effective Width Method
FSM : Finite Strip Method
G : Global Controlling Buckling Mode
IS : I - Sections
LG : Local-global Controlling Buckling Mode
LRFD : Load and Resistance Factor Design
NAS : North American Standart
PCS : Plain Channel Sections
RHS : Rectangular Hollow Sections
RMI : Rack Manufacturers Institute
S.S. : Simply Supported

NOTATIONS

A : Full unreduced cross-sectional area
A_e : Effective area at the stress F_n, effective net area.
A_g : Gross area of element including stiffeners
b : Effective design width of compression element
b_0 : Out-to-out flange width
b_1 , b_2 : Effective widths
B_{np} : Length of nonperforated sheet between perforations in a row perpendicular to column length
B_p : Total length of perforations in a row perpendicular to column length
C_w : Warping constant
D : Term determined by $Et^3/12(1-\mu^2)$
Overall depth of first lip
D_2 : Overall depth of second lip
D_3 : Overall depth of third lip
d_s : Reduced effective width of stiffener
d'_s : Effective width of stiffener
E : Modulus of elasticity
E_r : Reduced modulus
E_t : Tangent modulus
f : Stress in compression element computed on basis of effective design width
f_{cr} : Critical buckling stress for local buckling of plates and tubes
F_d : Elastic distortional buckling stress
F_e : The least of the applicable elastic flexural, torsional and flexural torsional buckling stress
F_n : Nominal buckling stress
$(F_n)_e$: Nominal elastic buckling stress
$(F_n)_I$: Nominal inelastic buckling stress
f_x : Compression stress in x direction
F_y : Yield stress of steel
G : Shear modulus
H : Total column width including complex lip lengths
h_0 , B : Out-to-out web depth
I : Moment of innertia
I_a : Adequate moment of innertia of stiffener, so that each component element will behave as a stiffened element
I_s : Actual moment of innertia of full stiffener about its own centroidal axis parallel to element to be stiffened
J : St. Venant torsion constant of cross section
k : Effective length factor
k_d : Plate buckling coefficient for distortional buckling

$\mathbf{K_t}$: Effective length factor for torsion

L : Column length,
Pitch length,
Laterally unbraced length of member

$\mathbf{L_{cr}}$: Critical unbraced length of distortional buckling

$\mathbf{L_m}$: Distance between discrete restraints that restrict distortional buckling

$\mathbf{L_{np}}$: Length of nonperforated sheet between perforations in a row parallel to column length

$\mathbf{L_p}$: Total length of perforations in a row parallel to column length

$\mathbf{L_t}$: Unbraced length of compression member for torsion

m : Number of half sine waves

n : Coefficient

P : Applied axial load

$\mathbf{P_e}$: Euler buckling load

$\mathbf{P_n}$: The nominal axial strength

$\mathbf{P_{ne}}$: Nominal axial strength for global(overall) buckling

$\mathbf{P_{crd}}$: Critical elastic distortional column buckling load

$\mathbf{P_{cre}}$: Critical elastic overall(global) column buckling load

$\mathbf{P_{cr\ell}}$: Critical elastic local column buckling load

$\mathbf{P_{nd}}$: Nominal axial strength for distortional buckling

$\mathbf{P_{n\ell}}$: Nominal axial strength for local buckling

$\mathbf{P_R}$: Reduced modulus load

$\mathbf{P_{RMI}}$: Yielding stress

$\mathbf{P_{RMI-n}}$: Nominal values of yielding stress

$\mathbf{P_t}$: Tangent modulus load

$\mathbf{P_{test}}$: Maximum axial load gathered from experimental test

$\mathbf{P_{ua}}$: Ultimate axial load of experimental results

$\mathbf{P_x}$: Euler flexural buckling load about x axis

$\mathbf{P_y}$: Yield load

$\mathbf{P_z}$: Torsional buckling load about z axis

Q : Stress and/or area factor to modify allowable axial stress

r : Radius of gyration of full unreduced cross-section about axis of buckling

$\mathbf{r_0}$: Polar radius of gyration of cross section about shear center

$\mathbf{R_I}$: I_s/I_a

$\mathbf{r_x}$, $\mathbf{r_y}$: Radii of gyration of cross-section about centrodial principal axes

S : $1.28\sqrt{E/f}$

t : Thickness of plate
Base steel thickness

$\mathbf{t_r}$: Reduced thickness

$\mathbf{t_{rD}}$: Reduced thickness for distortional buckling

$\mathbf{t_{rG}}$: Reduced thickness for global buckling

$\mathbf{t_{rL}}$: Reduced thickness for local buckling

w : Flat width of element exclusive of radii

$\mathbf{x_0}$: The distance from shear center to centroid along principal x-axis, taken as negative

α : Coefficient accounts for the benefit of an unbraced length

β : $1 - (x_0/r_0)^2$

θ : Lip angle

λ	: Length of half sine wave (Half wavelength)
λ_c	: Column slenderness parameter. Slenderness factor for global buckling
λ_d	: Slenderness factor for distortional buckling
λ_ℓ	: Slenderness factor for local buckling
μ	: Poisson's ratio for steel, = 0.30
ρ	: Local reduction factor
σ_e	: Euler stress of elastic column buckling
σ_{ex}	: P_x / A
σ_R	: Critical buckling stress based on reduced modulus method
σ_T	: Critical buckling stress based on tangent modulus method
σ_t	: P_z / A
σ_{TFO}	: Elastic flexural–torsional buckling stress
σ_{TFT}	: Inelastic flexural–torsional buckling stress
ω	: Deflection of plate perpendicular to surface
a , w	: Width of the plate, respectively
τ	: Shear stress

LIST OF TABLES

Page

Table 3.1 : Determination of plate buckling coefficient, k 51
Table 3.2 : Section properties of example solution 55
Table 3.3 : Effective widths of section's elements 59
Table 4.1 : Geometric properties of unperforated specimens having 500 mm column length 78
Table 4.2 : Geometric properties of unperforated specimens having 1000 mm column length 78
Table 4.3 : Geometric properties of unperforated specimens having 1500 mm column length 79
Table 4.4 : Critical elastic buckling loads obtained from CUFSM analysis for unperforated specimens having 500 mm column length 80
Table 4.5 : Critical elastic buckling loads obtained from CUFSM analysis for unperforated specimens having 1000 mm column length 81
Table 4.6 : Critical elastic buckling loads obtained from CUFSM analysis for unperforated specimens having 1500 mm column length 82
Table 4.7 : Nominal axial strengths of unperforated specimens having 500 mm column length 83
Table 4.8 : Nominal axial strengths of unperforated specimens having 1000 mm column length 83
Table 4.9 : Nominal axial strengths of unperforated specimens having 1500 mm column length 84
Table 4.10 : Limits of the model of reduced thickness 92
Table 4.11 : Geometric properties of perforated specimens having 500 mm column length 94
Table 4.12 : Geometric properties of perforated specimens having 1000 mm column length 94
Table 4.13 : Geometric properties of perforated specimens having 1500 mm column length 95
Table 4.14 : Critical elastic buckling loads obtained from CUFSM analysis for perforated specimens having 500 mm column length 98
Table 4.15 : Critical elastic buckling loads obtained from CUFSM analysis for perforated specimens having 1000 mm column length 99
Table 4.16 : Critical elastic buckling loads obtained from CUFSM analysis for perforated specimens having 1500 mm column length 100
Table 4.17 : Nominal axial strengths of unperforated specimens having 500 mm column length 101
Table 4.18 : Nominal axial strengths of unperforated specimens having 1000 mm column length 101
Table 4.19 : Nominal axial strengths of unperforated specimens having 1500 mm column length 102

LIST OF FIGURES

Page

Figure 1.1 : Cold formed steel member shapes. 1
Figure 1.2 : Cold roll-forming process (description). 2
Figure 1.3 : Cold roll-forming process (real). 3
Figure 1.4 : Cold formed steel building example 4
Figure 1.5 : Cold formed steel structure example. 4
Figure 1.6 : A cold formed steel hangar 5
Figure 1.7 : Some CFS section geometries. 5
Figure 1.8 : Cold formed steel roof deck sheet example. 6
Figure 1.9 : Cold formed steel roof deck example. 6
Figure 1.10 : An example of cold formed steel wall panel. 7
Figure 1.11 : A basic schematic sketch of a CFS storage rack structure. 8
Figure 1.12 : Pallet racking example from Turkey 9
Figure 1.13 : A drive-in model of rack structures. 9
Figure 1.14 : Pallet racking structure example. 10
Figure 2.1 : Flexural column buckling stress. 17
Figure 2.2 : An exaggerated flexural-torsional column buckling example. 18
Figure 2.3 : Flexural-torsional column buckling of an I section. 18
Figure 2.4 : Maximum stress for flexural-torsional buckling. 20
Figure 2.5 : Example of different local buckling modes 21
Figure 2.6 : Local buckling of stiffened compression flange of a hat-shaped section. 22
Figure 2.7 : Square plate subjected to compression stress. 22
Figure 2.8 : Rectangular plate subjected to compression stress. 22
Figure 2.9 : Buckling coefficient for flat rectangular plates. 23
Figure 2.10 : Values of k for determining critical buckling stress. 24
Figure 2.11 : Distortional buckling of a C channel with stiffened lips. 26
Figure 2.12 : Rack section column buckling stress versus half wavelength for concentric compression. 27
Figure 2.13 : Approach of finite element method and finite strip method 28
Figure 2.14 : An example of buckling curve. 28
Figure 2.15 : Local buckling mode of a Z section. 29
Figure 2.16 : Comparison of test strengths with design strengths. 30
Figure 2.17 : Buckling stress versus half-wavelength for a C-Section in compression. 31
Figure 2.18 : Comparison of the direct strength method predictor curves with test data for columns. 33
Figure 2.19 : Comparison design methods with test results. 34
Figure 2.20 : Comparison between the current DSM distortional curve and ultimate loads with different end conditions 36

Figure 2.21 : Comparison between the modified DSM distortional curve and column ultimate loads with different end conditions. 36
Figure 2.22 : Load versus displacement curves for f_y=250 MPa. 38
Figure 2.23 : Load versus displacement curves for f_y=320.23 MPa. 38
Figure 2.24 : Experimental collapsed specimens and deformed shapes from FE analysis. 39
Figure 2.25 : Effective area and centre of gravity comparisons 40
Figure 2.26 : Main geometric parameters of the column 42
Figure 3.1 : Stiffened elements. 50
Figure 3.2 : Elements with simple lip edge stiffener. 51
Figure 3.3 : Out-to-out dimensions of webs and stiffened elements 53
Figure 3.4 : C-channel column section with simple lip edge example 54
Figure 3.5 : Limits for pre-qualified columns 62
Figure 3.6 : DSM global buckling failure design curve and equations 66
Figure 3.7 : DSM local buckling failure design curve and equations 66
Figure 3.8 : DSM distortional buckling failure design curve and equations 67
Figure 3.9 : Centerline dimensions in CUFSM 68
Figure 3.10 : Yield load calculation 69
Figure 3.11 : Configuration of material properties 69
Figure 3.12 : Boundary condition selection 70
Figure 3.13 : Result of local Buckling in CUFSM 71
Figure 3.14 : Result of distortional buckling in CUFSM 71
Figure 3.15 : Result of flexural-torsional buckling in CUFSM 72
Figure 4.1 : General geometric details of specimen cross-sections 76
Figure 4.2 : Explanation of specimen's notation through its properties 77
Figure 4.3 : Nominal strength – lip length relationship of the unperforated specimens having 500 mm column length (lip continues outward) 85
Figure 4.4 : Nominal strength – lip length relationship of the unperforated specimens having 500 mm column length (lip continues inward) 85
Figure 4.5 : Nominal strength – lip length relationship of the unperforated specimens having 1000 mm column length (lip continues outward) .. 86
Figure 4.6 : Nominal strength – lip length relationship of the unperforated specimens having 1000 mm column length (lip continues inward) 86
Figure 4.7 : Nominal strength – lip length relationship of the unperforated specimens having 1500 mm column length (lip continues outward) .. 87
Figure 4.8 : Nominal strength – lip length relationship of the unperforated specimens having 1500 mm column length (lip continues inward) 87
Figure 4.9 : Comparison of nominal strength – lip length relationship of the unperforated specimens having 500 mm column length 88
Figure 4.10 : Comparison of nominal strength – lip length relationship of the unperforated specimens having 1000 mm column length 89
Figure 4.11 : Comparison of nominal strength – lip length relationship of the unperforated specimens having 1500 mm column length 89
Figure 4.12 : Comparison between nominal strength – lip length realtionships of the unperforated specimens having lips continuing outwards 90
Figure 4.13 : Comparison between nominal strength – lip length realtionships of the unperforated specimens having lips continuing inwards 91
Figure 4.14 : Typical model for perforation configuration of all perforated specimens 93
Figure 4.15 : Typical model for reduced thickness approach from CUFSM 97

Figure 4.16 : Nominal strength – lip length relationship of the perforated specimens having 500 mm column length (lip continues outward)..... 103
Figure 4.17 : Nominal strength – lip length relationship of the perforated specimens having 500 mm column length (lip continues inward)..... 103
Figure 4.18 : Nominal strength – lip length relationship of the perforated specimens having 1000 mm column length (lip continues outward)..... 104
Figure 4.19 : Nominal strength – lip length relationship of the perforated specimens having 1000 mm column length (lip continues inward)..... 104
Figure 4.20 : Nominal strength – lip length relationship of the perforated specimens having 1500 mm column length (lip continues outward)..... 105
Figure 4.21 : Nominal strength – lip length relationship of the perforated specimens having 1500 mm column length (lip continues inward)..... 105
Figure 4.22 : Comparison of nominal strength – lip length relationship of the perforated specimens having 500 mm column length..... 106
Figure 4.23 : Comparison of nominal strength – lip length relationship of the perforated specimens having 1000 mm column length..... 107
Figure 4.24 : Comparison of nominal strength – lip length relationship of the perforated specimens having 1500 mm column length..... 107
Figure 4.25 : Controlling buckling modes for inward and outward cases of perforated 1500 mm long columns with maximum lip length configuration 108
Figure 4.26 : Comparison between nominal strength – lip length realtionships of the perforated specimens having lips continuing outwards 109
Figure 4.27 : Comparison between nominal strength – lip length realtionships of the perforated specimens having lips continuing inwards 110
Figure 4.28 : Comparison between nominal strength – lip length relationships of the perforated and unperforated specimens having lips continuing outward and column length 500 mm..... 111
Figure 4.29 : Comparison between nominal strength – lip length relationships of the perforated and unperforated specimens having lips continuing inward and column length 500 mm..... 112
Figure 4.30 : Comparison between nominal strength – lip length relationships of the perforated and unperforated specimens having lips continuing outward and column length 1000 mm..... 112
Figure 4.31 : Comparison between nominal strength – lip length relationships of the perforated and unperforated specimens having lips continuing inward and column length 1000 mm..... 113
Figure 4.32 : Comparison between nominal strength – lip length relationships of the perforated and unperforated specimens having lips continuing outward and column length 1500 mm..... 113
Figure 4.33 : Comparison between nominal strength – lip length relationships of the perforated and unperforated specimens having lips continuing inward and column length 1500 mm..... 114

STRENGTH AND STABILITY OF THIN WALLED STEEL COLUMNS IN STORAGE RACK STRUCTURES

SUMMARY

Steel Storage Rack Systems play a vital role in logistics and storing goods.This has particularly increased over the last decade. In our country, importance of these systems is increasing through the demand of insufficient space to storage goods from various industries and fields. The structural strength and stability of steel storage rack structures became more important than before because the usage of these structures and value of the goods carried by these structures have increased.

Safety of columns used as part of the structral system of storage rack frames is particulary vital for safe use of the systems. Steel Storage Rack Columns can be assumed to be a specific version of general cold formed steel (CFS) columns. However, the behaviour of steel storage rack columns is different from general behavior of the CFS columns due to their thickness, lip configuration and the presence of the perforations. Steel storage rack columns may consist various lip types, lengths and perforations for the intended use. These two major variables affect the capacity of rack columns and hence the stability and strength of whole rack structure.

Determining the structural capacity of steel storage rack columns has been currently regulated with several standarts and methods. American Iron and Steel Institute S100-2007 Standart is one of these few standarts to regulate the method of calculation to determine the strength of cold formed steel columns. The standart presents Effective Width Method and Direct Strength Method for calculations.

Direct Strength Method, presented in Appendix 1 part of AISI S100-2007 standart has been newly developed method for determination of the strength of concentrically axially loaded cold formed steel members. The effects of perforations and lip configuration including lip type, lip forming direction and column length on nominal column strength are investigated using Direct Strength Method on a range of various specimens in this thesis.

The main parts of the present study can be summarized as follows;

- Review of previous studies conducted on steel storage rack columns and direct strength method.

- Assessment of current practise (AISI S100-700 provisions) with respect to calculation of cold formed steel column capacity with Effective Width Method and Direct Strength method.

- The analytical study carried out on 120 column models having different column lengths, lip directions, lip lengths and perforated and unperforated cases.

In AISI S100-700 standart, currently the effect of perforations on column strength is accounted for by physical testing. No design rules are given to consider the effect of perforations on the three major buckling modes including local, distortional and global. In this study, a recently developed analytical approach which integrates the

Direct Strength Method by a method called “Reduced Thickness Approach” was used. Comparisons were made between nominal strength values of columns with varying cross-section geometries (lip configuration) for both unperforated and perforated cases with three different column lengths.

İNCE CİDARLI ÇELİK DEPO RAF SİSTEMLERİ KOLONLARININ DAYANIM VE STABİLİTESİ

ÖZET

Çelik Depo Raf Sistemleri ürün depolama ve lojistik sektörlerinde hayati bir rol oynamaktadır. Son on yıllık periyotta bu sistemlerin öneminin bilhassa arttığı görülmüştür. Ülkemizde, çeşitli endüstriyel sektörler ve alanlardaki depolama alanlarının yetersizliği ile bu sistemlerin önemi gittikçe artmaktadır. Depo raf sistemlerinin kullanımının yaygınlaşması ve bu sistemlerde taşınan ürünlerin değerlerinin artması ile bu sistemlerin yapısal dayanımları önem kazanmaktadır.

Çelik depo raf sistemleri, ince cidarlı çelik elemanlardan oluşmaktadır. İnce cidarlı çelik elemanlar, çelik plakaların oda sıcaklığında işlenmesi ile elde edilirler. İşleme metodu, çelik plakalara soğuk merdaneli biçimleme veya sıkıştırma yapılmasıdır. İşlenen çelik plakaların kalınlıkları genellikle 0.10 mm ile 7.7 mm arasında değişmektedir. Plakaların akma gerilmeleri ise 230 MPa ile 380 MPa arasında değişmektedir. İnce cidarlı çelik elemanların, taşıyıcı sistemlerde kullanımının bazı avantaj ve dezavantajları bulunmaktadır. Hafiflik, toplu üretim, yüksek mukavemet, kolay kurulum, kalıp işçiliğinin gerekmemesi, paslanma korunumu, düşük taşıma giderleri, kesit çeşitliliği ve geri kazanılabilirlik gibi özellikler, ince cidarlı çelik elemanların kullanım avantajları arasında yer almaktadır. Eleman kalınlıklarının düşük olması sebebiyle burkulma problemleri ve yangın dayanımları ise ince cidarlı çelik elemanlar kullanımının dezavantajları arasında yer alabilmektedir.

İnce cidarlı elemanların taşıyıcı sistemi oluşturduğu iki tip depo raf sistemi yaygın olarak kullanılmaktadır. Bunlardan ilki ve en yaygını paletli depo raf sistemleridir. Paletli depo raf sistemlerinde, raflara konacak ürünler çeşitli yüksekliklerdeki raf kirişlerine paletler üzerinde yerleştirilirler. Sistemin bileşenlerini, kolon ve çaprazların oluşturduğu çerçeveler ve bu çerçeveleri birbirine bağlayan, paletlerin üzerlerine yerleştirildiği yatay kirişler oluşturmaktadır. Çapraz elemanlar ve kirişler, kolonlara genellikle bulonlu veya kaynaklı birleşimler ile bağlanırlar. Avrupa'da ve ülkemizde yaygın olarak bulonlu birleşimler kullanılmaktadır. İkinci tip depo raf sistemleri ise içine girilebilir raf sistemleridir. Bu sistemlerde kolonlara bağlanan yatay kirişler bulunmaz ve konulacak yükler forklift gibi araçlar ile sistem üzerine sürülürler. Paletli depo raf sistemlerinin daha yaygın kullanılmasının sebebi, ürünlere her iki yönden kolayca ulaşılabilmesidir.

Bu çalışmada öncelikle soğukta şekillendirilmiş genel çelik kolonların yapısal davranışı incelenmiştir. İnce cidarlı çelik kolonların eksenel yük altında taşıma kapasitelerini tayin edebilmek için dikkat edilmesi gereken başlıca unsurlar, akma, global burkulma, yerel burkulma ve çarpılmalı burkulmadır. Akma için kapasite hesabında kesit alanı ile malzemenin akma dayanımı kullanılır. Kesit kalınlıkları düşük olduğu için genelde kolon kapasitesi, akma dayanımına ulaşmadan burkulma problemleri oluşur. Global burkulmanın, eğilmeli burkulma, burulmalı burkulma ve bu iki burkulma modunun aynı anda olduğu durum olarak üç farklı türü mevcuttur.

İnce cidarlı çelik kolonları oluşturan elemanlar, şekil verilmiş çelik plak elemanlar olduğundan dolayı yerel burkulmayı basınca maruz kalan plakların davranışı belirlemektedir. Yerel burkulma için yapılan hesaplarda yaygın olarak efektif alan yöntemi kullanılmaktadır. Çarpılmalı burkulma, özellikle açık ağızlı kesitlerde karşılaşılan, kolonun kesit ağızlarının içe yada dışa doğru açılarak deforme olması ile oluşan burkulma durumudur. İnce cidarlı çelik kolonların kapasite hesabında kolonun taşıyabileceği maksimum yük, tüm bu etmenler dikkate alınarak hesaplanan kapasitelerin minimum olanı alınarak hesaplanmaktadır.

Depo raf sistemleri taşıyıcı çerçevelerinde kullanılan kolon elemanların güvenliği sistem güvenliği açısından özel ve önemli bir yer teşkil etmektedir. Çelik depo raf kolonları genel soğukta biçimlendirilmiş ince cidarlı çelik kolonların özel bir tipi olarak kabul edilebilir. Fakat, çelik depo raf kolonlarının yapısal davranışı; kalınlıkları, kolon ağzı konfigürasyonları ve delikli yapılarından dolayı soğukta şekillendirilmiş genel çelik kolonlardan farklılık göstermektedir. Çelik depo raf kolonları, çeşitli kolon ağzı tipleri ve uzunlukları ve kullanım amacına göre çeşitli delik konfigürasyonlarına sahip olabilirler. Bu iki ana değişken, raf kolonlarının taşıma kapasitesini ve bundan dolayı tüm raf yapısının dayanımı ve stabilitesini etkileyen başlıca etmenlerdir.

Çelik raf kolonlarının kapasitesinin hesabı şuan çeşitli yönetmelikler ve metotlar ile düzenlenmektedir. "Amerikan Demir ve Çelik Enstitüsü S100-2007" standardı, soğukta biçimlendirilmiş çelik kolonların dayanımlarının hesaplama yöntemlerini düzenleyen az sayıda yönetmelikten biridir. Bu standartta hesap yöntemleri olarak "Efektif Genişlik Yöntemi" ve "Doğrudan Dayanım Yöntemi" tarif edilmektedir.

Efektif genişlik yöntemi, eşmerkezli eksenel yüklenmiş ince cidarlı çelik elemanların dayanımları için kullanılan klasik yöntemdir. Yapılan çalışmalarda, basınç altında ince cidarlı çelik kolon kesitlerinin tüm alanları ile çalışmadıkları görülmüştür. Dolayısı ile kapasite hesabında öncelikle kesit alanı, gelen basınca dayanan kısma yaklaşacak şekilde yönetmelikte tarif edilen plakların yerel burkulma durumu dikkate alınarak azaltılır. Global burkulma gerilmesi, akma gerilmesi ile ilişkilendirilerek kolon narinliği hesaplanır. Bulunan kolon narinliği ve akma gerilmesi kullanılarak kolon kapasitesi tayin edilir.

Doğrudan dayanım yöntemi, eşmerkezli eksenel yüklenmiş ince cidarlı çelik elemanların dayanımlarının belirlenmesi için son zamanlarda geliştirilen bir yöntem olup AISI S100-2007 standardının EK-1 kısmında tarif edilmektedir. Yapılan çalışmalarda, birçok çelik kolon kapasitesinin test sonuçları biraraya getirilerek direk dayanım yöntemi için öngörü eğrileri çıkarılmıştır. Bu eğrilerden elde edilen analitik formüller ile her bir burkulma modu için kolon kapasitesi hesap edilebilmektedir. Elemanların kritik elastik burkulma yükleri, her bir burkulma modu için sonlu şerit yöntemi kullanan "CUFSM" paket programı veya sonlu eleman yöntemi ile hesaplanır. Kritik elastik burkulma yükleri, direk dayanım yöntemi formüllerinde kullanılarak her bir burkulma modu için kolon dayanımı hesap edilir. Elde edilen dayanımların en küçüğü alınarak kolon kapasitesi tayin edilir. Direk dayanım yönteminde yerel burkulma ve global burkulmanın etkileşimi dikkate alınmaktadır. Çarpılmalı burkulma, akma dayanımı ile ilişkilendirilmektedir. Direk dayanım yöntemi kullanılarak yapılan kapasite hesabında doğru sonuç elde edilebilmesi için ilgili yönetmelikteki kesit geometrisi limitleri dikkate alınmalıdır.

Bu tezde, çeşitli özelliklerde ve aralıklarda örnek kolonların dayanım hesabında doğrudan dayanım yöntemi kullanılarak kolon ağzı tipi, yönü ve uzunluğu, kolon boyu ve delik varlığının kolon dayanımı üzerindeki etkileri incelenmiştir.

Mevcut çalışma aşağıdaki şekilde özetlenebilir;

- Doğrudan dayanım yöntemi ve çelik depo raf kolonları ile ilgili yapılan önceki çalışmaların incelenmesi ve özetlenmesi.

- Soğukta biçimlendirilmiş çelik kolonların taşıma kapasitelerinin mevcut yönetmelikteki (AISI S100-700) Efektif genişlik yöntemi ve doğrudan dayanım yöntemi ile örnek çözümler verilerek değerlendirilmesi.

- Kolon boyları, kolon ağzı yönleri ve uzunlukları, delikli olup olamama gibi durumları bakımından çeşitlilik gösteren 120 adet kolon modelinin dayanım hesabı üzerinde analitik bir çalışma yapılması.

AISI S100-700 standardında deliklerin kolon dayanımı üzerindeki etkisinin, fiziksel test yapılarak bulunması tarif edilmektedir. Üç ana burkulma modu olan yerel burkulma, çarpılmalı burkulma ve global burkulma üzerinde delik etkisinin incelenebilmesi için bir tasarım kuralı verilmemiştir. Bu çalışmada, doğrudan dayanım yöntemi ile bütünleştirilerek son zamanlarda geliştirilen bir yöntem olan "Azaltılmış Kalınlık Yaklaşımı" kullanılmıştır. Üç farklı kolon boyunda, delilikli olup olmama durumları için kolon ağzı konfigürasyonundan dolayı değişken geometrili kesitlere sahip kolon modelleri dayanımları hesaplanarak karşılaştırmalar yapılmıştır.

1. INTRODUCTION

1.1 Overview of Cold Formed Steel

Cold-formed steel (CFS) is the term used for products which are made by rolling or pressing thin gauges of sheet steel. Usable products of cold-formed steel material can be achieved by stamping, rolling or pressing the steel sheets. These products are commonly used in various areas of manufacturing. Automobiles, industrial products, railway coaches, storage racks, highway products, bridges, types of equipment etc. However, cold-formed steel phrase is generally used to describe as a construction material. There are two main structural member families in steel construction. Hot-rolled shapes and cold-formed steel members. The use of cold-formed steel construction materials' popularity has increased since 1950s. In general expression, structural and non-structural elements in the construction industry are created from cold-formed members. These building materials form columns, beams, joists, studs, floor decking, built-up sections and other components. Cold formed steel members are also known as thin-walled steel members in construction industry. Some CFS member shapes are given in figure 1.1. The material thicknesses for these members usually range from 0.4 mm to about 6.4 mm [1-2].

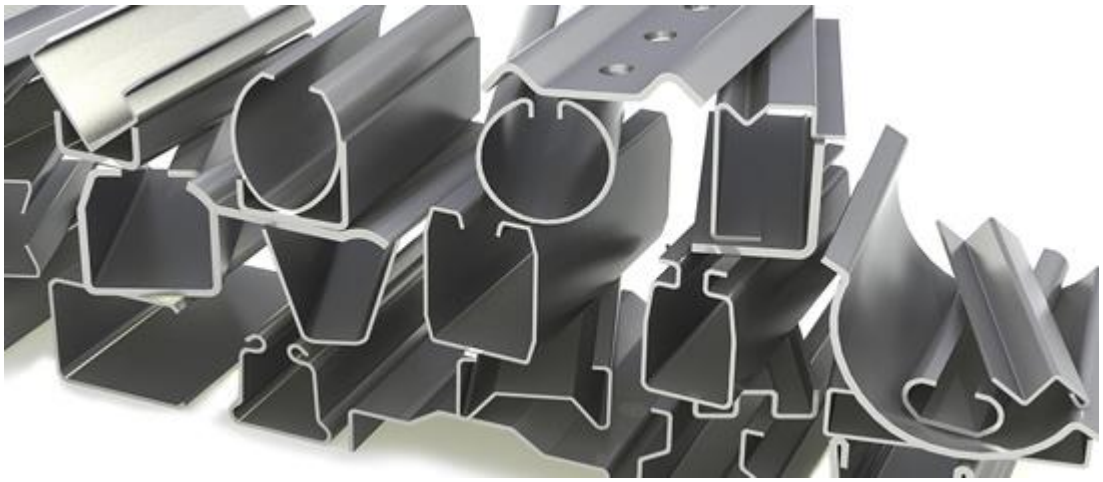

Figure 1.1 : Cold formed steel member shapes [3].

1.1.1 Production

The hot-rolled steel shapes are formed at elevated temperatures while the cold-formed steel shapes are formed at room temperature. Cold-formed steel structural members are shapes commonly manufactured from steel plate, sheet or strip material. The producing and manufacturing process includes forming the material by either cold roll-forming or press-breaking to achieve the desired shape. Cold roll-forming is the most widely used method for production of floor and wall panels, roof members and structural components like C, Z and hat sections. Sections can be made from sheet up to 1.5 m wide and from coils more than 1000 m long. Press-braking is often used for production of simple shapes.

Cold roll-forming process is shown in the figures 1.2 and 1.3. Flat sheets are given the desired shapes by cold-forming of the sheets between logitudinal rolls. Complex shapes can require 24 to 30 rolls whereas a simple section may require as few as six pairs of roll. Generally, the thickness of material that can be formed ranges between 0.10 mm up to 7.7mm, although heavy duty cold forming mills can handle steel up to 19 mm thick.

The manufacturing of cold-formed steel products occurs at room temperature. Design considerations for the strength of these elements are usually deals with the effects of buckling. The yield stress of the steels commonly used for cold-forming ranges from 230 to 380 MPa and higher. With regards to for the formability, tensile strength and ductility are the other distinctive properties. The ratio of tensile strength to yield strength for cold-formed steels commonly ranges from 1.2 to 1.8 [4].

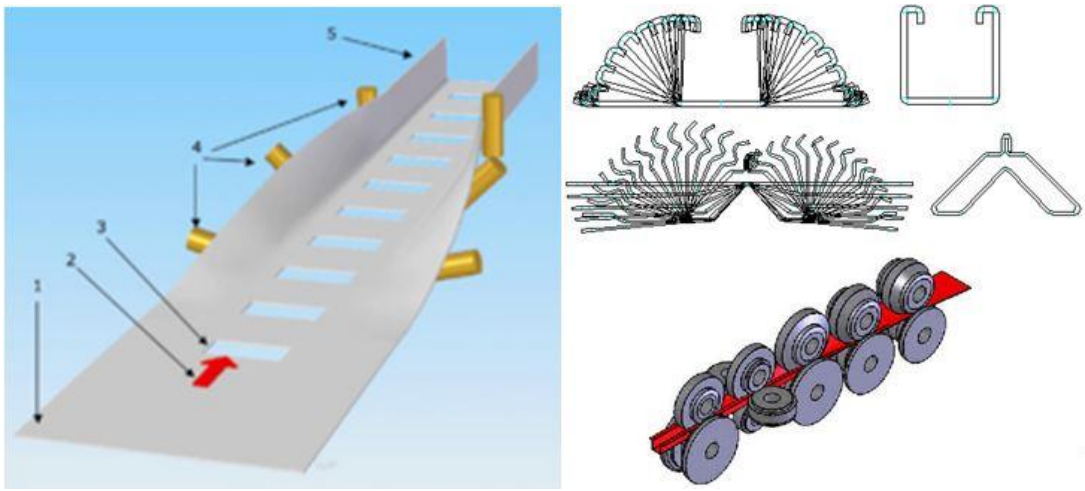

Figure 1.2 : Cold roll-forming process (description) [2].

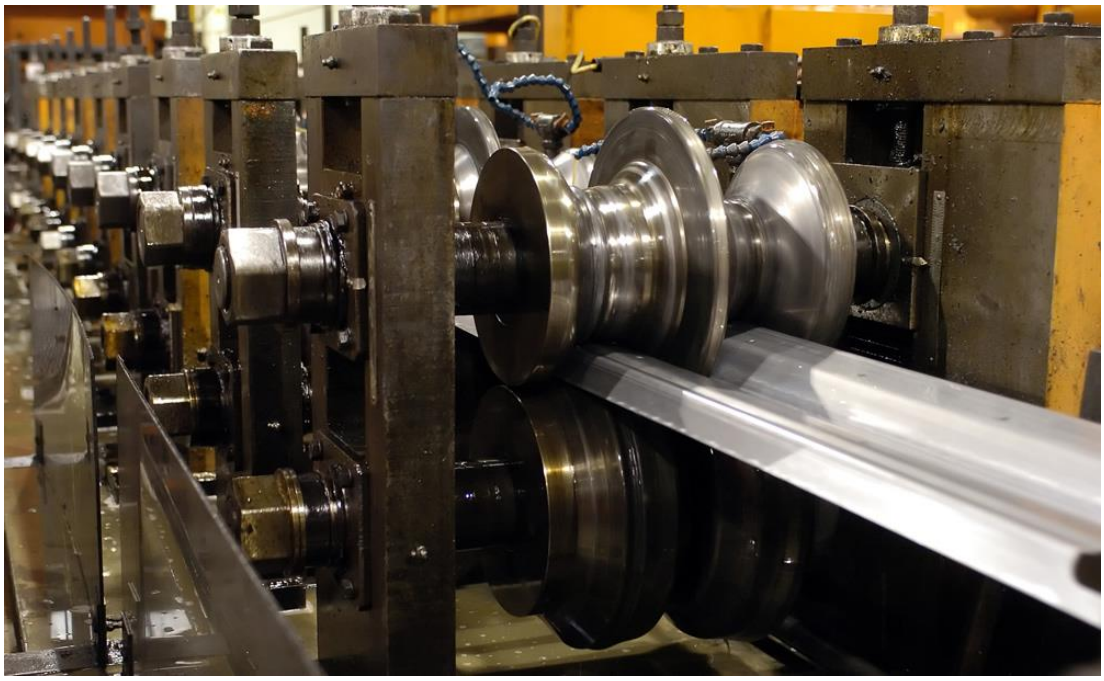

Figure 1.3 : Cold roll-forming process (real) [5].

1.1.2 Structural applications

There are many applications around the world which are related with the cold-formed elements. Applications for structural purposes cover around %50 of general usage around the world with cold formed steel. Industrialized housing, standardized metal buildings, steel storage rack structures, pre-engineered buildings are general structural areas related with cold formed steel materials.

Construction where cold-formed steel is finding wider application is in steel framing systems for residental, commercial, agricultural and industrial applications. Small buildings can be made entirely with cold formed steel sections as shown in Figure 1.4 Pre-engineered metal building manufacturers provide custom designed structures from small residental houses to sophisticated structures such as schools, hangars, and complex manufacturing facilities. Three adjacent building blocks shown in Figure 1.5 raised in Paris is very attractive due to a playful and optimized use of the cold formed steel structure as a good example. A cold-formed steel hangar can be seen in Figure 1.6.

Figure 1.4 : Cold formed steel building example [6].

Figure 1.5 : Cold formed steel structure example [7].

Figure 1.6 : A cold formed steel hangar [8].

More specifically, cold formed steel elements can be grouped in two major headline according to their role in structural applications; individual structural members, panels and decks.

Individual structural members consist of various shapes and sections for cold-formed construction. Channels (C-sections), I sections, T sections, tubular members, Z-sections, hat sections, angles are usual shapes used in cold-formed structural framing. Generally, depth of members ranges from 50 to 305 mm and the thickness ranges from 1.20 to 6.35 mm. In some cases, depth may be up to 457mm and thickness also maybe up to 12.7 mm or thicker in building construction and transportation.

Some of the sections are shown in Figure 1.7.

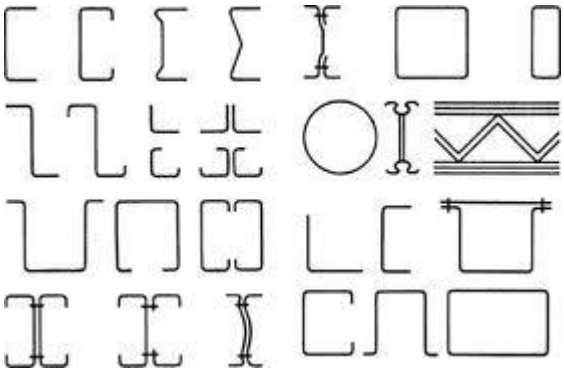

Figure 1.7 : Some CFS section geometries [1].

Stiffness, structural strength and load carrying properties are the main design considerations of an individual framing member.

The second major headlines of cold-formed sections are panels and decks. These sections are generally used for floor decks, roof decks, bridge forms, wall panels and siding materials. In general, the depth of panels ranges from 40 to 200 mm and thickness ranges 0.5 to 2 mm. Besides their role to carry loads, these section also provide a surface on which roofing, flooring or concrete fill can be applied. Some perforations can be made on these sections combining with sound absorption material to form an acoustically conditioned ceiling. As a result of their geometry, they provide space for electrical conduits, communications and data cable distribution as well as heating and air conditioning ducts. In Figures 1.8 and 1.9, typical roof decks are shown. In figure 1.10, an example of cold formed wall panel is given.

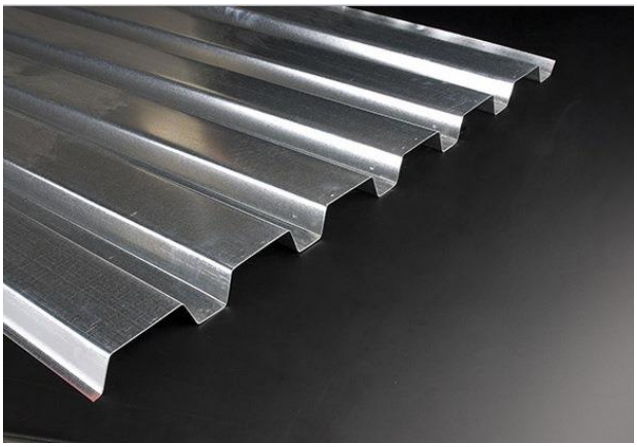

Figure 1.8 : Cold formed steel roof deck sheet example [9].

Figure 1.9 : Cold formed steel roof deck example [10].

Figure 1.10 : An example of cold formed wall panel [11].

Cold formed steel storage rack systems are another important category of cold form steel structures. Rack systems are widely used throughout the world for storing materials. Due to their vertical character these systems provide high storage density, allowing the storage of a great amount of products in reduced areas. They also allow great accessibility to the stored materials. These systems are used by many companies to store their products in large scale. There are various models which fit to the conditions demanded accessing each product to be stored in the available room. These models vary from simple shelves to automated structures of more than 30 m height. Within these various models, Pallet and Drive-in Systems are widely-used ones [12].

Pallet Racking Systems allow for the storage of palletized materials in horizontal rows with multiple levels. Main parts of these systems are upright frames, load carrying beams, braces and base plates. A basic schematic sketch is given in Figure 1.11.

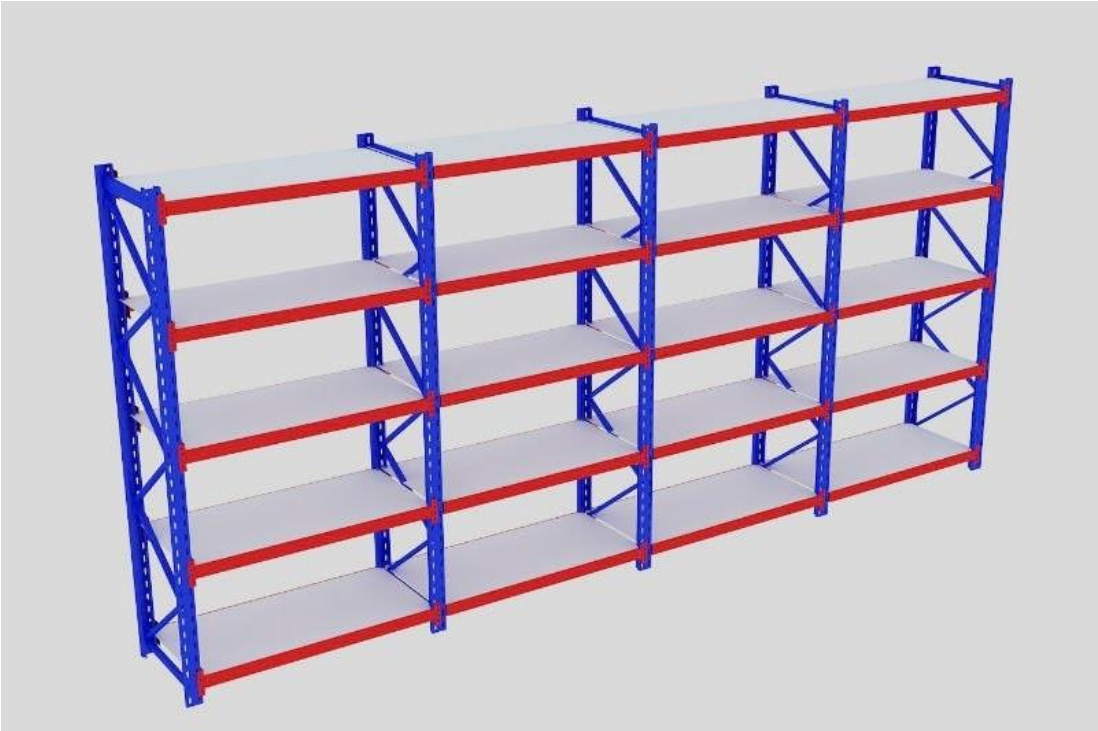

Figure 1.11 : A basic schematic sketch of a CFS storage rack structure [13].

Upright frames are in blue color which include cold formed columns and braces, beams are in orange color. The most widely used beam sections are box sections. On the other hand, open C sections and many different configurations of perforated cold formed sections are used as columns forming uprights. Braces are the members of upright frame lacing can be welded or bolted between two upright columns to form upright frames. One of the peculiar structural concepts is Drive-In models. In these models the absence of transversal beams allows fork-lifts to move inside the structure and the presence of perforations on columns also facilitate the assemblage. Drive-in and pallet racking examples are shown in Figures 1.12 to 1.14.

Pallet racking systems are used more often with regard to Drive-in models. Accessibility to goods from both sides makes pallet-racking systems more preferable. In Europe, the designers prefer bolted connection types more than the welded connection types on connections between beam-columns and beam-braces. In US, the welded connections are preferred mostly.

Figure 1.12 : Pallet racking example from Turkey [Personal Photo].

Figure 1.13 : A drive in model of rack stuctures [14].

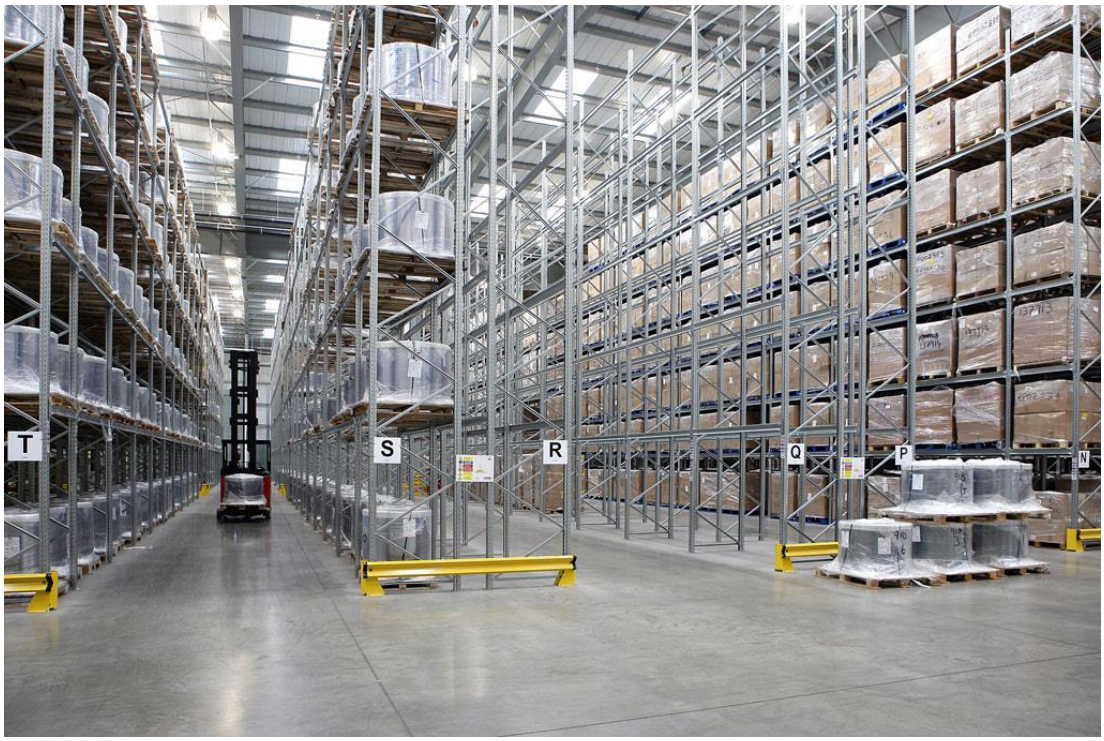

Figure 1.14 : Pallet racking structure example [15].

1.1.3 Advantages and disadvantages of cold formed steel

Cold-formed steel offers many advantages. If compared with other materials, like timber or concrete; cold formed steel structural members have following characteristics;

- Lightness
- Mass production and prefabrication ease
- High strength and stiffness
- Easy, quick and facilitated assembly
- Delays due to weather conditions
- Accurate detailing
- Formwork is not needed
- Rot and termite proof
- Low transportation and handling expenses
- Recyclability
- Shape variability

- Uniform of quality

Also, cold-formed steel structural members provide structural and constructional advantages. For short spans and relatively light loads, cold formed light members can be manufactured in comparison with thicker hot-rolled sections. Some of cold formed sections can be nested which allows compact packaging and transportation. Various sectional configurations can be produced with cold-forming operations economically. A useful surface can be provided for floor, roof and wall construction by load carrying cold-formed panels and decks. Load carrying panels act like a shear diaphragm to resist force in their own planes if they are adequately interconnected with each other and supports beside withstanding loads normal to their surfaces. Favorable strength to weight ratios can be obtained by variation of cold formed steel sections [1].

Designing with cold-formed steel shapes and with hot-rolled structural shapes differs.With the hot-rolled, primarily concerns are about two types of instability: lateral buckling of unbraced beams and column buckling. Local buckling of individual constituent elements generally will not occur before yielding due to the dimensions of hot-rolled shapes. However, this is not the case with cold-formed members. In most cases, the material used is thin relative to its width which causes to local and distortional buckling hence these failure modes must also be considered. This can result in premature buckling of individual flat, or plate, elements at stresses well below the yield stress point [4].

Sometimes, high unit-prices, low fire resistance, more careful requirement of treatment during assembly and difficult connections may be considered as disadvantages.

1.2 Aim and Layout of the Thesis

This study mainly focuses on the approaches to predict the strength and stability of thin walled steel columns in storage rack structures. Direct Strength Method, which is a recently proposed approach on this topic is investigated in detail. The major differences between columns in steel storage rack structures and general cold formed steel columns are lip configuration and perforations. The effects of perforations and lip configuration including lip type, lip forming direction and column length on

nominal column strength are investigated using Direct Strength Method on a range of various specimens in this thesis.

Chapter 1 includes an overwiev on Cold-Formed Steel. This chapter discusses production phases, structural applications, advantages and disadvantages of CFS.

The thesis moves on with a detailed literature review on cold-formed steel columns. Under the “General Remarks” title in Chapter 2, the behaviour of cold formed steel columns with respect to phenomenas like yielding, buckling and other buckling types is summarized. Second part of Chapter 2 focuses on the studies conducted using Direct Strength Method. The third part of this chapter summarizes various studies conducted on perforated cold-formed steel storage rack columns.

Chapter 3 consists of an overview of the design rules given in American Iron and Steel Institute S100-2007 Standart on concentrically loaded compression CFS members. These design rules include the widely used Effective Width Method and recently proposed Direct Strength Method. (Appendix 1 of AISI S100-2007) Example Solution of a C-Channel Column with a Simple Lip Edge Stiffener is presented via Effective Width Method and Direct Strength Method.

Main focus of Chapter 4 is on the investigation of nominal strength of various rack columns through Direct Strength Method. This investigation includes the analysis of 120 column models having different lip configurations and column lengths. Both perforated and unperforated columns were considered.

Chapter 5 presents the final conclusions drawn from the present study and suggestions for future work.

2. LITERATURE REVIEW ON COLD FORMED STEEL COLUMNS

There have been many studies made on cold-formed steel columns since 1970s. Design methods are improved due to many experimental results and numerical studies. Effective width method is traditional method for determining strength of cold formed steel sections. Direct strength method can also be considered as new method for determining specifically cold formed steel column sections. This method has been validated by many experiments and studies that will be summerized under this topic. Besides, many studies have been made on perforated storage rack columns which needs a different approach. It is necessary to realize the importance of perforations on strength and behaviour of the columns. In this chapter, literature survey is grouped into three parts. General Remarks on Cold-Formed Steel Column Behaviour, Studies on Direct Strength Method and Studies on Perforated Cold-formed Steel Storage Rack Columns.

2.1 General Remarks on Cold Formed Steel Column Behaviour

Thin walled cold formed steel compression members are used to carry a compressive load through centroid of their cross-section. Cross-sections may be composed of stiffened elements, unstiffened elements or combination of stiffened and unstiffened elements. Most of the time, shear center of cross-sections may not coincide with the centroid of the section. Thus; during the design phase; following limit states must be considered depending on the configuration of the section, column lengths used and thickness of the material;

- Yielding
- Global (overall) Column Buckling including;

  Flexural Buckling (bending about a principal axis)

  Torsional Buckling (twisting about shear center)

  Flexural-Torsional Buckling (bending and twisting simultaneously)

- Local Buckling
- Distortional buckling (buckling of open sections with edge stiffened flanges)

Design provisions of global (overall) buckling and effect of local buckling on column strength have been included in the AISI Specification [16]. These provisions were added to Specification in 1968 by detailed investigations of George Winter, Alexander Chajes, Pen Jeng Fang and Teoman Peköz at Cornell University [17-19].

Unified approach of design provisions developed in 1986 and discussed by Peköz in [20]. In this approach, following steps for the design of axially loaded compression members are given;

- Calculate the elastic column stress (flexural, torsional, or flexural-torsional) for the full unreduced section
- Determine the nominal failure stress (elastic buckling, inelastic buckling or yielding)
- Calculate the nominal column load based on the governing failure stress and the effective area
- Determine the design column load from the nominal column load using the specified safety factor or the resistance factor

North American Specification had the design provisions for determining the distortional buckling strength of I, Z, C, hat and other open sections having edge-stiffened flanges in 2007.

2.1.1 Yielding

Yield load can simply be described as;

$$P_y = A * F_y \qquad \textbf{(2.1)}$$

Where "A" is the cross-sectional are of column and "F_y" is the yield stress of steel.

Very short, compact columns under axial load may fail by yielding.

2.1.2 Global (overall) column buckling

Global buckling of steel columns can be inspected into three parts. Flexural Column Buckling, Torsional Column Buckling and Flexural-Torsional Column Buckling.

2.1.2.1 Flexural column buckling

Elastic buckling

Slender axially loaded cold formed steel column sections such as doubly symmetric shapes, closed shapes, point-symmetric shapes or cylindrical shapes can easily be subjected to fail by overall flexural buckling. The elastic critical buckling load for a long steel column can be calculated by the Euler formula given in **(2.2)**.

$$P_e = \frac{\pi^2 EI}{(KL)^2} \qquad \textbf{(2.2)}$$

Where;

P_e is the Euler Buckling Load

E is the Modulus of Elasticity

I is the Moment of Inertia

L is the column length

K is the effective length factor

If substitution made on **(2.2)** by $I = Ar^2$, where A is the cross-section area, Euler stress for elastic column buckling is obtained and given in **(2.3)**;

$$\sigma_e = \frac{\pi^2 E}{(KL/r)^2} \qquad \textbf{(2.3)}$$

Where KL/r is the effective slenderness ratio and r is the least radius of gyration.

Inelastic buckling

There are two different approach in the literature for inelastic buckling concept. The tangent modulus method, firstly proposed by Engesser in 1889. Tangent modulus load equation is given in **(2.4)** according to this method:

$$P_T = \frac{\pi^2 E_t I}{(KL)^2} \qquad \textbf{(2.4)}$$

Where E_t is the tangent modulus. Critical buckling stress is;

$$\sigma_T = \frac{\pi^2 E_t}{(KL/r)^2} \quad \textbf{(2.5)}$$

As the second method, reduced or double modulus concept including effect of elastic unloading has been developed by Janisky in 1895. Equations used by this method are as follows;

$$P_R = \frac{\pi^2 E_r I}{(KL)^2} \quad \textbf{(2.6)}$$

And

$$\sigma_R = \frac{\pi^2 E_r}{(KL/r)^2} \quad \textbf{(2.7)}$$

Where E_r is the reduced modulus which can be defined as $E\ (I_1 / I) + E_t\ (I_2 / I)$ I_1 is moment of inertia about neutral axis of the area on unloading side after buckling. I_2 is moment of inertia about neutral axis of the area on loading side after buckling.

Francis R. Shanley's contributions on this topic are revealed in [21];

- Tangent modulus concept gives the maximum load up to which an initially straight column remains straight.
- The actual maximum load exceeds the tangent modulus load, but it cannot reach the reduced modulus load.

Other investigations and experiments improved Shanley's concepts and Galambos stated in [22] that the maximum load is usually higher than the tangent modulus load by %5 or less.

The Structural Stability Research Council has pointed that if the effect of residual stress is considered and the effective proportional limit is assumed to be equal to one-half the yield stress, Eq. **(2.5)** can be approximated by the following equation:

$$\sigma_T = F_y\left(1 - \frac{F_y}{4\sigma_e}\right) = F_y - \left(\frac{F_y^2}{4\pi^2 E}\right)\left(\frac{KL}{r}\right)^2 \quad \textbf{(2.8)}$$

Where F_y is the minimum yield stress. Figure 2.1 shows that the value of $\sqrt{2\pi^2 E/F_y}$ is the limiting KL/r ratio corresponding to a stress equal to $F_y/2$. Elastic buckling governs when this ratio is greater than limiting ratio. Inelastic buckling governs when this ratio is smaller than limiting ratio.

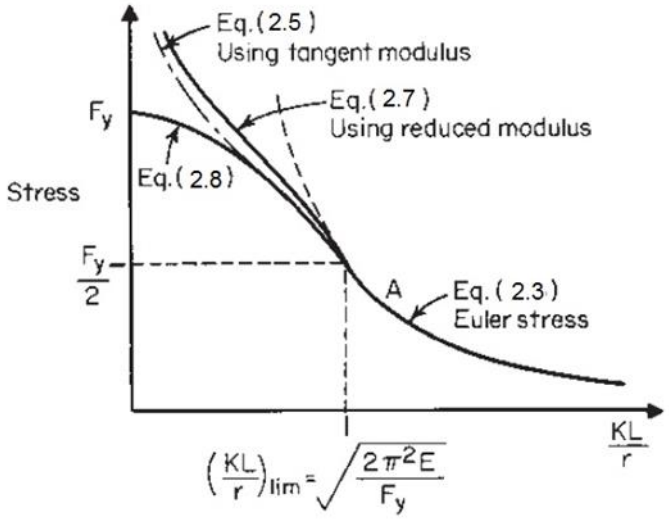

Figure 2.1 : Flexural column buckling stress [1].

These basic equations have changed during years due to lots of investigations and tests. Finally, AISI Specification states that the design equations calculating the nominal inelastic and elastic flexural buckling stresses are calculated as follows:

$$(F_n)_I = \left(0.658^{\lambda_c^2}\right)F_y \quad \text{when } \lambda_c \leq 1.5 \qquad \textbf{(2.9)}$$

$$(F_n)_e = \left[\frac{0.877}{\lambda_c^2}\right]F_y \qquad \text{when } \lambda_c > 1.5 \qquad \textbf{(2.10)}$$

Where $(F_n)_I$ is the nominal inelastic buckling stress, $(F_n)_e$ is the nominal elastic buckling stress, $\lambda_c = \sqrt{F_y/\sigma_e}$ is the column slenderness parameter, σ_e is the theoretical elastic buckling stress of the column which can be calculated by Eq. **(2.3)**.

2.1.2.2 Torsional buckling and flexural-torsional buckling

Due to their large torsional rigidity, closed sections are not always vulnerable for torsional buckling. However, for open thin-walled members, three main buckling modes should be considered during the analysis. These are flexural, torsional and

flexural-torsional buckling modes. As a definition of open-section columns in flexural-torsional buckling mode, bending and twisting occur simultaneously. The first investigations known on this problem were made by Goodier, Timoshenko and Bleich [23-25]. Further studies conducted by George Winter and Alexander Chajes in [18] and the same authors with Pen Jeng Fang in [19]. These further studies formed a basis for the development of the AISI design criteria. In Figures 2.2 and 2.3 , flexural-torsional buckling examples on different sections are given.

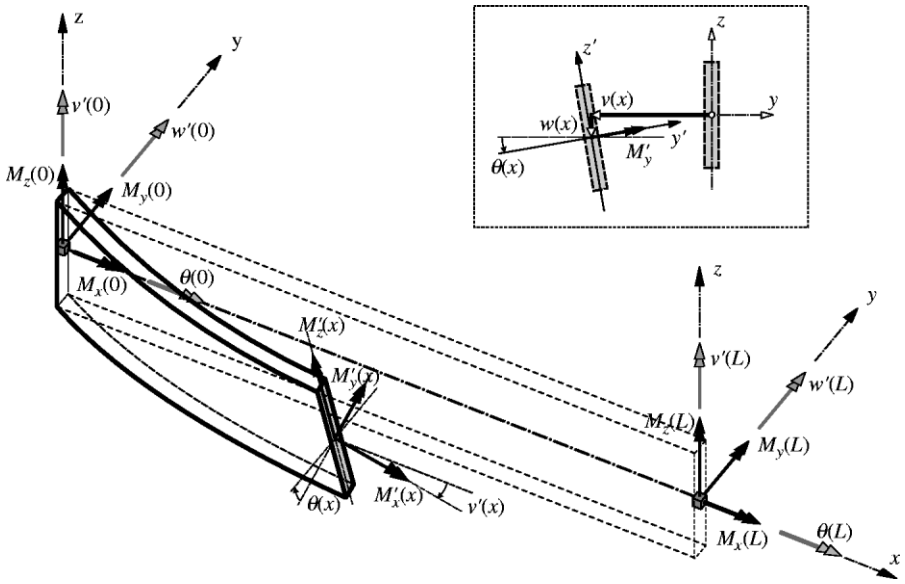

Figure 2.2 : An exaggerated flexural-torsional column buckling example [26].

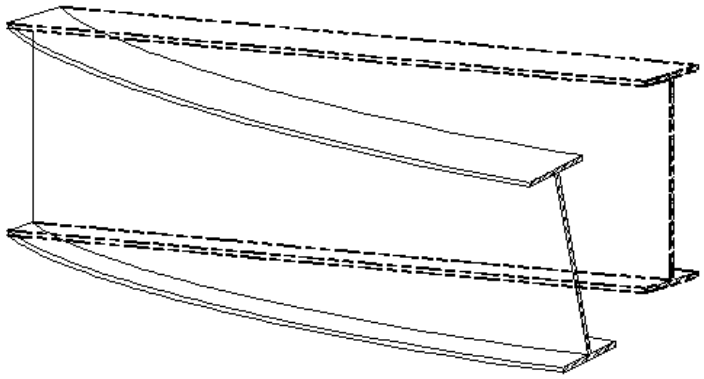

Figure 2.3 : Flexural-torsional column buckling of an I section [27].

Besides the calculation of the critical stress for flexural buckling discussed in previous section, torsional buckling stress can ben calculated by the following equation;

$$\sigma_t = \frac{1}{Ar_0^2}\left[GJ + \frac{\pi^2 EC_W}{(K_t L_t)^2}\right] \quad \textbf{(2.11)}$$

Where A is the area of the section, r_0 is the polar radius of gyration of cross section about shear center, G is the shear modulus, J is St. Venant torsion constant of cross section, E is the modulus of elasticity, C_w is the warping constant of torsion of cross section, K_t is effective length factor for torsion and L_t is unbraced length of compression member for torsion. GJ describes the torsional rigidity and also EC_w describes the warping rigidity.

For the doubly symmetric sections like I sections, H sections etc. the shear center coincides with the centroid of the section. Usually column fails with pure bending or pure torsion. So, formulas given above can be used to calculate the desired stresses. However, mostly in singly-symmetric sections like C sections, hat sections etc., flexural-torsional buckling possibility is higher than pure failure modes.

Elastic Flexural-Torsional buckling stress can be calculated by the following equation;

$$\sigma_{TFO} = \frac{1}{2\beta}\left[(\sigma_{ex} + \sigma_t) - \sqrt{(\sigma_{ex} + \sigma_t)^2 - 4\beta\sigma_{ex}\sigma_t}\right] \quad \textbf{(2.12)}$$

Where; $\sigma_{ex} = \frac{P_x}{A}$ and $\sigma_t = \frac{P_z}{A}$

P_x is the Euler flexural buckling load about x axis and P_z is the torsional buckling load about z axis. Equations **(2.13)** and **(2.14)** are about the calculation of P_x and P_z.

$$P_x = \frac{\pi^2 EI_x}{(K_x L_x)^2} \quad \textbf{(2.13)}$$

$$P_z = \left[\frac{\pi^2 EC_W}{(K_t L_t)^2} + GJ\right]\left(\frac{1}{r_0^2}\right) \quad \textbf{(2.14)}$$

In case of inelastic flexural-torsional buckling, following formula is used for calculating inelastic flexural-torsional buckling stress:

$$\sigma_{TFT} = F_y\left(1 - \frac{F_y}{4\sigma_{TFO}}\right) \quad \textbf{(2.15)}$$

Equations **(2.12)** and **(2.15)** are graphically plotted in Figure 2.4.

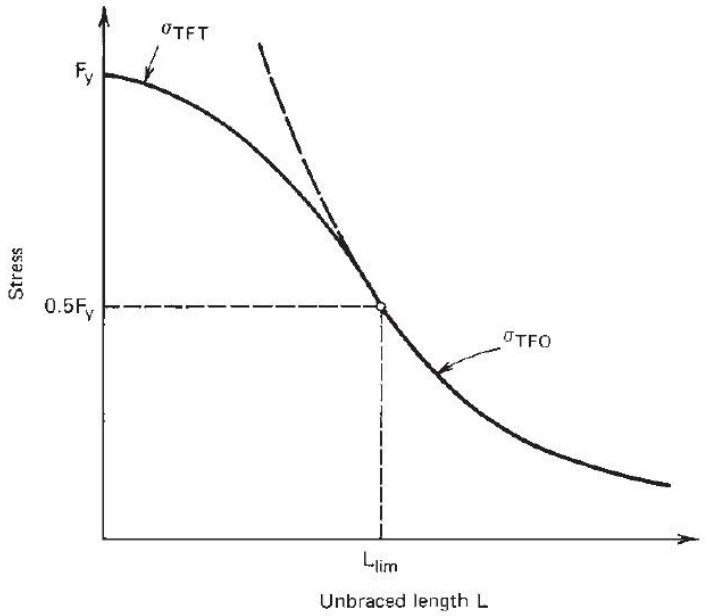

Figure 2.4 : Maximum stress for flexural-torsional buckling [1].

Eq. **(2.15)** has been used in AISI specificaion up to 1996, similar to the case for flexural column buckling. After 1996, the nominal inelastic flexural-torsional buckling stress was computed by equation **(2.9)** in which;

$$\lambda_c = \sqrt{F_y/\sigma_{TFO}} \qquad \textbf{(2.16)}$$

2.1.3 Local buckling

Local buckling of individual component plates usually occurs before the applied load passes the limit of the overall collapse load limit of the column in cold formed steel compression members. Local and global column buckling interaction is very important and may cause a reduction of the overall column strength. Following factors form a basis for the influence of local buckling on column strength;

- Slenderness ratio of column
- Cross section shape
- Governing global column buckling type (flexural, torsional or flexural-torsional)
- Steel material's mechanical properties and type

- Imperfections
- Welding
- Perforations
- Residual Stress
- Plane components' interaction
- Effect of cold work

Investigations on the interaction of local and global buckling on steel columns have been conducted by Amos Henry Chilver, V. Kalyanaraman, Teoman Peköz, Paulus Pieter Bijlaard, G. P. Fisher, Victor Gioncu and more during past 60 years [1].

Local buckling can be understood in more detail by determining the structural behaviour of plates. Because in general, cold formed steel column sections are formed with plates which are in interaction.

If a stiffened compression element's width / thickness ratio is relatively small, the strength of that element may be governed by yielding. If its width / thickness ratio is relatively large, it may be governed by local buckling at a stress level less than yield stress. In Figure 2.5, different local buckling modes of a box section are shown.

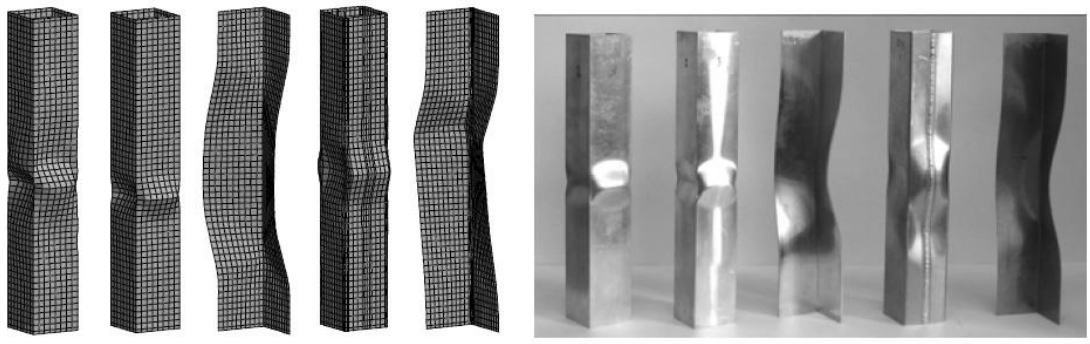

Figure 2.5 : Example of different local buckling modes [28].

If a simply supported square plate is subjected to a uniform compression stress in one direction, it will buckle in a single curvature in both directions as shown in Figure 2.7. The length of the element is usually much larger than the width for individual elements. Figure 2.6 shows the local buckling of stiffened compression flange of a hat-shaped section.

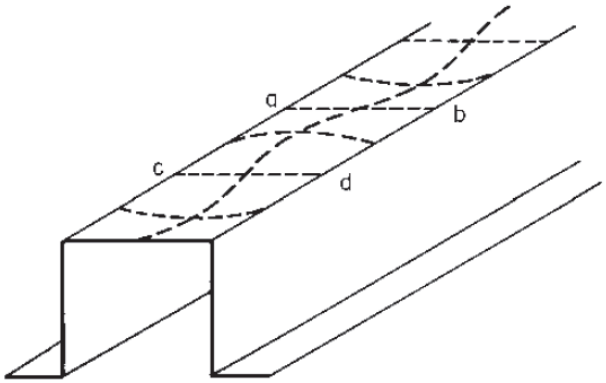

Figure 2.6 : Local buckling of stiffened compression flange of a hat-shaped section [17].

The critical buckling stress of a plate can be calculated by solving Bryan's differential equation based on small deflection theory. Figures 2.7 , 2.8 and Eq. **(2.17)** describe the situation of a plate subjected to compression stress.

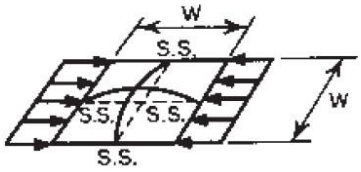

Figure 2.7 : Square plate subjected to compression stress [1].

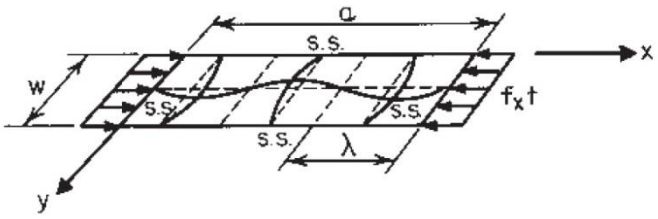

Figure 2.8 : Rectangular plate subjected to compression stress [1].

$$\frac{\partial^4 \omega}{\partial x^4} + 2\frac{\partial^4 \omega}{\partial x^2 \partial y^2} + \frac{\partial^4 \omega}{\partial y^4} + \frac{f_x t}{D}\frac{\partial^2 \omega}{\partial x^2} = 0 \qquad \textbf{(2.17)}$$

Where;

$$D = \frac{Et^3}{12(1-\mu^2)} \qquad \textbf{(2.18)}$$

E is the modulus of elasticity of steel, t is the thickness of plate, μ is the Poisson's ratio = 0.3 for steel, ω is the deflection of plate perpendicular to surface, f_x is the compression stress in x direction, λ is the halfwave length , a and w is the width of the plate, respectively and s.s. meaning the simply supported.

Solution of this differential equation represents a general equation for critical load buckling stress for a rectangular plate subjected to compression stress in one direction which is given in Eq. **(2.19)**.

$$f_{cr} = k\frac{\pi^2 E}{12(1-\mu^2)(\omega/t)^2} \qquad \textbf{(2.19)}$$

Investigations on k values conducted with George Gerrard and Herbert Becker in 1957 and given in [29]. Figure 2.9 shows the k values used in eq. **(2.19)** for different a/ω ratios where m is the numbers of half sine waves occur during local buckling and it can be assumed that length of the half sine waves, $\lambda = a/\omega = m$ for respectively for long plates.

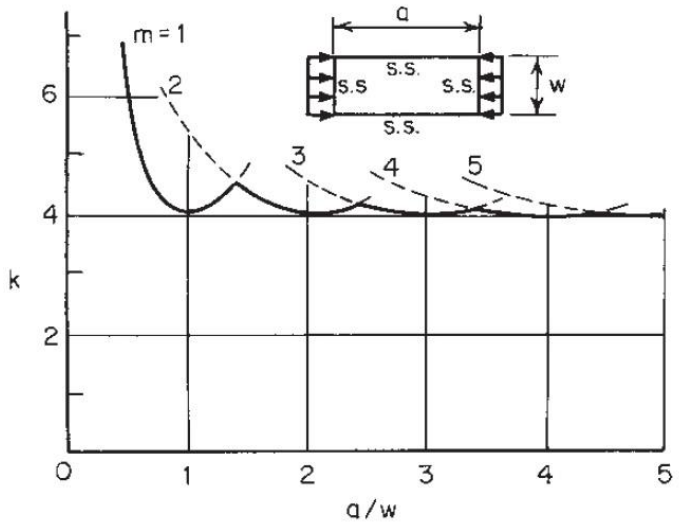

Figure 2.9 : Buckling coefficient for flat rectangular plates [29].

It should be notified that a/ω ratio is an integer the value of k equals 4. K can be taken as 4 for relatively large a/ω ratios. The values of k for a long rectangular plate subjected different types of stresses and within different kind of boundary conditions have been investigated with Stephen P. Timoshenko and Stephen M. Gere and given in [30]. Figure 2.10 shows the results of studies on values of k for determining critical buckling stress.

Case	Boundary Condition	Type of Stress	Value of k for Long Plate
(a)	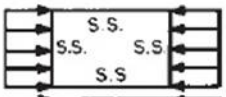	Compression	4.0
(b)	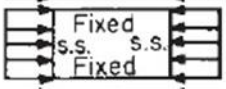	Compression	6.97
(c)	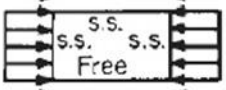	Compression	0.425
(d)		Compression	1.277
(e)	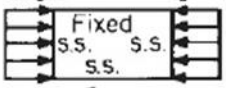	Compression	5.42
(f)	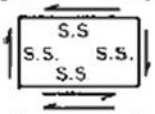	Shear	5.34
(g)	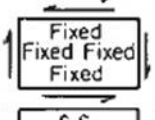	Shear	8.98
(h)	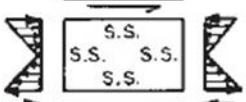	Bending	23.9
(i)	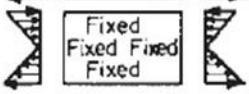	Bending	41.8

Figure 2.10 : Values of k for determining critical buckling stress [30].

For the analysis of the buckling plates in the inelastic range, equations used were modified by Bleich [25]. Basically, plate becomes an anisotropic plate which means different properties in different directions of plate when the compression stresss in only one direction exceeds the proportional limit of the steel. For this inelastic case, Friedrich Bleich proposed following differential equation, **(2.20)**, in [25].

$$\left(\tau\frac{\partial^4\omega}{\partial x^4}+2\sqrt{\tau}\frac{\partial^4\omega}{\partial x^2\,\partial y^2}+\frac{\partial^4\omega}{\partial y^4}\right)+\frac{f_x t}{D}\frac{\partial^2\omega}{\partial x^2}=0 \qquad \textbf{(2.20)}$$

Where $\tau = E_t/E$ and E_t is the tangent modulus of steel. After applying the modified boundary conditions and solving this differential equation, following critical buckling stress for plastic buckling of plate formula is obtained;

$$f_{cr}=\frac{k\pi^2 E\sqrt{\tau}}{12(1-\mu^2)(\omega/t)^2}=\frac{k\pi^2\sqrt{EE_t}}{12(1-\mu^2)(\omega/t)^2} \qquad \textbf{(2.21)}$$

The wavelength for a long plate can be obtained by $\lambda = \sqrt{\tau}\omega$

AISI specification used Q-factor method during the period from 1946 to 1986 for the effects of local buckling on column strength. This method developed by contributions of Winter and Fahy [17]. Q-factor method basically aims to assume a reduced stress in yield stress equation previously given in Eq. **(2.1)**. Because in cold-formed steel members, if w/t ratios of compressions are relatively large, local buckling may occur before yielding.

$$P = A(QF_y) \tag{2.22}$$

Where Q is a factor which weakens the yield strength and less than unity due to the effects of local buckling. This factor depends on the shape and form of the section.

Even though this method has been used for years, the recent stuides and developments have shown that this method needs improvement. With the contributions of DeWolf, Winter, Peköz, Kalyanaraman and Loh; test results and analytical studies have shown that for compression members having stiffened elements with large width/thickness ratios and for those members having slenderness ratios around 100, Q-factor method can give unconservative results [20]. Q factor method was really precise on especially I sections which have unstiffened flanges with small slenderness ratios. After 1986, Q-factor method has been eliminated in AISI specification and Effective Area approach has been accepted. This area basically focus on reducing the total cross-section area of cold formed steel compression members for the influence of local buckling in yielding equation calculating the nominal column load given in Eq. **(2.23)**.

$$P = A_e F_y \tag{2.23}$$

Where, the effective area of section is indicated by A_e. In case of effective area can not be calculated by generalized effective width calculations of AISI specification, it can be calculated by stub column tests which is described by Peköz in [20]. Kim Rasmussen and Gregory Hancock conducted studies on channel sections given in [31] and also Rasmussen conducted another study on unstiffened flanges given in [32] so that all of these studies guided building up the latest version of AISI Specification and North American Design Provisions. These provisions of AISI Specification on cold formed steel sections under uniform compression will also be

discussed in the "Codified Design of Cold-Formed Steel Columns" chapter in this thesis.

2.1.4 Distortional buckling

The distortional buckling mode involves the rotation of each flange and lip about the flange-web junction of cold-formed steel columns under compression stress. This mode is usually seen in open sections like Z and C channels as their geometry is suitable for this kind of failure. In Figure 2.11, distortional buckling of a C channel with stiffened lips is given.

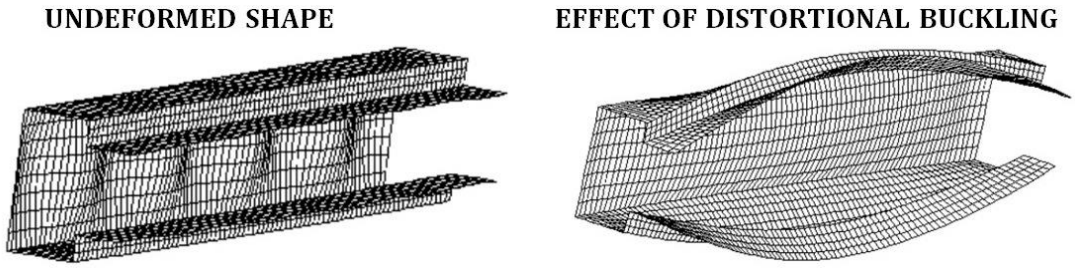

Figure 2.11 : Distortional buckling of a C channel with stiffened lips [33].

Distortional buckling is one of the important failure modes for open cross-sectional members having stiffened flanges which should be precisely considered in column design. Gregory Hancock have conducted many studies and research on distortional buckling mode. Figure 2.12 shows an example of rack section column buckling stress versus half wavelength for concentric compression from Hancock's investigations [34].

Many other researchers like Kwon, Schafer, Merrick, Tovar, Sputo, Camotim, Davies, Jiang and Silvestre have been made contributions on this specific buckling mode and all summerized in [34]. North American Specification included a new section 4.2, for determining the distortional buckling strength of open sections compression members like I, Z, C and hat shapes. In this thesis, distortional buckling stregth section of AISI Specification will also be discussed in the "Codified Design of Cold-Formed Steel Columns" chapter.

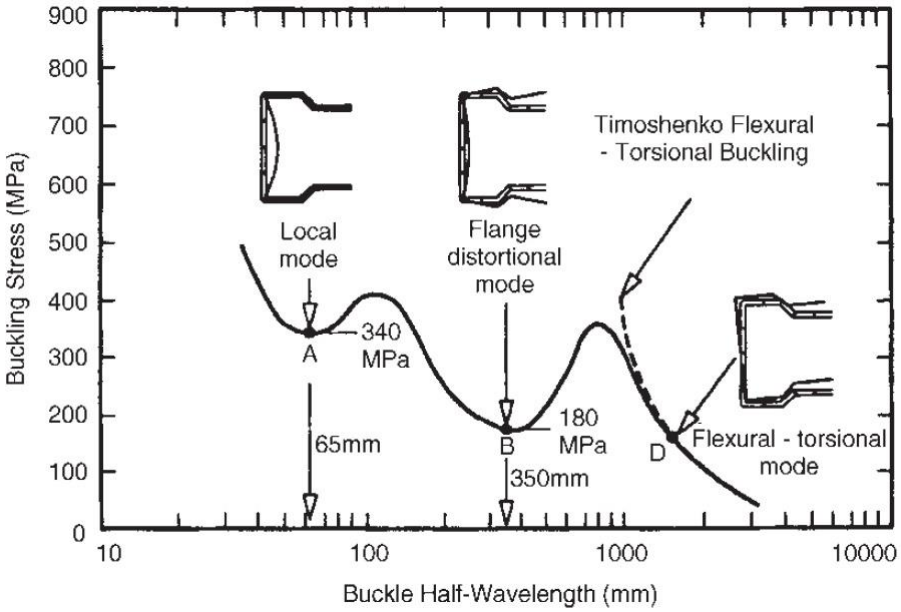

Figure 2.12 : Rack section column buckling stress versus half wavelength for concentric compression [34].

2.2 Studies on Direct Strength Method

The direct strength method has been adopted as an alternative design methodology in Appendix 1 of the North American Specification including the design of cold-formed steel structural members [16]. Practicaly, DSM (Direct Strength Method) brings a new perspective and a relatively different approach for calculating the nominal strength of cold formed steel structural sections. DSM needs numerical methods such as finite strip method and generalized beam theory in calculation of member elastic behavior primarily for accurate solution. Computer software "Cornell University Finite Strip Method, CUFSM" using finite strip method is programmed by Benjamin W. Schafer, Zhanjie Li and Sándor Ádány to explore elastic buckling behaviour and calculate the buckling stress buckling mode of arbitrarily shaped, simply supported, thin-walled members. Outputs of these calculations are used in DSM equations for prediction of nominal strengths of cold formed steel sections. Some important headlines related with DSM will be defined under this topic. Detailed information on AISI Specification about DSM will be described under "Codified Design of Cold-formed Steel Columns" chapter in this thesis.

Finite strip method

Finite Strip Method is a specialized finite element method used by CUFSM. Element shape functions use polynomials in the transverse direction. However, they use

trigonometric functions in the longitudinal direction. Judicious choice of the longitudinal shape function allows a single element which is called “strip” to be used. Finite strip method uses a single half sine wave (sin(πx/a)) for the longitudinal direction. In Figure 2.13, approach difference between an example sketch of finite element method and finite strip method is shown.

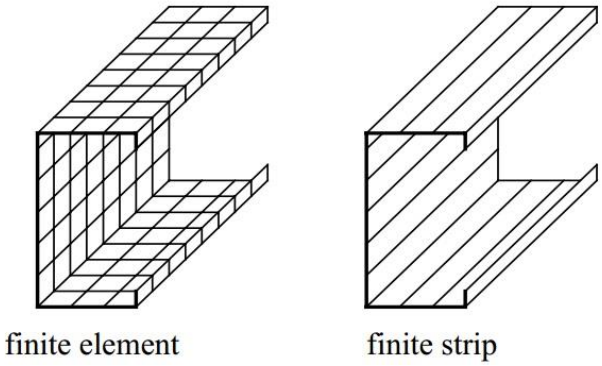

Figure 2.13 : Approach of finite element method and finite strip method [35].

Buckling curve

The buckling curve is a graphical representation showing a section’s elastic buckling behaviour and also the primary result from a finite strip analysis. A typical buckling curve is shown in Figure 2.14. The minima of curvatures on this curve indicate the critical halfwavelength and load factor for a given buckling mode.

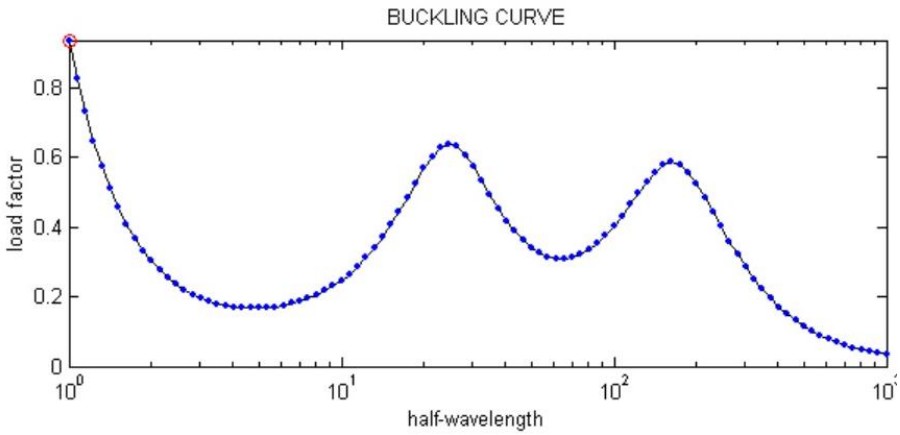

Figure 2.14 : An example of buckling curve [35].

Buckling mode

Basically, the buckling mode means the shape that a member buckles into. A buckling mode represents a secondary deformed shape that has the same potential energy as the primary deformation. As an example, local buckling mode shape of a Z section is given in Figure 2.15.

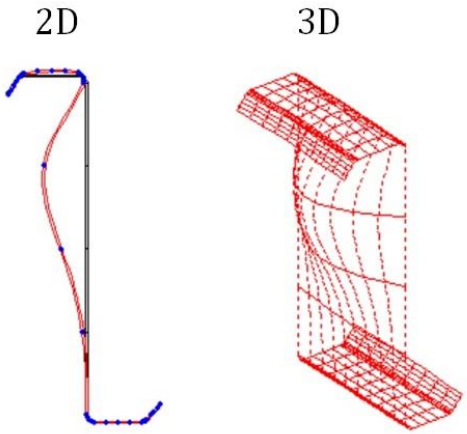

Figure 2.15 : Local buckling mode of a Z section [35].

Half-Wavelength

Half-Wavelength is 1/2 of the sine waves assumed during the finite strip analysis which is performed for systematically increasing halfwavelengths to determine the buckling behavior of a member.

Load factor

During the finite strip analysis, the member assumed to be loaded with a reference stress distribution. Buckling stress is found by multiplying the load factor with the reference stress distribution. In more detail, the load factor is the eigenvalue of the relevant eigenvalue buckling problem where the buckling mode is the eigenvector. Reference stresses are generally chosen as yield stresses during the analysis of cold formed steel members which are under compression.

There have been several studies on DSM which will also be summarized under this chapter.

Design of Cold Formed Steel Channel Columns with Complex Edge Stiffeners by Direct Strength Method;
Ben Young, Jintang Yan (2004)

Mainly, this paper focuses on the comparisons between the failure modes observed in the tests with the failure modes predicted by the direct strength method [36]. The test program and results are taken from a previous study of Ben Young and Jintang Yan [37], has a total of 30 column specimens were tested. Comparison of test strengths with design strength for a serie of specimens shown in Figure 2.16. Design Strengths have been found by DSM (Direct Strength Method), The Australian/New Zealand Standard (AS/NZS) and North American Standart (NAS).

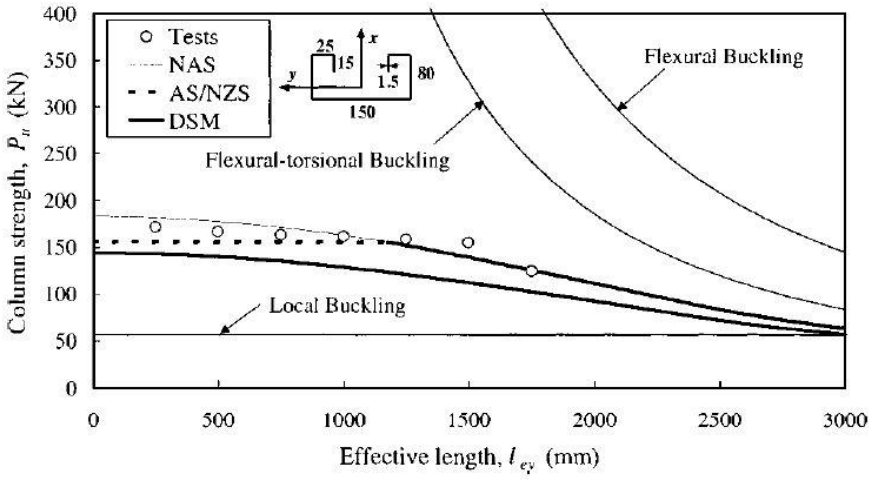

Figure 2.16 : Comparison of test strengths with design strengths [36].

The test specimens were tested between fixed end supports. It is shown that in the prediction of column strengths of the fixed-ended cold-formed steel channels with complex edge stiffeners having slender flanges, accurate results are achieved by using the direct strength method. For sections having less slender flanges, direct strength method conversatively predicts the column strengths. As another point shown in this paper is for the failure modes. For the tests of long columns, the failure modes predicted by direct strength method are generally in parallel with the failure modes observed in the tests. However, for short columns and intermediate columns, this agreement of predictions is not valid.

Direct Strength Design of Hot Rolled and Cold-Formed Steel Compression Members;
Gregory J Hancock, Daniel O Cook, Robert E. Moisy and Andy Yen (2005)

This paper focuses on the analysis of hot rolled sections like I-sections, square hollow sections and fabricated sections with Direct Strength method due to put its simplicity forward than Effective Width Method [38]. Paper begins with a computation that shows the analysis results of an opened channel section under compression given in Figure 2.17. Finite Strip Buckling Analysis given in Figure 2.17, conducted by Papangelis and Hancock in 1995 [39].

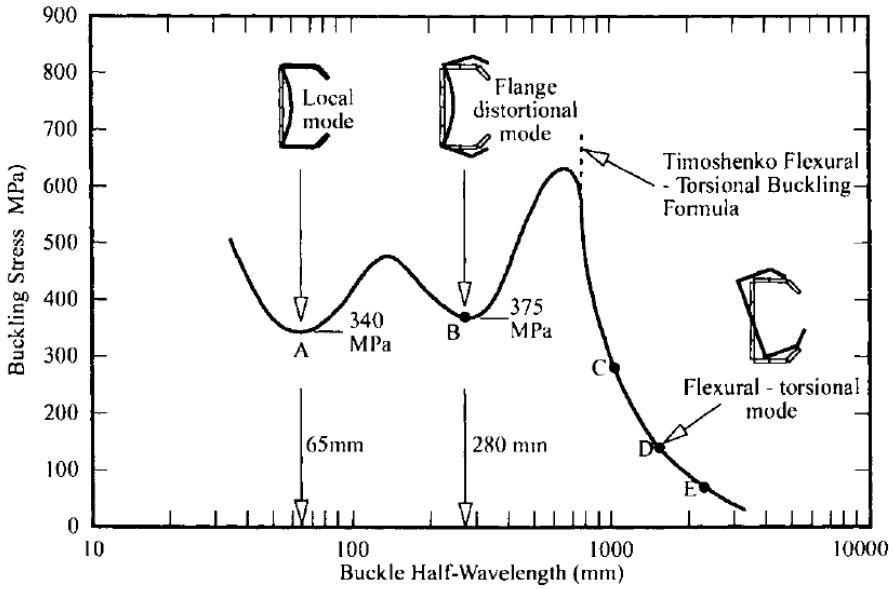

Figure 2.17 : Buckling stress versus half-wavelength for a C-Section in compression [39].

Figure 2.17 clearly shows the the three basic buckling modes for design of thin-walled C-section used under compression which are the local, distortional and overall modes. Paper indicates that these three modes are characteristic of thin-walled open-section members in compression or bending. Than, studies on hot rolled sections, welded series and unlipped channel sections have been conducted. In conclusion; the DSM was found to give better design accuracy than the Effective Width Method (EWM) in all cases except for the very slender unlipped channel section. The local buckling stress was much lower than the yield stress and the effective centroid of the locally buckled section moved creating a premature failure compared with the DSM in the case of the very slender unlipped channel. DSM design is suggested for all other sections investigated except this type of sections.

Buckling Analysis of Cold-formed Steel Members Using CUFSM: Conventional and Constrained Finite Strip Methods;
B.W. Schafer & S. Ádány (2006)

This paper provide technical background and examples for stability analysis of cold-formed steel members using the conventional and constrained finite strip methods [40]. CUFSM software uses finite strip method. Conventional Finite Strip Method is used to examine all the possible instabilities in a cold-formed steel member under longitudinal stresses like axial, bending, or combinations). The constratinted finite strip method provides stability solutions to be focused only a given buckling mode

(modal decomposition). Modal decomposition is completed by forming a series of constraint equations that describe a particular buckling class. For exploring cross-section stability in cold-formed steel members, the conventional finite strip method combined with the constrained finite strip method provide a powerful tool. Elastic and geometric stiffness matrices are formed from a summation of cross-section strips and employed in an eigenvalue stability analysis in the conventional finite strip method. In this paper the stiffness matrices are explicitly derived and can readily be used in the software. The provided solution is identical to that employed in the CUFSM software. The strength of this new extension to finite strip solutions is the ability to decompose and identify conventional finite strip solutions as related to buckling classes of interest like global, distortional, or local buckling. The potential use of the constrained finite strip method is shown in this paper with the examples provided, and the algorithms discussed are implemented in CUFSM [40].

Review: The Direct Strength Method of Cold-Formed Steel Member Design; Benjamin W. Schafer (2008)

This paper of Benjamin W. Schafer summarizes general remarks of DSM studies and developments [41]. Especially, DSM for columns development part of this paper will be described due to the relation with this thesis. The beginning of the Direct Strength Method for columns most clearly be traced to research into distortional buckling of rack postsections at the University of Sydney. Lau S. C. W. and Hancock G. J. conducted studies on columns published in distortional buckling formulas for channel columns [42]. Also, Kwon and Hancock conducted Strength tests of cold-formed channel sections undergoing local and distortional buckling and published their studies in Journal of Structural Engineering [43]. Hancock et al. collected the research and demonstrated that for a large variety of cross-sections the measured compressive strength in a distortional failure correlated well with the slenderness in the elastic distortional mode. Hancock attributes his methodology to Trahair's work on the strength prediction of columns undergoing flexural–torsional buckling [44]. As a final regard, it seems clear that the Direct Strength Method is not a new idea, but rather the extension of an old one to new instability limit states. Development of the Direct Strength Method beyond distortional buckling was completed using a much wider set of cold-formed steel cross-sections and tests that included failures in local, distortional, and global flexural or flexural–torsional modes in the papers by Schafer [45-46]. Hand solutions and numerical (finite strip) solutions for the elastic

buckling of 187 columns were gathered in these papers. Also lots of test has been conducted and graphically compared with the Direct Strength Method predictor curves given in Figure 2.18.

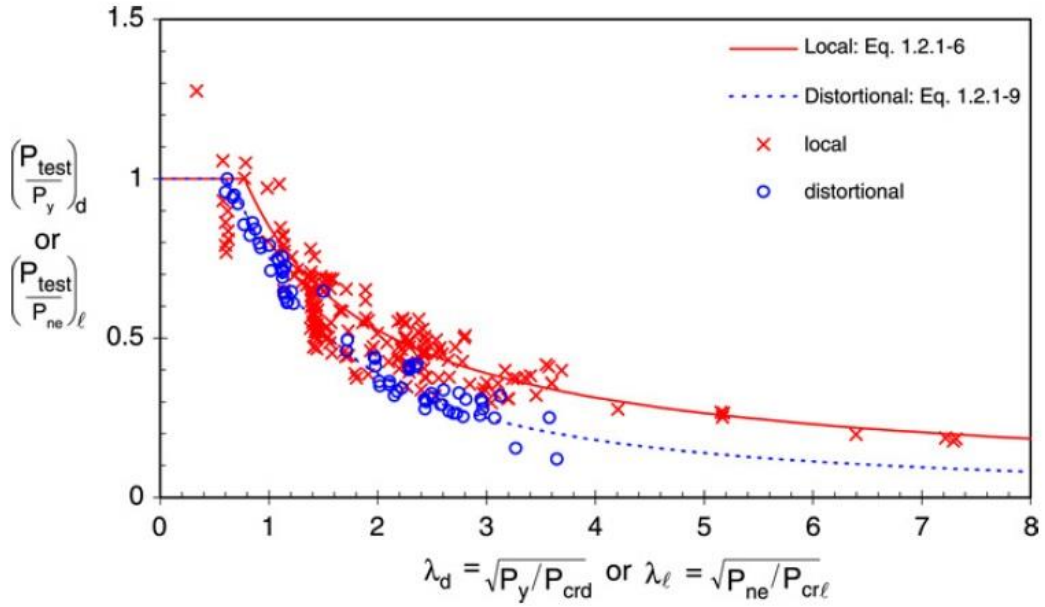

Figure 2.18 : Comparison of the direct strength method predictor curves with test data for columns (equation numbers refer to those used in the North American Specification) [41].

This figure indicates that DSM is a reasonable predictor of strength over a wide range of slenderness. Interaction of the buckling modes were systematically studied for local–global, distortional–global, and local–distortional buckling of the columns. Based on overall test-to-predicted ratios, and when available the failure modes noted by the researchers in their testing, it was concluded that local–global interaction should be included, but not distortional–global, or local–distortional interaction. As a result, it was recommended to only include local–global interaction in the Direct Strength Method. Recent work by Hancock, Camotim, Yang and Silvestre is focused on the investigations for the effect of local-distortional interactions [47-48]. Work is ongoing to determine the most appropriate way to identify and predict the strength for the small number of columns that do have potential local–distortional interaction. In conclusion, Direct Strength Method is on path to be a completely viable alterative design procedure for cold-formed steel member design according to many research groups' efforts around the world [41].

Evaluation of Direct Strength Method for CFS Compression Members without Stiffeners;
M. V. Anil Kumar, V. Kalyanaraman (2010)

This paper includes the results of a study on the suitability of Direct Strength Method to evaluate the compressive strength of plain channel, I and rectangular tubular members [49]. For calculating the strength of compression members such as tubular, plain channel, and I-sections consisting stiffened and unstiffened elements, without either lip stiffener or intermediate stiffener it is known that the Direct Strength Method has not been adequately evaluated. These members do not have edge or intermediate stiffeners. Hence, these sections are not vulnerable to distortional/stiffener buckling and experience interaction of only local and overall buckling before failure. Authors used the test results data from following studies previously conducted: Test results on fixed plain channel compression members [50-52, 20], hinged ended rectangular tubular members [53-55], hinged ended I-Sections [56]. Calculations have been made via Effective Width Method with CUFSM and Direct Strength Method. The graphs in Figure 2.19 shows the comparison of design methods with test results for Plain Channel Sections (PCS), I-Sections (IS), and Rectangular Hollow Sections (RHS).

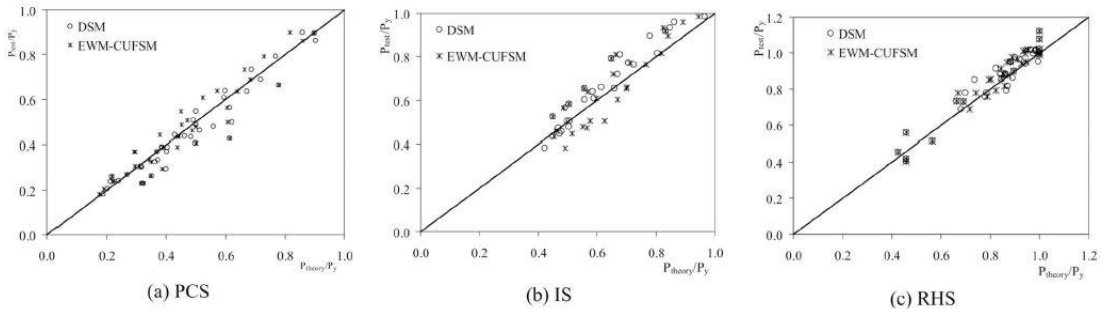

Figure 2.19 : Comparison design methods with test results [49].

In conlusion, authors observed the applicability of Direct Strength Method on sections mentioned above. DSM estimates the strength of these compression members within acceptable accuracy, for practical purposes according to the comparative study with test results and EWM-CUFSM results.

On the Direct Strength Method (DSM) Design of Cold-formed Steel Columns Against Distortional Failure;
A. Landesmann, D. Camotim (2013)

This study includes many numerical investigations have been made to determine the influence of the cross-section geometry and end support conditions on the post-

buckling behaviour and Direct Strength Method (DSM) design of cold-formed steel columns buckling and failing in distortional modes [57]. ANSYS computer software has been used for elastic and elastic-plastic shell finite element analysis of the columns which are analyzed exhibit, four end support conditions (fixed, pinned-pinned, pinned and fixed-free end supports) , different cross-section shapes, dimensions and lengths and several yield stresses. During the investigations, studies are carefully conducted to ensure that all the columns selected have been failed in "pure" distortional buckling mode cover a wide distortional slenderness range. From the performance of a parametric study involving 648 columns the ultimate strength data acquired and then used to show that, the current DSM distortional design curve is only able to predict adequately the ultimate loads of fixed columns, regardless of the column geometry. This design curve was shown to clearly over estimate the numerical ultimate loads in the moderate-to-high slenderness range for the columns with the remaining end support conditions (pinned-fixed, pinned and fixed-free). Fig.2.20 shows a comparison between these studies and current DSM distortional curve where P_u is ultimate load, P_y is column squash load, P_{crd} is critical distortional buckling load and $\lambda_D = \left(P_y/P_{crd}\right)^{0.5}$ is the distortional slenderness.

As shown in the Figure 2.20, analyzes other than fixed end condition points a modification on current DSM distortional curve which may be an alternative and shown in Figure 2.21.

These studies show that the proposed preliminary DSM-based distortional strength curves require further validation, in order to assess their reliability and universality to find out whether they remain valid for any column cross-section shape.

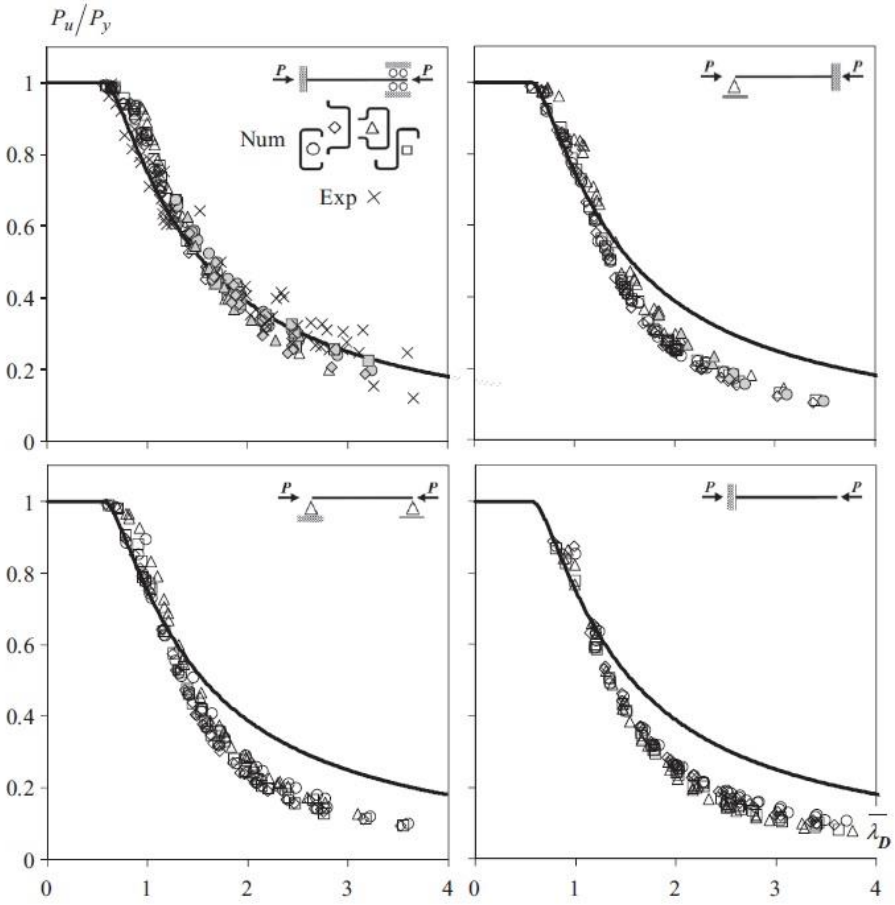

Figure 2.20 : Comparison between the current DSM distortional curve and column ultimate loads with different end conditions [57].

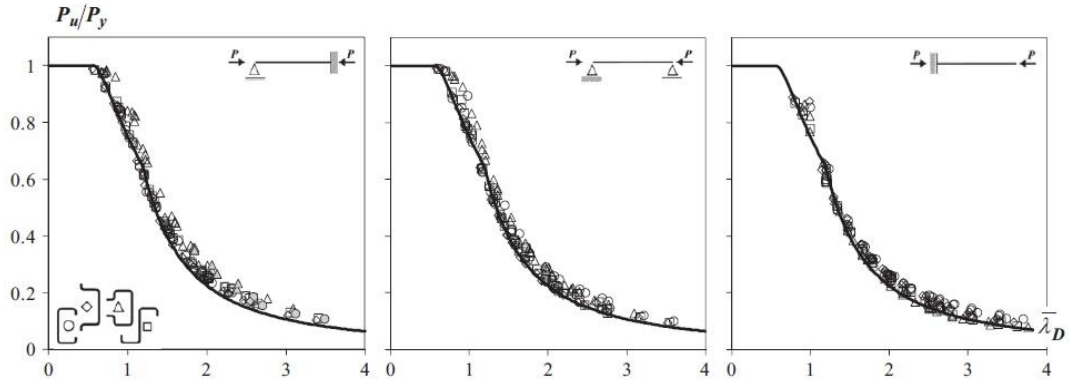

Figure 2.21 : Comparison between the modified DSM distortional curve and column ultimate loads with different end conditions [57].

2.3 Studies on Perforated Cold Formed Steel Storage Rack Columns

There have been many studies on this specific topic of cold formed steel columns. Rack columns are a specific version of CFS columns having perforations which have

different shapes and sizes. Placement of these holes vary depending on configuration of beams, rack type and purpose of usage.

Analysis of Steel Storage Rack Columns,
A.M.S Freitas, M.S.R. Freitas, F.T. Souza (2005)

In this article, authors used experimental and numerical methods to quantify the influence of the perforations on the load capacity of the steel storage rack columns [12]. Finite element analysis has been done on the column types that tested before by using "ANSYS" software and comparisons have been made. Shell, solid and contact finite elements were used to represent the stub column analyzed in the model. 4 specimens tested by "stub column test" and ultimate compressive strengths of these specimens were evaluated. Different cross-sectional areas have been used for the numerical simulation of perforation influence in the load capacity. Four different area-types are used which can be described as;

Nominal column: Actual cross section of the column, considering the perforations with nominal dimensions.

Actual column: Actual cross section of the column, considering the perforations with actual dimensions.

Gross column: Full cross section of the column, without perforations with nominal dimensions.

Net column: Cross section of the column without perforations considering the area as the minimum net area of the column.

Nominal and experimental steel properties used during the numerical analysis. Comparisons have been made with numerical results, experimental output and the RMI prescriptions values using experimental results (P_{ua} - ultimate axial load of experimental results) to yielding stress (P_{RMI}) and using nominal values to yielding stress (P_{RMI-n}). Result graphs are given in Figures 2.22 and 2.23

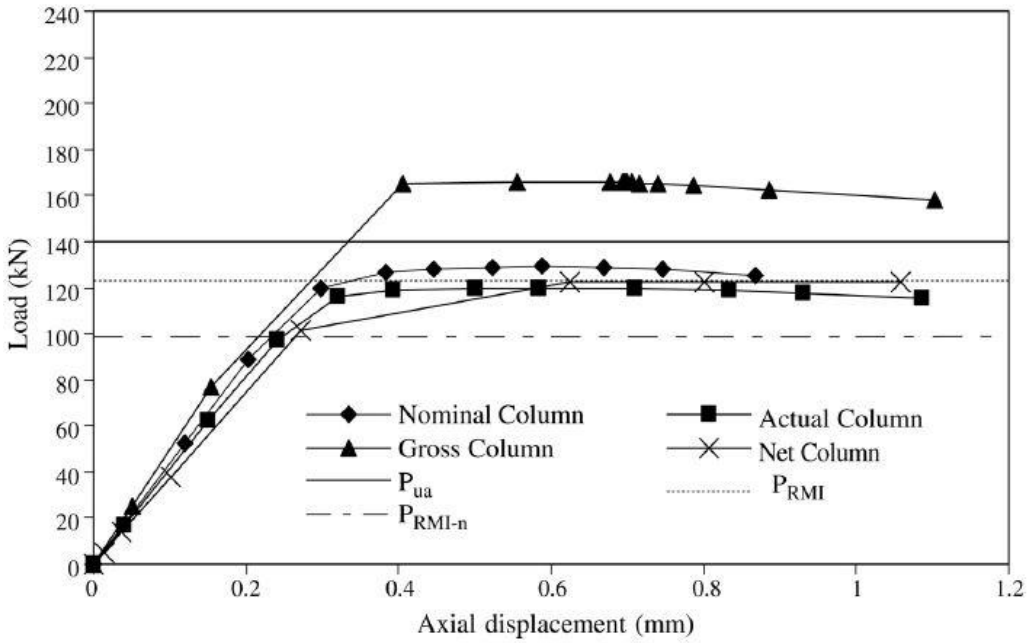

Figure 2.22 : Load versus displacement curves for f_y = 250 MPa [12].

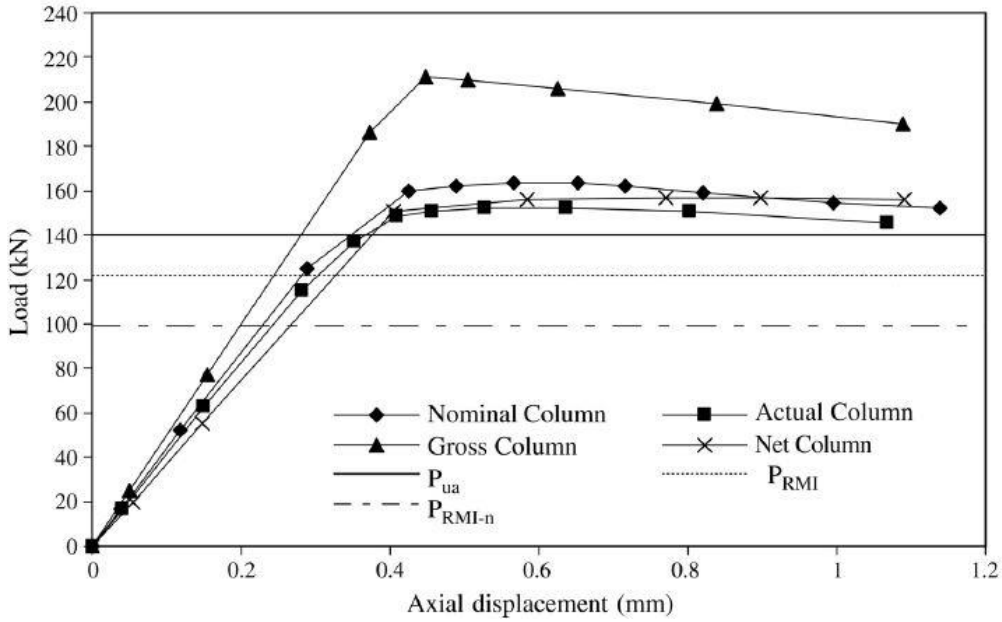

Figure 2.23 : Load versus displacement curves for f_y = 320.23 MPa [12].

The authors have mentioned that the representative curves of the nominal, net and actual columns indicate similar values to experimental data, varying from 8% to 17% from the average experimental ultimate loads. Actual column and net column indicated good agreement with experimental results when nominal yielding stress is used in finite element analysis of the nominal column. Another observation have been made on the failure mode. When measured imperfections are not included, the

collapse mode was caused by the perforations of the cross section in the middle height of the column in region of minimum area. When measured imperfections are included, similar collapse mode like in the experimental test have been observed showing the strong influence of imperfections on stub columns.

Stub Column Tests for Racking Design: Experimental Testing, FE Analysis and EC3;
F. Roure, M. M. Pastor, M. Casafont, M. R. Somalo (2010)

This research has been conducted in the Laboratory of Elasticity and Strength of Materials , in the School of Engineering of Barcelona [58]. Twenty pallet rack column specimens have been tested aiming to evaluate alternative methods for testing as a design option. An analytical and numerical method have been followed to compare the results with the ones gained from experimental tests. Analytical method have been followed by applying the European Standard EN 1993-1-3 involvilng the effective width determination for each part of the section subject to compression [59]. The numerical method have been followed by applying finite element analysis, including non-linear material and geometrical behaviour. The test specimens were formed with a piece of an upright, whose length was more than three times greater than the longest dimension of the upright section, and more than five times the distance between perforations. As an example, experimental collapsed specimens and deformed shapes from finite element analysis have been given in Figure 2.24.

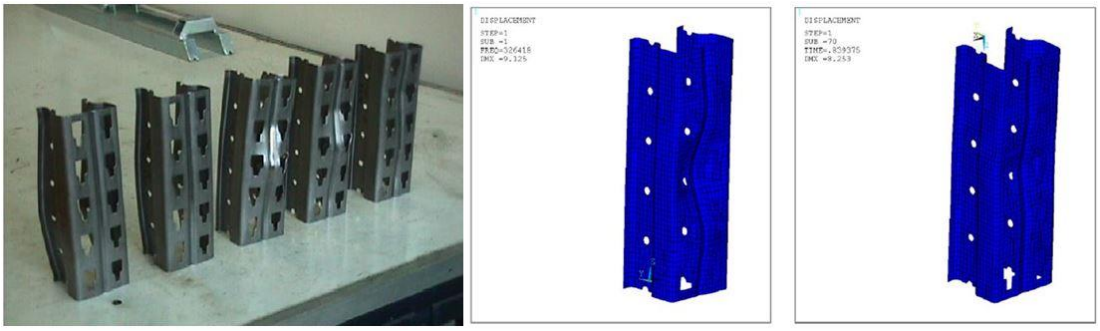

Figure 2.24 : Experimental collapsed specimens and deformed shapes from FE analysis [58].

After experimental, numerical and analytical testing a comparison have been made between the effective areas and effective centre of gravities. Results of these comparisons are also shown in Figure 2.25.

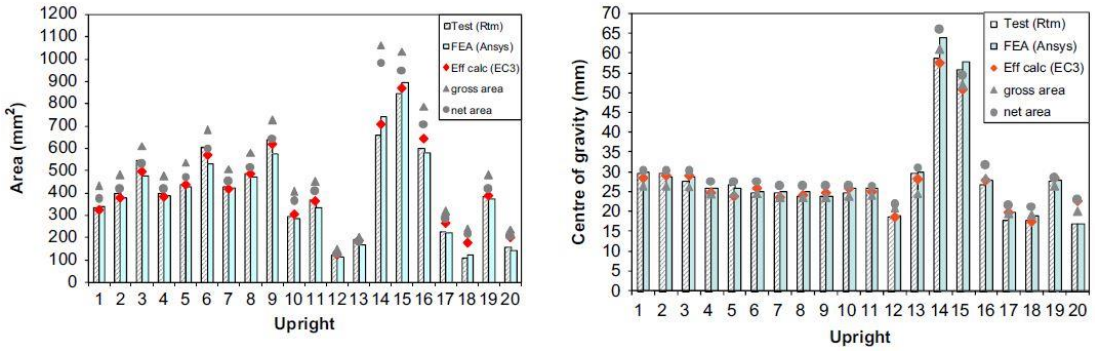

Figure 2.25 : Effective area and centre of gravity comparisons [58].

In conclusion, two methods are suitable determining the effective area and centre of gravity with some precautions. When working with the effective net area and effective net centre of gravity, the analytical method used with Euro Code 3 gives good results [59]. Finite Element Analysis also gives good results when the following precautions are considered. The model must reproduce the upright faithfully and the increments in displacement must be small, and also the force-displacement curve must show that the point of the maximum force is clearly reached. Authors elaborate that at the present time, none of the methods can completely replace experimental testing. Factors such as actual boundary conditions, geometric imperfections, or residual stresses, for instance, are not usually totally known; therefore physical testing is necessary. However, the analytical and the simulation by finite element methods come rather close to the experimental results which is confirmed by these investigations. Finite Element Analysis seems like most advantageous method in the design and optimization phase. Using Finite Element Analysis can cause a decrease in number of tests mandatory in Euro Code by reproducing most of the factors involved in the problems [58].

An Experimental Investigation of Distortional Buckling of Steel Storage Rack Columns;
Miquel Casafont, Maria Magdalena, Francesc Roure, Teoman Peköz (2011)

This study includes experimental investigation of steel storage columns under compression for distortional buckling failure mode [60]. The study mainly focused in moderately long specimens which are longer than the stub columns used for the determination of the local buckling strength and short enough to avoid the effects of global buckling. The objective of the study is to formulate experimental and analytical approaches to the design of industrial rack columns against distortional buckling. Four different type of rack cross-sections having medium load carrying

capacity produced by European manufacturers are used in analysis and testing. These investigations made possible to study failure modes combining distortional buckling and global buckling. Determination of distortional buckling strength from test results have been gathered using a modification to Rack Manufacturers Institute (RMI) specification, European Code and Direct Strength Method. Better results are obtained if the interaction between distortional buckling and global modes is considered when the strength of a member is determined from experimental tests according to the American RMI specification. Another point is coming from the results; if this interaction is not considered, the strength overestimation can be up to about 15% for the cross-sections analyzed. Another keypoint from paper is an evaluation has been done for Direct Strenght Method calculations for distortional buckling. The method includes two important changes for the effect of perforations; usage of the net are of cross-section and Finite Element Analysis for calculation of determining elastic buckling loads. The calculated results are in good agreement with experimental results and showed that DSM equations provide interaction between distortional buckling and global modes. This paper also forms a start for ongoing and new studies like the Research on the behavior of upright frames aimed at checking whether the experimental tests on individual columns are useful for assessing the strength of complete frames.

Design of Steel Storage Rack Columns via the Direct Strength Method; Miquel Casafont, Maria Magdalena Pastor, Francesc Roure, Jorde Bonada, Teoman Peköz (2013)

This paper presents an attempt for prediction of the load carrying capacity of perforated rack columns by the direct strength method [61]. Investigations are focused on the prediction of the elastic buckling loads of members with multiple perforations and the accuracy of the current DSM buckling curves on rack columns. Currently there is no calculation procedure is adopted by the main design codes of rack structures in Eurocode. Design is simply based on expreimental physical tests. Non-linear finite element analysis is most probably the best alternative to experimental approach. Reduced Thickness formulas given below form another alternative for the effect of perforations on calculating strength of a cold formed column. Casafont et al. found these formulas in 2012 [62]. Reduced Thickness can be used in DSM or EWM calculations instead of thickness for the effect of perforations on Rack Columns.

Reduced Thickness for local buckling;

$$t_{rL} = 0.61t\frac{L_{np}B_{np}}{LH} + 0.18t\frac{B_p}{L_p} + 0.11 \quad \textbf{(2.24)}$$

Reduced Thickness for distortional buckling;

$$\mathrm{t_{rD}} = 0.9\mathrm{t}\left(\frac{\mathrm{L_{np}}}{\mathrm{L}}\right)^{1/3} \quad \textbf{(2.25)}$$

Reduced Thickness for torsional-flexural buckling;

$$\mathrm{t_{rG}} = 0.7\mathrm{t}\left(\frac{\mathrm{L_{np}}}{\mathrm{L}}\right) \quad \textbf{(2.26)}$$

Where the terms are the geometric parameters on a rack column given in Figure 2.26.

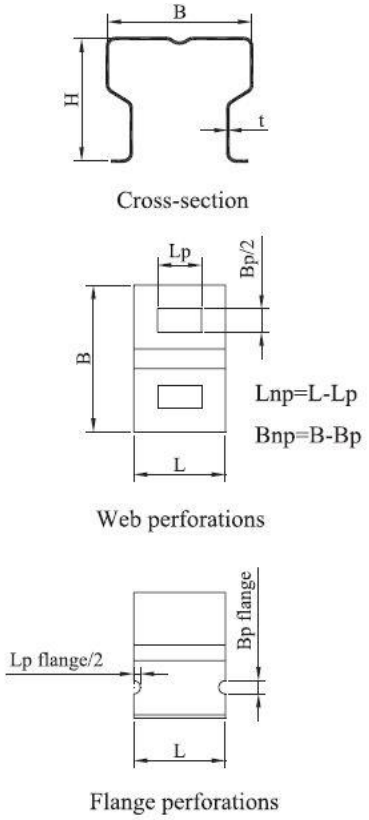

Figure 2.26 : Main geometric parameters of the column [61].

Five different rack column types have been used in this study. Elastic buckling load have been calculated via Finite Strip Method. For the results, the performance of the distortional buckling and global buckling reduced thickness equations are correct. Concerning the global buckling loads of columns with large flange holes, some small

problems have only arisen. For the accuracy of DSM, authors have tried different methods and parameters like minimum net area, Finite Element Analysis and CUFSM for comparison. In determining elastic buckling loads using Finite Element Method, the results were not good if the failure is governed by local buckling. Predictions were accurate on the columns have failed in the modes of distortional buckling and torsional-flexural buckling. In determining elastic buckling loads using CUFSM, the results are quite parallel and even better for those cross sections with large web stiffeners.

3. CODIFIED DESIGN OF COLD FORMED STEEL COLUMNS UNDER PURE COMPRESSION

The present study is based on the design rules given in American Iron and Steel Institute S100-2007 standart [16]. The same standart is also called as "North American Specification for the Design of Cold-Formed Steel Structural Members". This chapter consists of an overview of this standart on Concentrically loaded compression CFS members. Approaches with Effective Width Method and Direct Strength Method are discussed by example solutions.

3.1 Review of American Iron and Steel Institute S100-2007 Standart

Section-C of American Iron and Steel Institute S100-2007 (AISI S100-2007) Standart describes the limitations and calculations for Members of Cold-Formed Structural Steel family[16]. C4-Concentrically Loaded Compression Members part is related with the scope of this thesis. Allowable Stress Design (ASD) and Load and Resistance Factor Design (LRFD) considerations and methods are also two different approaches proposed for the design of these members which are described in the standart. In this thesis, nominal column capacities are considered instead of design strength. There are two main methods to calculate ultimate capacity of the concentrically loaded compression members which are Effective Width Method and Direct Strength Method. The standart and its main sections describe the limitations and calculations for traditional method (EWM). In Appendix 1, the standart describes DSM method and its provisions. Members and Column Design part in Appendix 1 is an alternative approach for traditional method.

3.1.1. Effective width method for concentric axially loaded compression members

Studies have shown that cross-section of a thin walled steel member may not be fully effective under compression. Basically, some parts of the cross-section resists the load instead 100% of the member cross-sectional area. The reduced area is used

during the calculation of maximum strength of the section which is also called Effective Area; can be calculated by multiplying the thickness of the member with the Effective Width. The standart aims to calculate the available axial strength which shall be smaller of the values obtained from section C4. For usage of the effective widths in the calculations; standart also describes the calculation of effective widths of elements under B Section.

3.1.1.1 The nominal axial strength calculations

The nominal axial strength which is also called compressive resistance of a compression member, P_n , can be calculated in accordance with C4.1 section of related standart.

$$P_n = A_e F_n \tag{3.1}$$

Where A_e is the effective area calculated at stress F_n. Effective area shall be calculated in accordance with section B of the related standart. F_n shall be calculated as follows depending on slenderness factor, λ_c:

For $\lambda_c \leq 1.5$;

$$F_n = \left(0.658^{\lambda_c^2}\right) F_y \tag{3.2}$$

For $\lambda_c > 1.5$;

$$F_n = \left[\frac{0.877}{\lambda_c^2}\right] F_y \tag{3.3}$$

Where;

$$\lambda_c = \sqrt{\frac{F_y}{F_e}} \tag{3.4}$$

And F_e is the least of the applicable elastic flexural, torsional and flexural-torsional buckling stress determined in accordance with section C4.1.1-5 of the related standart.

For any sections that can be shown not to be subjected to torsional or flexural-torsional buckling, the elastic flexural buckling stress, F_e , shall be found as follows;

$$F_e = \frac{\pi^2 E}{(KL/r)^2} \quad \textbf{(3.5)}$$

Where;

E is the modulus of elasticity of steel. K is the effective length factor. L is laterally unbraced length of member and r is the radius of gyration of full unreduced cross-section about axis of buckling. In frames where lateral stability is provided by diagonal bracing, the effective length factor, K, for compression members that do not depend upon their own bending stiffness for lateral stability of the frame shall be taken as unity, unless analysis shows that a smaller value is suitable. Otherwise, the effective length, KL, of the compression members shall be found by rational method and can not be less than the actual unbraced length.

For singly-symmetric sections subject to flexural-torsional buckling, F_e can be taken as the smaller value obtained from Eq. **(3.5)** or **(3.6)**.

$$F_e = \frac{1}{2\beta}\left[(\sigma_{ex} + \sigma_t) - \sqrt{(\sigma_{ex} + \sigma_t)^2 - 4\beta\sigma_{ex}\sigma_t}\right] \quad \textbf{(3.6)}$$

Where;

$$\beta = 1 - (x_0/r_0)^2 \quad \textbf{(3.7)}$$

x_0 is the distance from shear center to centroid along principal x-axis, taken as negative. r_0 is the polar radius of gyration of cross section about shear center calculated from E.q.**(3.8).** r_x and r_y are the radii of gyration of cross-section about centrodial principal axes.

$$r_0 = \sqrt{r_x^2 + r_y^2 + x_0^2} \quad \textbf{(3.8)}$$

$$\sigma_{ex} = \frac{\pi^2 E}{(K_x L_x/r_x)^2} \quad \textbf{(3.9)}$$

Torsional buckling stress can be calculated as follows:

$$\sigma_t = \frac{1}{Ar_0^2}\left[GJ + \frac{\pi^2 EC_w}{(K_t L_t)^2}\right] \quad \textbf{(3.10)}$$

G is the shear modulus, J is Saint-Venant torsional constant of cross-section, C_w is torsional warping constant of cross-section, K_t is effective length factors for twisting, L_t is the unbraced length of member for twisting, K_x is effective length factor for buckling about x-axis, L_x is the unbraced length of compression member for for bending about x-axis and A is full unreduced cross-sectional area of member.

An alternative also conservative estimation F_e shall be permitted to be calculated as in Eq. **(3.11)**.

$$F_e = \frac{\sigma_t \sigma_{ex}}{\sigma_t + \sigma_{ex}} \quad \textbf{(3.11)}$$

For singly-symmetric sections, the x-axis shall be selected as the axis of symmetry. For doubly-symmetric sections subject to torsional buckling, F_e shall be taken as the smaller value obtained from eq. **(3.5)** and $F_e = \sigma_t$. For non-symmeytic sections, F_e shall be determined by rational analysis.

3.1.1.2 Effective area calculations

For the calculation of nominal strength of a member given in eq. **(3.1)**, effective area, A_e , should also be calculated. Following sections of related standart describes the methods for calculating effective areas:

B2 – Effective Widths of Stiffened Elements

B3 – Effective Widths of Unstiffened Elements

B4 – Effective Width of Uniformly Compressed Elements with a Simple Lip Edge Stiffener

B5 – Effective Widths of Stiffened Elements with Single or Multiple Intermediate Stiffeners or Edge Stiffened Elements with Intermediate Stiffeners

Since this thesis mainly focuses on DSM calculations, only B2 and B4 sections will be discussed covering general remarks and methods for effective area calculations. Example solution is also a suitable member for this section.

Section B2 describes the effective width calculations for stiffened element which is also used in general. b, the effective width shall be calculated as follows:

b = w when $\lambda \leq 0.673$ **(3.12)**

b = ρw when $\lambda > 0.673$ **(3.13)**

Where;

w = Flat width as shown in Figure 3.1.

ρ = Local Reduction factor, given in eq. **(3.14)**.

$$\rho = (1 - 0.22/\lambda)/\lambda \quad \textbf{(3.14)}$$

λ = Slenderness factor, given in eq. **(3.15)**.

$$\lambda = \sqrt{\frac{f}{F_{cr}}} \quad \textbf{(3.15)}$$

f = Stress in compression element. In flexural members, when the initial yielding is in compression element is considered, $f = f_y$.

F_{cr} = Plate elastic buckling stress

$$F_{cr} = k\frac{\pi^2 E}{12(1-\mu^2)}\left(\frac{t}{w}\right)^2 \quad \textbf{(3.16)}$$

k = Plate buckling coefficient. It can be taken as "4" for stiffened elements supported by a web on each longitudinal edge. It's also shown as Case (a) in Figure 2.10.

E = Modulus of elasticity of steel

t = Thickness of the section

μ = Poisson's ratio of steel

For compression members, f is also taken equal to nominal buckling stress, F_n.

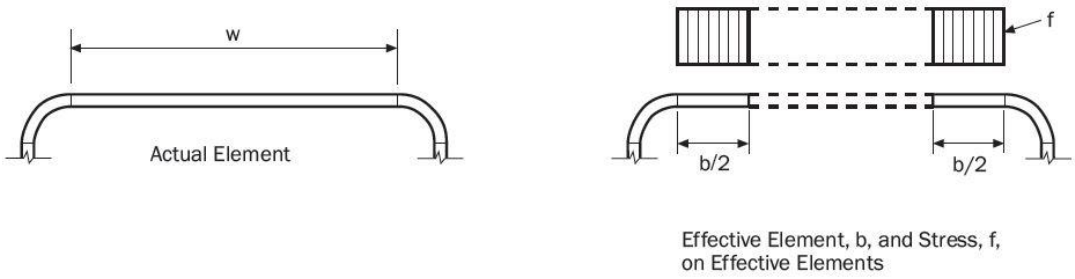

Figure 3.1 : Stiffened elements [16].

The effective widths of uniformly compressed elements with a simple edge stiffener shall be calculated in accordance with for Strength Determination and for Serviceability Determination calculations according to strength determination shall be as follows;

For $w/t \leq 0.328S$:

$I_a = 0$ (no edge stiffener is needed. **(3.17)**

$b = w$ (effective design width) **(3.18)**

$b_1 = b_2 = w/2$ (portions of effective design widths as shown in fig.3.1) **(3.19)**

$d_s = d'_s$ (reduced effective width of stiffener shown in fig.3.1) **(3.20)**

For $w/t > 0.328S$:

$b_1 = (b/2)\,(R_I)$ **(3.21)**

$b_2 = b_2 = w/2$ **(3.22)**

$d_s = d'_s\,(R_I)$ **(3.23)**

where;

$S = 1.28\sqrt{E/f}$ **(3.24)**

w = Flat dimensions defined in Figure 3.1 and Figure 3.2.

I_a = Adequate moment of inertia of stiffener, so that each component element will behave as a stiffened element, given in eq. **(3.25)**.

$$I_a = 399t^4\left[\frac{w/t}{S} - 0.328\right]^3 \leq t^4\left[115\frac{w/t}{S} + 5\right] \quad \textbf{(3.25)}$$

d'_s = Effective width of stiffener seen in Figure 3.1.

$(R_I) = I_s/I_a \leq 1$ **(3.26)**

I_s = Moment of inertia of full section of stiffener about its own centrodial axis

parallel to element to be stiffened. For edge stiffeners, the round corner between stiffener and element to be stiffened is not considered as a part of the stiffener, given in eq. **(3.27)**.

$$I_s = (d^3.t.\sin^2\theta)/12 \tag{3.27}$$

The effective width, b in equations **(3.21)** and **(3.22)** shall be calculated in accordance with previously described section B2 with eq. **(3.16)**, plate buckling coefficient, k, as given in table 3.1.

Table 3.1 : Determination of plate buckling coefficient, k [16].

Simple Lip Edge Stiffener ($140° \geq \theta \geq 40°$)	
$D/w \leq 0.25$	$0.25 < D/w \leq 0.8$
$3.57(R_I)^n + 0.43 \leq 4$	$\left(4.82 - \frac{5D}{w}\right)(R_I)^n + 0.43 \leq 4$

Where;

$$n = \left(0.582 - \frac{w/t}{4S}\right) \geq \frac{1}{3} \tag{3.28}$$

Figure 3.2 shows the definitions of dimensional variables on elements with a simple lip edge stiffener;

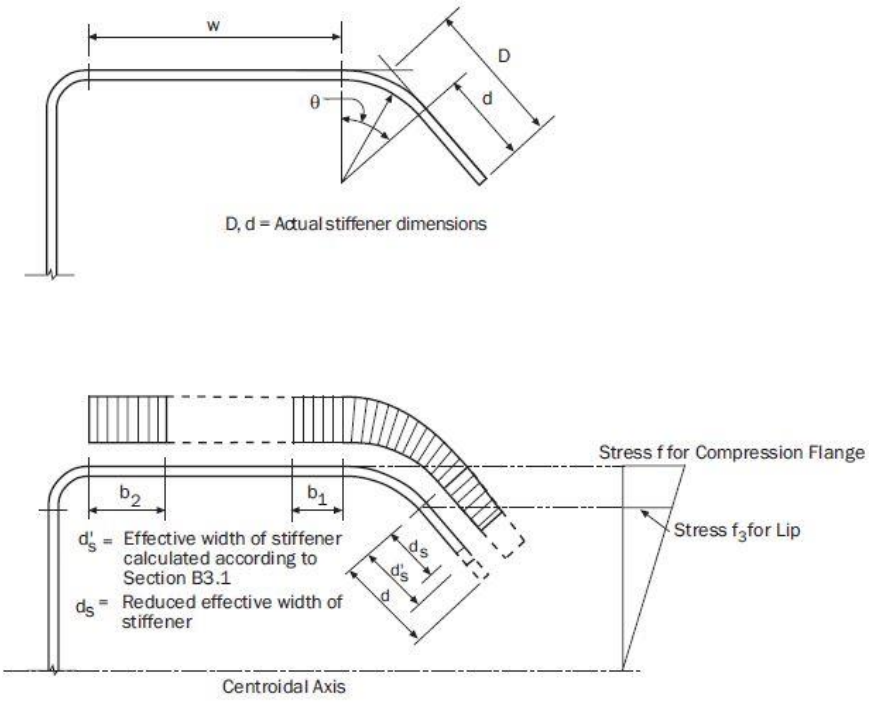

Figure 3.2 : Elements with simple lip edge stiffener [16].

3.1.1.3 Distortional buckling strength calculations

C4.2 section of AISI S100-2007 standart describes the calculations of distortional buckling strength for concentrically loaded compression members [16]. The provisions of this section shall apply to I, Z, C, hat and any other open-sections which will be affected by distortional buckling. Nominal axial strength, P_n will be calculated for distortional buckling as one found for general in previous section and will be compared with previous strength.

For $\lambda_d \leq 0.561$;

$$P_n = P_y \tag{3.29}$$

For $\lambda_d > 0.561$;

$$P_n = \left(1 - 0.25\left(\frac{P_{crd}}{P_y}\right)^{0.6}\right)\left(\frac{P_{crd}}{P_y}\right)^{0.6} P_y \tag{3.30}$$

Where;

λ_d = Slenderness factor for distortional buckling, given in eq. **(3.31)**.

$$\lambda_d = \sqrt{P_y/P_{crd}} \tag{3.31}$$

P_n is the nominal axial strength and P_y is the member yield strength given in Eq. **(3.32)**.

$$P_y = A_g F_y \tag{3.32}$$

A_g is the gross area of element including stiffeners. F_y is the yield stress of steel. P_{crd} is the distortional buckling load given in eq. **(3.33)**.

$$P_{crd} = A_g F_d \tag{3.33}$$

F_d is elastic distortional buckling stress. For C and Z sections that have no rotational restraint of flange and that are within the dimensional limits provided below, a conservative prediction of distortional buckling stress can be made with eq. **(3.34)**. Geometric definitions are shown on Figure 3.2 and Figure 3.3.

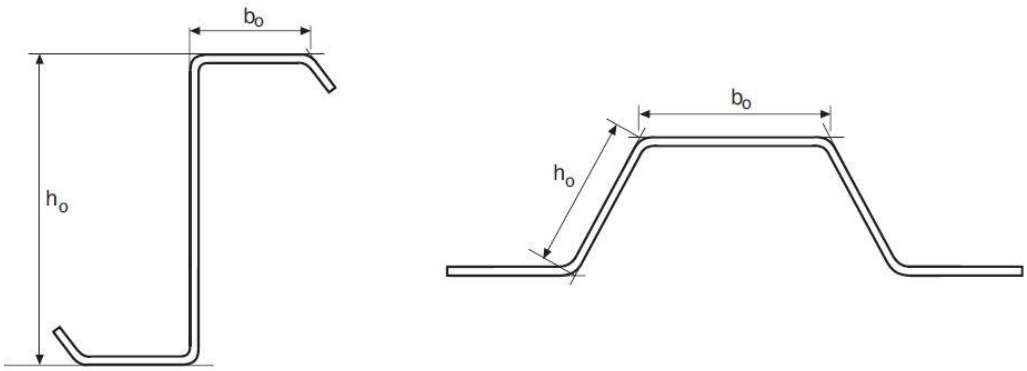

Figure 3.3 : Out-to-out dimensions of webs and stiffened elements [16].

h_0 is out-to-out web depth, b_0 is out-to-out flange width, D is out-to-out lip dimension, t is base steel thickness and θ is the lip angle. Following dimensional limits shall apply:

- $50 \leq h_0/t \leq 200$,
- $25 \leq b_0/t \leq 100$,
- $6.25 < D/t \leq 50$,
- $45° \leq \theta \leq 90°$,
- $2 \leq h_0/b_0 \leq 8$, and
- $0.04 \leq D.sin\theta/b_0 \leq 0.5$

$$F_d = \alpha * k_d * \frac{\pi^2 E}{12(1-\mu^2)}\left(\frac{t}{b_0}\right)^2 \quad \textbf{(3.34)}$$

Where;

α is a value that accounts for the benefit of an unbraced length, L_m , shorter than L_{cr} , but can be conservatively taken as "1".

For $L_m \geq L_{cr}$ $\alpha = 1$ **(3.35)**

For $L_m < L_{cr}$ $\alpha = (L_m/L_{cr})^{\ln(L_m/L_{cr})}$ **(3.36)**

L_m is the distance between discrete restraints that restrict distortional buckling, basically unbraced length. L_{cr} is the critical unbraced length of distortional buckling, given in eq. **(3.37)**.

$$L_{cr} = 1.2h_0\left(\frac{b_0 D\sin\theta}{h_0 t}\right)^{0.6} \leq 10h_0 \quad \textbf{(3.37)}$$

k_d is the plate buckling coefficient for distortional buckling, given in eq. **(3.38)**.

$$k_d = 0.05 \leq 0.1\left(\frac{b_0 D\sin\theta}{h_0 t}\right)^{1.4} \leq 8.0 \quad \textbf{(3.38)}$$

A rational elastic buckling analysis that considers distortional buckling shall be permitted to be used with these expressions given.

3.1.2. Example solution of a c-channel column with a simple lip edge stiffener via effective width method

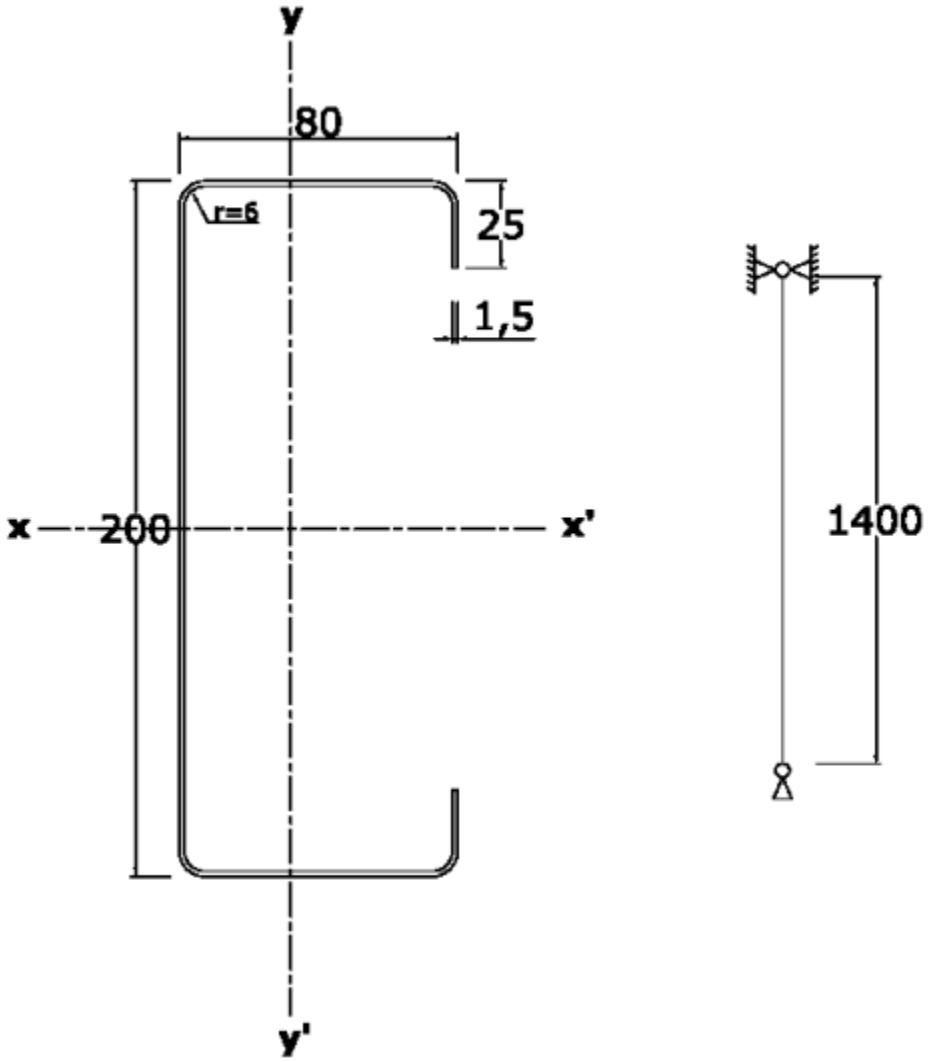

Figure 3.4 : C-channel column section with simple lip edge example.

Table 3.2 : Section properties of example solution.

Section Properties	**Calculated Section Properties**
t = 1.5 mm	**A** = 588.21 mm^2
b = 80 mm	$\mathbf{r_x}$ = 79.03 mm
h = 200 mm	$\mathbf{r_y}$ = 30.02 mm
$\mathbf{f_y}$ = 235 MPa	**J** = 441.16 mm^4
E = 200000 MPa	$\mathbf{x_0}$ = -61.96 mm
G = 80000 MPa	$\mathbf{r_0}$ = 104.81 mm
inner curvature radius = 6 mm	$\mathbf{C_w}$ = 4487970571.77 mm^6

Section is pin connected from both ends, concentrically loaded and effective length factors of this column are;

$\mathbf{K_x} = \mathbf{K_y} = \mathbf{K_t} = 1.0$

Nominal Capacity of this cold-formed steel column will be calculated using Effective Width Method and distortional buckling calculations according to AISI S100-2007 standart [16].

Nominal Section Strength

- Check for flexural buckling;

$$\frac{K_x L_x}{r_x} = \frac{(1.0)(1400)}{(79.03)} = 17.72 \qquad \frac{K_y L_y}{r_y} = \frac{(1.0)(1400)}{(30.02)} = 46.64$$

Since $\frac{K_y L_y}{r_y} > \frac{K_x L_x}{r_x}$, flexural buckling will control about y-axis

Using eq. **(3.5)**;

$$F_e = \frac{\pi^2 E}{\left(K_y L_y / r_y\right)^2} = \frac{\pi^2 (200000)}{(46.64)^2} = 907.43 \text{ MPa} \qquad \textbf{(3.5)}$$

- Check for flexural- torsional buckling, eq. **(3.6)** will be used. For the terms used in eq. **(3.6)**; equations **(3.7)** , **(3.9)** and **(3.10)** will be used.

$$\beta = 1 - \left(\frac{x_0}{r_0}\right)^2 = 1 - \left(\frac{-61.96}{104.81}\right)^2 = 0.651 \qquad \textbf{(3.7)}$$

$$\sigma_{ex} = \frac{\pi^2 E}{(K_x L_x / r_x)^2} = \frac{\pi^2 (200000)}{(17.72)^2} = 6286.4 \text{ MPa} \qquad \textbf{(3.9)}$$

$$\sigma_t = \frac{1}{Ar_0^2}\left[GJ + \frac{\pi^2 EC_w}{(K_t L_t)^2}\right] \quad \textbf{(3.10)}$$

$$\sigma_t = \frac{1}{(588.21)(104.81)^2}\left[(80000)(441.16) + \frac{\pi^2(200000)(4487970571.77)}{(1*1400)^2}\right]$$

$$\sigma_t = 704.96 \text{ MPa}$$

$$F_e = \frac{1}{2\beta}\left[(\sigma_{ex} + \sigma_t) - \sqrt{(\sigma_{ex} + \sigma_t)^2 - 4\beta\sigma_{ex}\sigma_t}\right] \quad \textbf{(3.6)}$$

$$F_e = \frac{1}{(2)(0.651)}$$

676.49 MPa < 907.43 MPa therefore, flexural-torsional buckling governs.

F_e = 676.49 Mpa will be used in eq. **(3.4)** to calculate the slenderness factor:

$$\lambda_c = \sqrt{\frac{F_y}{F_e}} = \sqrt{\frac{235}{676.49}} = 0.59 < 1.5 \quad \textbf{(3.4)}$$

Therefore in Eq. **(3.2)** nominal buckling stress, F_n , will be calculated as follows for $\lambda_c \leq 1.5$;

$$F_n = \left(0.658^{\lambda_c^2}\right)F_y = \left(0.658^{(0.59)^2}\right) * 235 = 203.14 \text{ MPa} \quad \textbf{(3.2)}$$

For calculating the nominal section capacity P_n , Effective area of the section should be calculated and multiplied by nominal buckling stress, F_n according to section C4.1 of related standart.

Effective Area Calculations (for F_n = 203.14 MPa)

- Calculations for compression flanges

f = 203.14 MPa, **E** = 200000 Mpa, **t** = 1.5 mm

w = 80 – 2 (6+1.5) = 65 mm (clear width of flange)

From Eq. **(3.24)**;

$S = 1.28\sqrt{E/f} = 1.28\sqrt{200000/203.14} = 40.16$

0.328 x S = 0.328 x 40.16 = 13.17 and w / t = 65 / 1.5 = 43.33

Since $\frac{w}{t} > 0.328S$, check on effective width of flange:

$$I_a = 399t^4\left[\frac{w/t}{S} - 0.328\right]^3 \leq t^4\left[115\frac{w/t}{S} + 5\right] \quad \textbf{(3.25)}$$

$$I_a = 399(1.5)^4\left[\frac{43.33}{40.16} - 0.328\right]^3 \leq (1.5)^4\left[115\frac{43.33}{40.16} + 5\right]$$

$855.35\ mm^4 > 653.45\ mm^4$ so $I_a = 653.45\ mm^4$ should be used.

Calculating I_s of the stiffener with eq. **(3.27)** (d is the clear width of stiffener = 25 - 6 - 1.5 = 17.5 mm)

$$I_s = \frac{d^3.t.\sin^2\theta}{12} = \frac{(17.5)^3(1.5)\sin^2(90)}{12} = 669.92\ mm^4 \quad \textbf{(3.27)}$$

From Eq. **(3.26)**; $(R_I) = I_s/I_a \leq 1$

$R_I = I_s/I_a = 669.92/653.45 = 1.025 > 1$ so $R_I = 1$

From Eq**. (3.24)**;

$$n = \left(0.582 - \frac{w/t}{4S}\right) \geq \frac{1}{3} \quad \textbf{(3.24)}$$

$$n = \left(0.582 - \frac{43.33}{4(40.16)}\right) = 0.312 < \frac{1}{3}$$

So n = 1/3. From table 3.1 plate buckling coefficient can be calculated as;

$D/w = 25/65 = 0.38$ $0.25 < D/w \leq 0.8$

$$k = \left(4.82 - \frac{5D}{w}\right)(R_I)^n + 0.43 \leq 4$$

$$k = \left(4.82 - \frac{5(25)}{65}\right)(1)^{1/3} + 0.43 = 3.33 < 4 \quad \textbf{OK!}$$

So k = 3.33

Calculating plate elastic buckling stress using Eq. **(3.16)**

$$F_{cr} = k\frac{\pi^2 E}{12(1-\mu^2)}\left(\frac{t}{w}\right)^2 \quad \textbf{(3.16)}$$

$$F_{cr} = 3.33\frac{\pi^2(200000)}{12(1-(0.3)^2)}\left(\frac{1}{43.33}\right)^2 = 320.6 \text{ Mpa}$$

Slenderness factor will be found using Eq. **(3.15)**

$$\lambda = \sqrt{\frac{f}{F_{cr}}} = \sqrt{\frac{203.14}{320.6}} = 0.796 \quad \textbf{(3.15)}$$

According to Eq. **(3.13)** b = ρw when $\lambda > 0.673$ **(3.13)**

$\lambda = 0.796 > 0.673$ Flange is subjected to local buckling.

Effective reduction factor will be found using Eq. **(3.14)**

$$\rho = (1 - 0.22/\lambda)/\lambda = (1 - 0.22/0.796)/0.796 = 0.909 \quad \textbf{(3.14)}$$

Effective width of the flange is $b = \rho w = 0.909 * 65 = 59.09\ mm$

- Calculations for stiffener lips

f = 203.14 Mpa k = 0.43 (from fig.2.10 case c)

clear width w = d = 17.5 mm From Eq. **(3.16)**;

$$F_{cr} = 0.43\frac{\pi^2(200000)}{12(1-(0.3)^2)}\left(\frac{1.5}{17.5}\right)^2 = 571.06 \text{ Mpa}$$

Using Eq. **(3.15);**

$$\lambda = \sqrt{\frac{f}{F_{cr}}} = \sqrt{\frac{203.14}{47.53}} = 2.07$$

According to Eq. **(3.13)** b = ρw when $\lambda > 0.673$ **(3.13)**

$\lambda = 2.07 > 0.673$ Web is subjected to local buckling.

Effective reduction factor will be found using Eq. **(3.14)**;

$$\rho = (1 - 0.22/\lambda)/\lambda = (1 - 0.22/2.07)/2.07 = 0.432 \quad \textbf{(3.14)}$$

Effective width of the flange is $b = \rho w = 0.432 * 185 = 79.92$ mm

- Calculations for Total Effective Area

Table 3.3 : Effective widths of section's elements.

Element	**Effective Widths (mm)**
Top Flange	59.09
Bottom Flange	59.09
Web	79.92
Top Inside Corner	10.6
Bottom Inside Corner	10.6
Top Outside Corner	10.6
Bottom Outside Corner	10.6
Top Lip	17.5
Bottom Lip	17.5
Total Length	275.5

Effective area of the section can be obtained by multiplying total effective width with the thickness:

$$A_e = t * \sum L = 1.5 * 275.5 = 413.25 \text{ mm}^2$$

Computation of P_n for local buckling

Effective area, A_e , of the section is calculated 413.25 mm^2 under 203.14 MPa nominal buckling stress, F_n.

From Eq. **(3.1)** nominal capacity of the section is;

$$P_n = A_e F_n = 413.25 * 203.14 = 83.9 \text{ kN} \quad \textbf{(3.1)}$$

Calculations for distortional buckling strength

Distortional buckling strength is calculated in accordance with AISI 100-2007 Section C4.2

Controlling dimensional limits for calculations

- $50 \leq h_0/t \leq 200$, $h_0/t = 200/1.5 = 133.33$ **OK!**
- $25 \leq b_0/t \leq 100$, $b_0/t = 80/1.5 = 53.33$ **OK!**
- $6.25 < D/t \leq 50$, $D/t = 25/1.5 = 16.67$ **OK!**
- $45° \leq \theta \leq 90°$, $\theta = 90°$ **OK!**
- $2 \leq h_0/b_0 \leq 8$, and $h_0/b_0 = 200/80 = 2.5$ **OK!**
- $0.04 \leq D.\sin\theta/b_0 \leq 0.5$ $D.\sin\theta/b_0 = 25.\sin(90)/80 = 0.313$ **OK!**

Controlling critical unbraced length of distortional buckling using Eq. **(3.37)**

$$L_{cr} = 1.2h_0\left(\frac{b_0 D\sin\theta}{h_0 t}\right)^{0.6} \leq 10h_0 \qquad \textbf{(3.37)}$$

$$L_{cr} = 1.2(200)\left(\frac{(80)(25)\sin(90)}{(200)(1.5)}\right)^{0.6} \leq 10(200)$$

$$L_{cr} = 749.13 < 2000 \qquad \textbf{OK!}$$

In Eq. **(3.35)** ;

For $L_m \geq L_{cr}$ $\alpha = 1$ **(3.35)**

$L_m = 1400\ \text{mm} > L_{cr} = 749.13\ \text{mm}$ so $\alpha = 1$

Calculating the distortional plate buckling coefficient by using Eq. **(3.38)**;

$$k_d = 0.05 \leq 0.1\left(\frac{b_0 D\sin\theta}{h_0 t}\right)^{1.4} \leq 8.0 \qquad \textbf{(3.38)}$$

$$k_d = 0.05 \leq 0.1\left(\frac{(80)(25)\sin(90)}{(200)(1.5)}\right)^{1.4} \leq 8.0 \qquad \textbf{(3.33)}$$

$$k_d = 1.423 \qquad 0.05 < 1.423 < 8.0 \qquad \textbf{OK!}$$

Calculating the elastic distortional buckling stress using Eq. **(3.29)**;

$$F_d = \alpha * k_d * \frac{\pi^2 E}{12(1-\mu^2)}\left(\frac{t}{b_0}\right)^2 \qquad \textbf{(3.34)}$$

$$F_d = (1.0) * (1.423) * \frac{\pi^2(200000)}{12(1-(0.3)^2)}\left(\frac{1.5}{80}\right)^2 = 90.43\ \text{MPa}$$

Calculating member yield strength using Eq. **(3.27)**;

$$P_y = A_g F_y = 588.21 * 235 = 138.23\ \text{kN} \qquad \textbf{(3.32)}$$

Calculating distortional buckling load using Eq. **(3.33)**;

$$P_{crd} = A_g F_d = 588.21 * 90.43 = 53.19\ \text{kN} \qquad \textbf{(3.33)}$$

Calculating slenderness factor for distortional buckling using Eq. **(3.31)**;

$$\lambda_d = \sqrt{P_y/P_{crd}} = \sqrt{138.23/53.19} = 1.61 \quad \textbf{(3.31)}$$

Since $\lambda_d > 0.561$ Eq. **(3.30)** will be used for calculating nominal distortional buckling strength;

$$P_n = \left(1 - 0.25\left(\frac{P_{crd}}{P_y}\right)^{0.6}\right)\left(\frac{P_{crd}}{P_y}\right)^{0.6} P_y \quad \textbf{(3.30)}$$

$$P_n = \left(1 - 0.25\left(\frac{53.19}{138.23}\right)^{0.6}\right)\left(\frac{53.19}{138.23}\right)^{0.6} (138.23)$$

$$P_n = 66.95 \text{ kN}$$

Since P_n obtained from distortional buckling strength calculations is critical than the one obtained from local buckling strength calculations, the nominal capacity of this section is:

From Distortional buckling strength $P_n = 66.95$ kN

From Local buckling strength $P_n = 83.9$ kN

$66.95 < 83.9$ kN $\rightarrow$ $P_n = 66.95$ kN

3.1.3 Direct strength method for concentric axially loaded compression members

In Appendix 1 of AISI 100-2007 standart, provisions, descriptions and details of Direct Strength Method is given. Since this thesis is focused on this method, codified view for DSM will be summarized in more detail.

The provisions of this appendix shall be permitted to be used to determine the nominal axial (P_n) and flexural (M_n) strengths of cold formed steel members. Section 1.2.1 of the standart presents a method applicable to all cold-formed steel columns meeting the geometric and material limitations.

These limitations are given under “pre-qualified columns” chart in the standart [16]. Basically, this means that DSM method is applicable for unperforated columns falling within these limits as a result of many studies and investigations. However, more studies and investigations are continuing to improve this pre-qualified column

chart for DSM method. This thesis also aims to bring a different perspective to this pre-qualified column chart by trial of different sections standing outside of this geometrical limitations. This pre-qualified column chart is given below in Figure 3.5.

Lipped C-Sections Simple Lips: 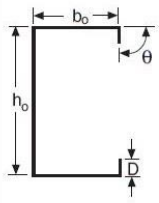 Complex Lips: 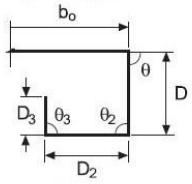 	For all C-sections: $h_o/t < 472$ $b_o/t < 159$ $4 < D/t < 33$ $0.7 < h_o/b_o < 5.0$ $0.05 < D/b_o < 0.41$ $\theta = 90°$ $E/F_y > 340$ [$F_y < 86$ ksi (593 MPa or 6050 kg/cm²)] For C-sections with complex lips: $D_2/t < 34$ $D_2/D < 2$ $D_3/t < 34$ $D_3/D_2 < 1$ Note: a) θ_2 is permitted to vary (D_2 lip is permitted to angle inward, outward, etc.) b) θ_3 is permitted to vary (D_3 lip is permitted to angle up, down, etc.)
Lipped C-Section with Web Stiffener(s) 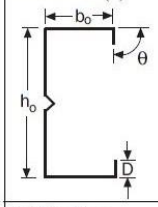 	For one or two intermediate stiffeners: $h_o/t < 489$ $b_o/t < 160$ $6 < D/t < 33$ $1.3 < h_o/b_o < 2.7$ $0.05 < D/b_o < 0.41$ $E/F_y > 340$ [$F_y < 86$ ksi (593 MPa or 6050 kg/cm²)]
Z-Section 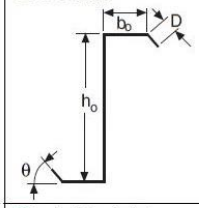 	$h_o/t < 137$ $b_o/t < 56$ $0 < D/t < 36$ $1.5 < h_o/b_o < 2.7$ $0.00 < D/b_o < 0.73$ $\theta = 50°$ $E/F_y > 590$ [$F_y < 50$ ksi (345 MPa or 3520 kg/cm²)]
Rack Upright 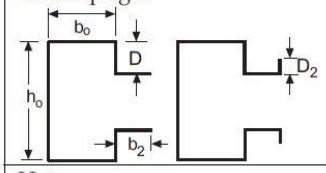 	See C-Section with Complex Lips
Hat 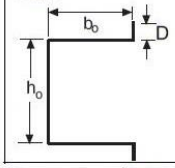 	$h_o/t < 50$ $b_o/t < 20$ $4 < D/t < 6$ $1.0 < h_o/b_o < 1.2$ $D/b_o = 0.13$ $E/F_y > 428$ [$F_y < 69$ ksi (476 MPa or 4850 kg/cm²)]

Note: * $r/t < 10$, where r is the centerline bend radius
b_o = overall width; D =overall lip depth; t = base metal *thickness*; h_o = overall depth

Figure 3.5 : Limits for pre-qualified columns [16].

3.1.3.1 Determination of elastic buckling loads

Section 1.1.2 of Appendix 1 describes the determination of elastic buckling loads in AISI 100-2007 standart. For columns, this includes the local, distortional and overall (global) buckling loads which are; $P_{cr\ell}$ P_{crd} and P_{cre} . It should be noted that in some cases, for a given column all three modes may not exist. These non-existent mode shall be ignored in such cases. These elastic buckling loads shall be calculated using software programs like CUFSM which uses Finite Strip Method in analysis. Finite element analysis is also another option to obtain these critical loads. Software programs like ABAQUS, ANSYS etc. can be used for finite element analysis.

3.1.3.2 Column analysis

The nominal axial strength, P_n, shall be the minimum of nominal axial strengths obtained from three major checks. These checks are for;

- Flexural, Torsional, or Flexural-Torsional Buckling

- Local Buckling

- Distortional Buckling

Nominal axial strength values should be calculated from mentioned checks are P_{ne} , $P_{n\ell}$, P_{nd} respectively.

Flexural, torsional, or flexural-torsional buckling

The nominal axial strength, P_{ne} , for flexural, torsional, or flexural-torsional buckling shall be calculated in accordance with the following formulas and method;

For $\lambda_c \leq 1.5$

$$P_{ne} = \left(0.658^{\lambda_c^2}\right)P_y \quad \textbf{(3.39)}$$

For $\lambda_c > 1.5$

$$P_{ne} = \left(\frac{0.877}{\lambda_c^2}\right)P_y \quad \textbf{(3.40)}$$

Where λ_c , is the global slenderness factor and can be calculated with Eq. **(3.41)**;

$$\lambda_c = \sqrt{P_y/P_{cre}} \quad \textbf{(3.41)}$$

P_y is the member yield strength previously given in Eq. **(3.32)**;

$$P_y = A_g F_y \tag{3.32}$$

A_g is the gross area of the section. F_y is the yield stress of steel.

P_{cre} is the minimum of the critical elastic column buckling load in flexural, torsional or flexural-torsional buckling determined by analysis in accordance with section 3.1.3.1.

Local buckling

The nominal axial strength, $P_{n\ell}$, for local buckling shall be calculated in accordance with the following formulas and method;

For $\lambda_\ell \leq 0.776$

$$P_{n\ell} = P_{ne} \tag{3.42}$$

For $\lambda_\ell > 0.776$

$$P_{n\ell} = \left[1 - 0.15\left(\frac{P_{cr\ell}}{P_{ne}}\right)^{0.4}\right]\left(\frac{P_{cr\ell}}{P_{ne}}\right)^{0.4} P_{ne} \tag{3.43}$$

Where λ_ℓ , is the local slenderness factor and can be calculated with Eq. **(3.44)**;

$$\lambda_\ell = \sqrt{P_{ne}/P_{cr\ell}} \tag{3.44}$$

P_{ne} is the nominal axial strength value obtained from Flexural, Torsional, or Flexural-Torsional Buckling section using eq. 3.39 or 3.40

$P_{cr\ell}$ is the critical elastic local column buckling load determined by analysis in accordance with section 3.1.3.1.

Distortional buckling

The nominal axial strength, P_{nd} , for distortional buckling shall be calculated in accordance with the following formulas and method;

For $\lambda_d \leq 0.561$

$$P_{nd} = P_y \tag{3.45}$$

For $\lambda_d > 0.561$

$$P_{nd} = \left[1 - 0.25\left(\frac{P_{crd}}{P_y}\right)^{0.6}\right]\left(\frac{P_{crd}}{P_y}\right)^{0.6} P_y \quad \textbf{(3.46)}$$

Where λ_d , is the distortional slenderness factor and can be calculated with Eq. (**3.47);**

$$\lambda_d = \sqrt{P_y/P_{crd}} \quad \textbf{(3.47)}$$

P_y is the member yield strength given in Eq. **(3.32)**

P_{crd} is the critical elastic distortional column buckling load determined by analysis in accordance with section 3.1.3.1.

3.1.3.3 Summary and design curves of direct strength method

As a summary, DSM method will be explained shortly in this section. Also Design Curves for Direct Strength Method will be given.

To calculate the capacity of a cold-formed steel member with DSM, the elastic buckling properties of a CFS cross-section are obtained from an elastic buckling curve. The curve should be generated using a software progra like CUFSM performing eigenbuckling analyses over a range of buckled half-wavelengths with finite strip method. Local buckling occurs as plate buckling of individual slender elements in whole cross-section. Only open cross-sections such as C and hat section will be faced to existence of distortional buckling where the compressed flanges buckle inward or outward along the length of the member. Global buckling defines buckling of the full member at long half-wavelengths which is also known as Euler buckling. Global buckling includes both flexural and flexural-torsional effects. For columns, the critical elastic buckling loads related with global, local, and distortional buckling (P_{cre} , $P_{cr\ell}$, P_{crd}) can be obtained directly from the elastic buckling curve of that member. Then, these values are used to find that member's slenderness factors ($\lambda_c, \lambda_\ell, \lambda_d$) defining the sensitivity to each type of buckling at failure. Then the nominal strengths (P_{ne} , $P_{n\ell}$, P_{nd}) shall be obtained by inserting the slenderness factors into DSM equations. The minimum of the global, local and distortional

nominal strengths will be the actual nominal strength of the member. For design of steel columns using Direct Strength Method and as an explanation of DSM calculations, three empirical design curves are given in Figures 3.6 to 3.8.

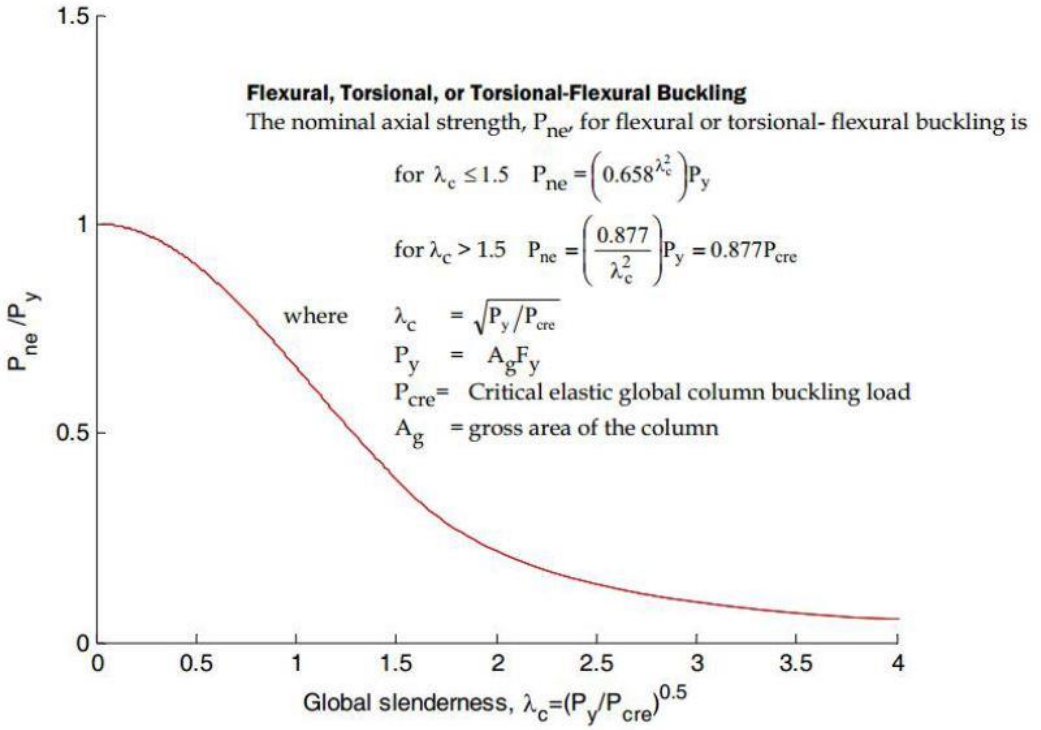

Figure 3.6 : DSM global buckling failure design curve and equations [63].

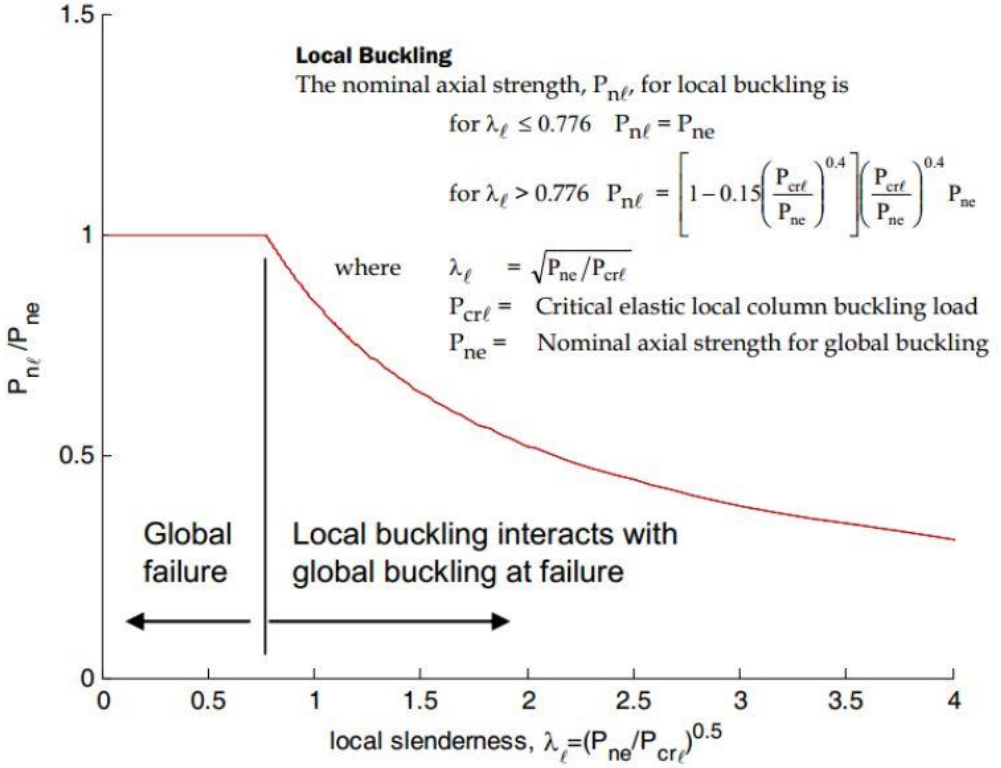

Figure 3.7 : DSM local buckling failure design curve and equations [63].

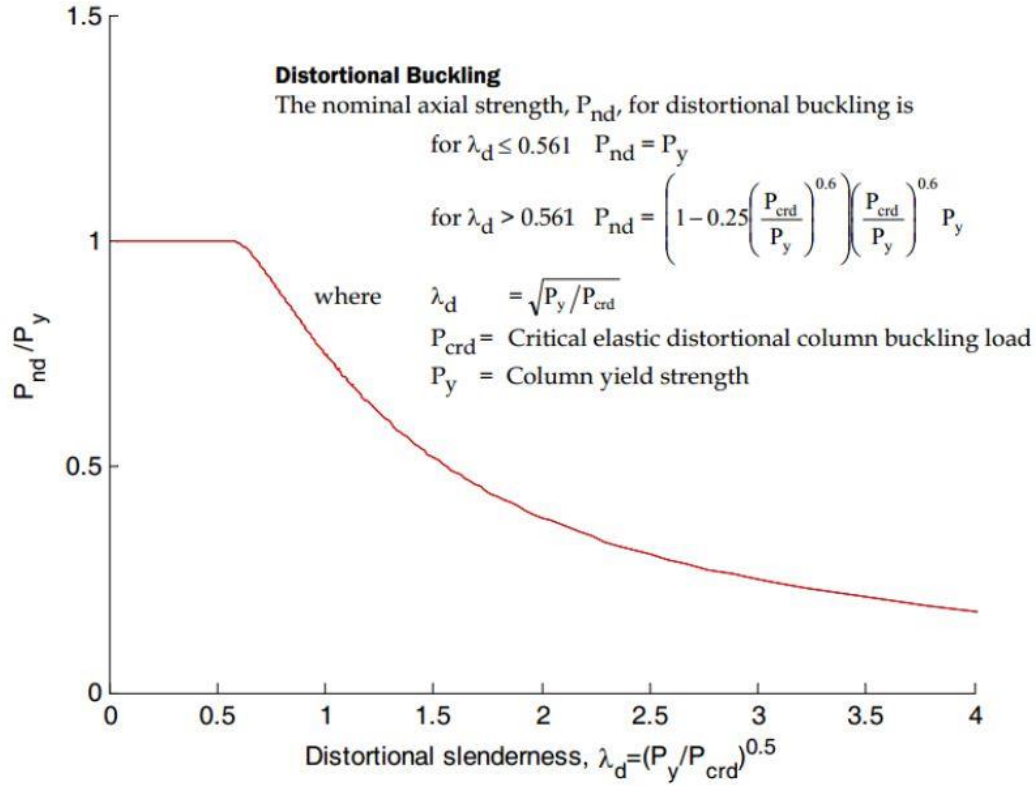

Figure 3.8 : DSM distortional buckling failure design curve and equations [63].

3.1.4 Example solution of a c-channel column with a simple lip edge stiffener via direct strength method

Same example will be used with DSM which have been previously solved with Effective Width Method. Geometric details of the example can be gathered from Figure 3.4 and Table 3.2.

Section is pin connected from both ends, concentrically loaded and effective length factors of this column are; $K_x = K_y = K_t = 1.0$

Dimension controls for DSM using "Limits for Pre-Qualified Columns Chart" given in Figure 3.5;

For all C Sections:

$h_0/t = 200/1.5 = 133.33 < 472$ **OK!**

$b_0/t = 80/1.5 = 53.33 < 159$ **OK!**

$4 < D/t < 33 \rightarrow D/t = 25/1.5 = 16.67 \rightarrow 4 < 16.67 < 33$ **OK!**

$0.7 < h_0/b_0 < 5.0 \rightarrow h_0/b_0 = 200/80 = 2.5 \rightarrow 0.7 < 2.5 < 5.0$ **OK!**

$0.05 < D/b_0 < 0.41 \rightarrow D/b_0 = 25/80 = 0.31 \rightarrow 0.05 < 0.31 < 0.41$ **OK!**

$\theta = 90°$ **OK!**

$E/F_y > 340\ [F_y < 593\ MPa] \rightarrow \ \ 200000/235 = 851.06\ > 340\ \ [235 < 593]$

OK!

Example column is in the Pre-qualified column limits. This means that nominal section strength can be calculated using Direct Strength Method.

Determination of Critical Elastic Buckling Loads Using CUFSM Software

Centerline dimensions of the section of this example column has been built in CUFSM v4.5. shown in Figure 3.9. Simple support boundary conditions and the yield load which is based on maximum yield stress (235 MPa) have been set on the section shown in Figure 3.10.

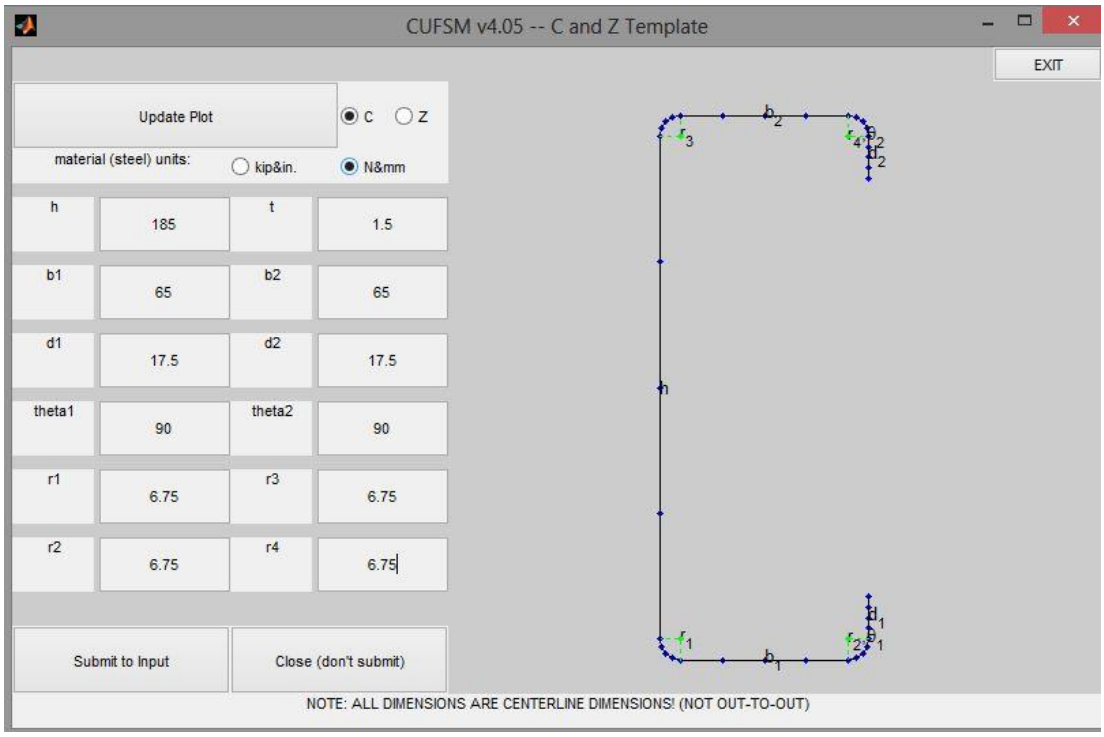

Figure 3.9 : Centerline dimensions in CUFSM.

Material properties and boundary conditions which is simply supported has been set in CUFSM which are shown in Figures 3.11 and 3.12.

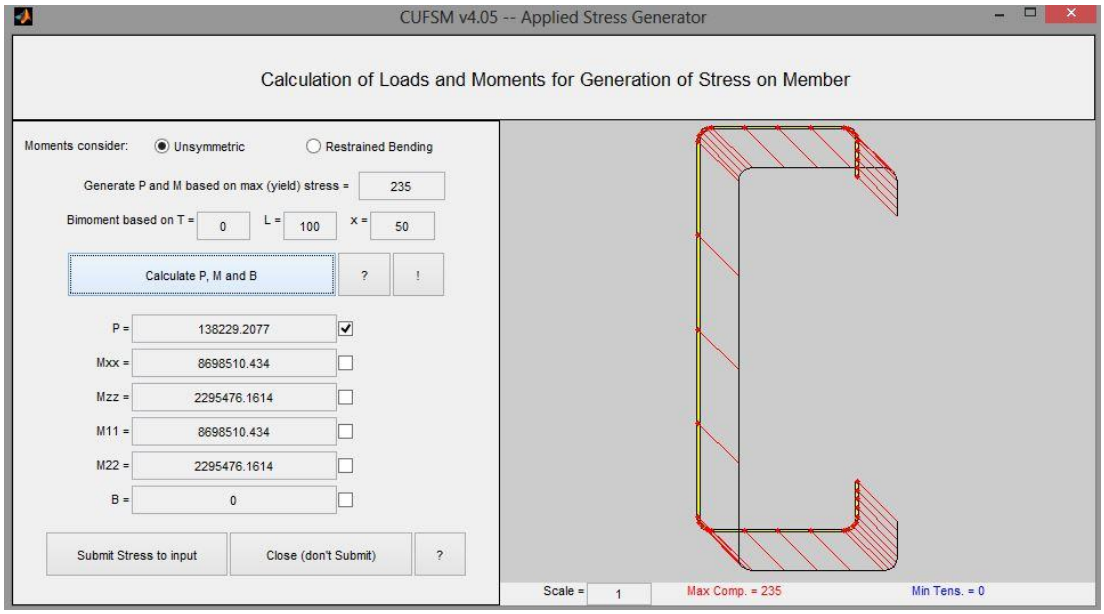

Figure 3.10 : Yield load calculation.

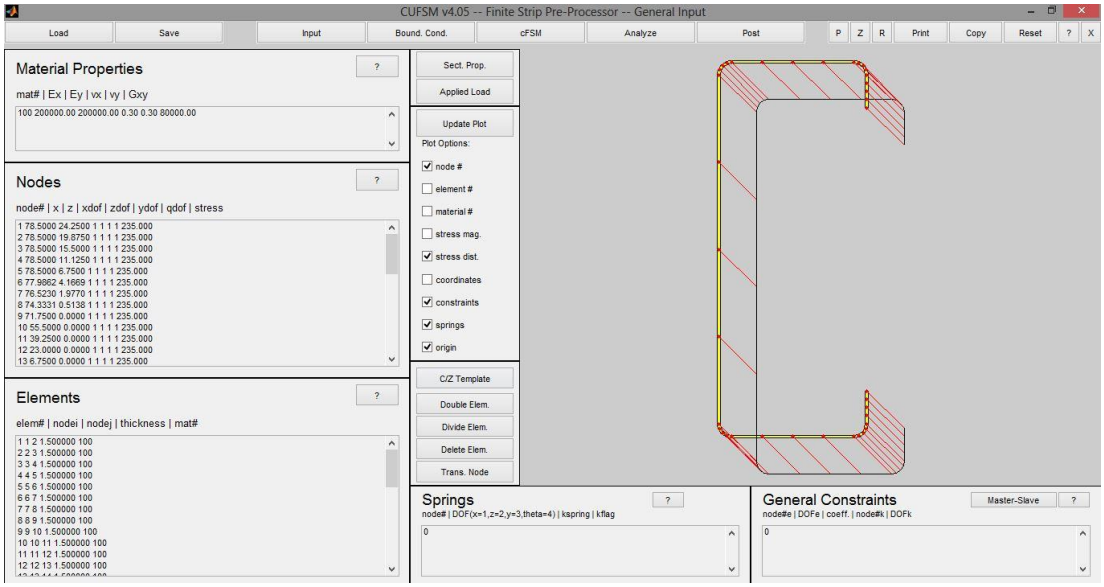

Figure 3.11 : Configuration of material properties.

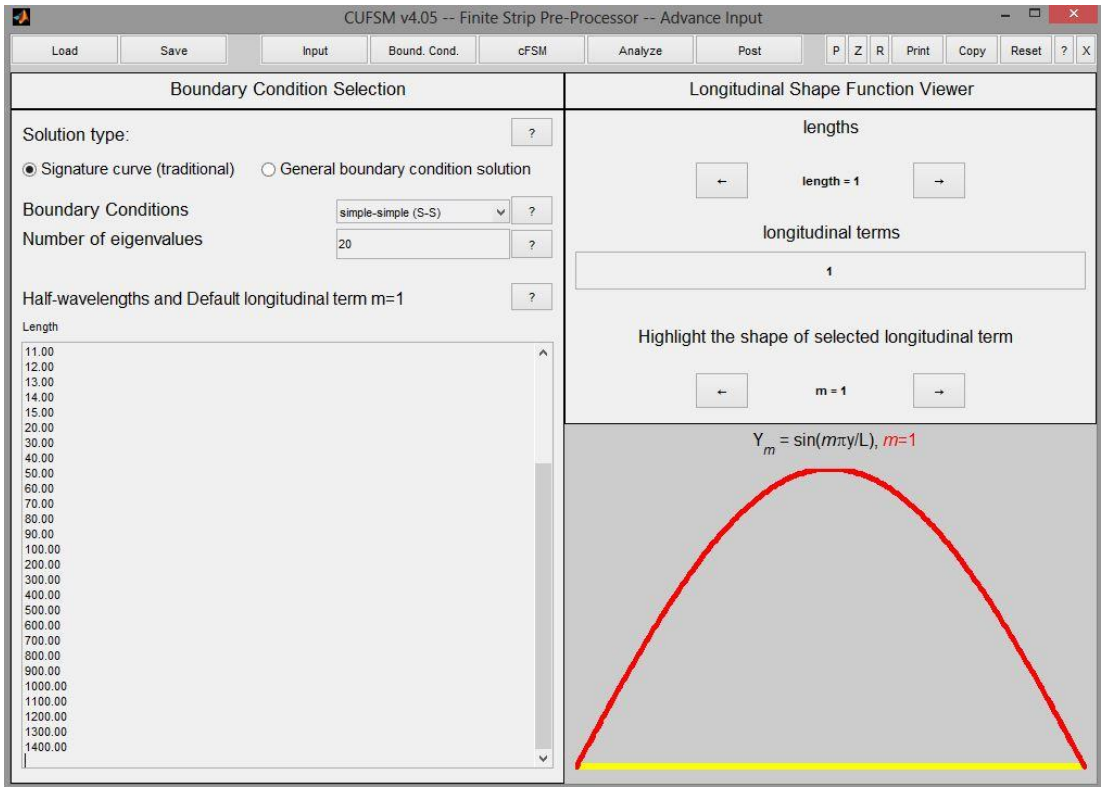

Figure 3.12 : Boundary condition selection.

The load factor on the elastic buckling curve of the section represents the ratios of $P_{cr\ell}/P_y$, P_{crd}/P_y , and P_{cre}/P_y according to the type of the buckled shape (local, distortional and global) on the minimas of the curve. Results of the finite strip analysis conducted in CUFSM are given in Figures 3.13 to 3.15. Load factors for local buckling, distortional buckling and flexural-torsional (global) buckling are obtained in order to calculate critical elastic column buckling loads.

It has been seen that load factor for flexural-torsional buckling mode caught on the 2nd mode in 1400 mm of half-wave length for this section. Member yield strength will be calculated using Eq. **(3.32)**;

$$P_y = A_g F_y = 588.21 \times 235 = 138.22 \text{ kN} \qquad \textbf{(3.32)}$$

According to the results of CUFSM;

$$P_{cr\ell}/P_y = 0.27787 \quad \rightarrow \quad P_{cr\ell} = 0.27787 \times 138.22 = 38.41 \text{ kN}$$

$$P_{crd}/P_y = 0.69067 \quad \rightarrow \quad P_{crd} = 0.69067 \times 138.22 = 95.46 \text{ kN}$$

$$P_{cre}/P_y = 2.1965 \quad \rightarrow \quad P_{cre} = 2.1965 \times 138.22 = 303.60 \text{ kN}$$

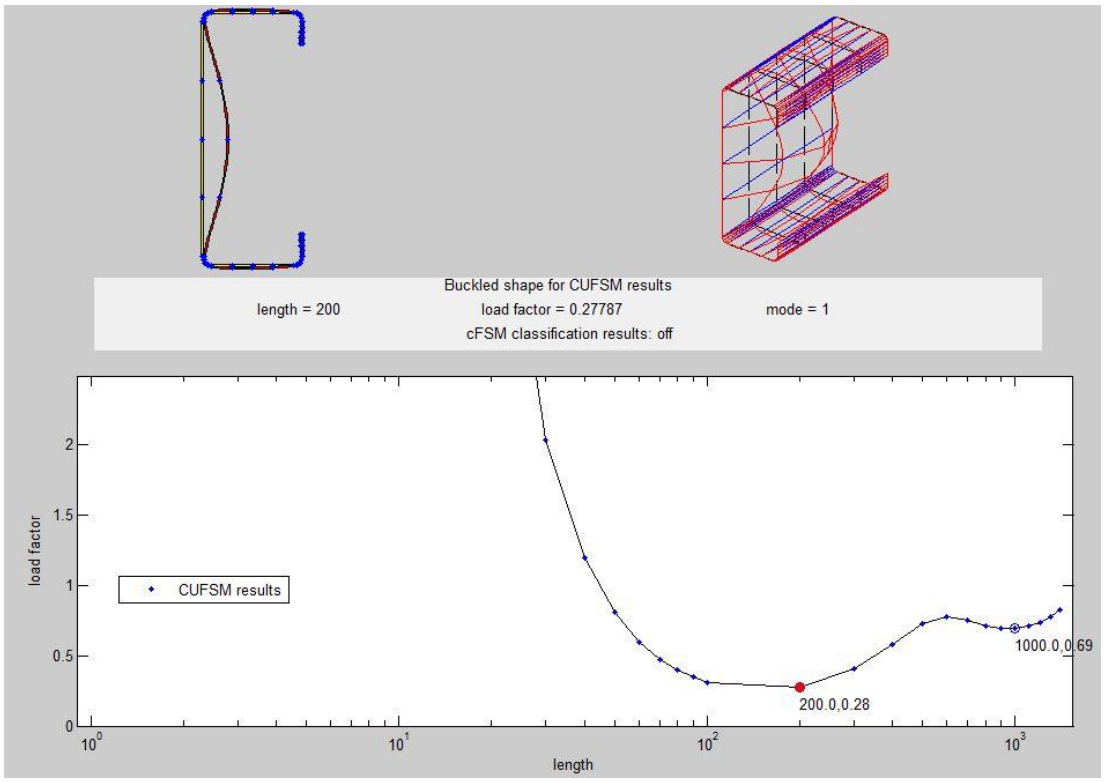

Figure 3.13 : Result of local buckling in CUFSM.

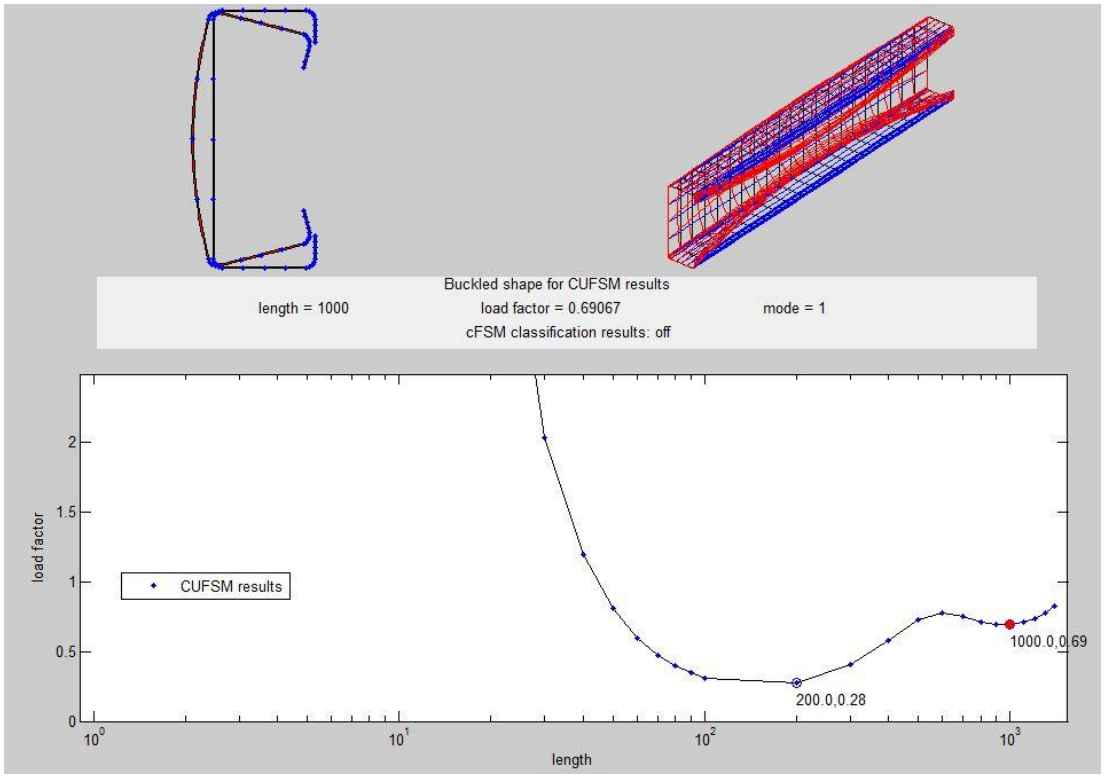

Figure 3.14 : Result of distortional buckling in CUFSM.

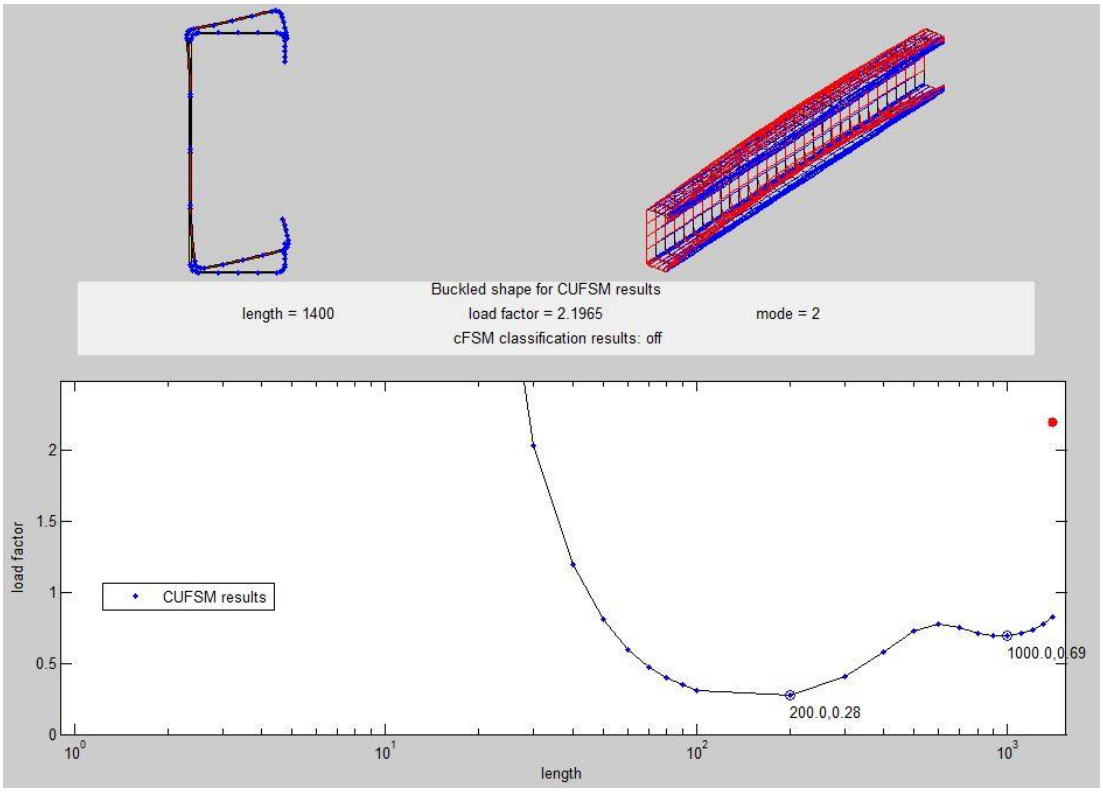

Figure 3.15 : Result of flexural-torsional buckling in CUFSM.

Calculations for flexural-torsional buckling

The global slenderness factor is calculated with Eq. **(3.41)**;

$$\lambda_c = \sqrt{P_y/P_{cre}} = \sqrt{138.22/303.6} = 0.675 \qquad \textbf{(3.41)}$$

The nominal axial strength, P_{ne} , for flexural-torsional buckling is calculated with eq. **(3.39)**;

For $\lambda_c \leq 1.5$

$$P_{ne} = \left(0.658^{\lambda_c^2}\right)P_y = \left(0.658^{0.675^2}\right)138.22 = 114.22 \text{ kN} \qquad \textbf{(3.39)}$$

P_{ne} = 114.22 kN

Calculations for local buckling

The local slenderness factor is calculated with eq. **(3.44)**;

$$\lambda_\ell = \sqrt{P_{ne}/P_{cr\ell}} = \sqrt{114.22/38.41} = 1.724 \qquad \textbf{(3.44)}$$

The nominal axial strength, $P_{n\ell}$, for local buckling is calculated with eq. **(3.43)**;

For $\lambda_c > 0.776$

$$P_{n\ell} = \left[1 - 0.15\left(\frac{P_{cr\ell}}{P_{ne}}\right)^{0.4}\right]\left(\frac{P_{cr\ell}}{P_{ne}}\right)^{0.4} P_{ne} \quad \textbf{(3.43)}$$

$$P_{n\ell} = \left[1 - 0.15\left(\frac{38.41}{114.22}\right)^{0.4}\right]\left(\frac{38.41}{114.22}\right)^{0.4} 114.22 = 66.70\text{kN}$$

$P_{n\ell}$ = 66.70 kN

Calculations for distortional buckling

The distortional slenderness factor is calculated with eq. **(3.47)**;

$$\lambda_d = \sqrt{P_y/P_{crd}} = \sqrt{138.22/95.46} = 1.203 \quad \textbf{(3.47)}$$

The nominal axial strength, P_{nd} , for distortional buckling is calculated with eq. **(3.46)**;

For $\lambda_d > 0.561$

$$P_{nd} = \left[1 - 0.25\left(\frac{P_{crd}}{P_y}\right)^{0.6}\right]\left(\frac{P_{crd}}{P_y}\right)^{0.6} P_y \quad \textbf{(3.46)}$$

$$P_{nd} = \left[1 - 0.25\left(\frac{95.46}{138.22}\right)^{0.6}\right]\left(\frac{95.46}{138.22}\right)^{0.6} 138.22 = 88.53\text{kN}$$

P_{nd} = 88.53 kN

Nominal axial strength of section

From the calculated nominal axial strengths, it can be seen that the minimum value is $P_{n\ell}$ among others. Nominal axial strength of this column is found **P_n = 66.70 kN** using Direct Strength Method.

4. INVESTIGATION OF RACK COLUMN BEHAVIOUR THROUGH DIRECT STRENGTH METHOD

This study consists of investigation on nominal section strength of various rack columns through a newly developed analytical method which is known as Direct Strength Method.

120 column models having different lip configurations and column lengths are used in this study. Half of these specimens have web perforations with same cross-section geometries.

In Figure 4.1, general specimen geometric cross-sectional details are shown. All cross-sections have same b_0 and h_0 values which are 50 mm and 140 mm. Lip length starts from 0 and increases with 5 mm intervals. After reaching the 20 mm length of first lip (as simple lip section) second lip continues inwards or outwards which makes the section a complex lipped section. After reaching the 30 mm length of second lip, third lip starts and ends at 10 mm length. Cross-sections are generated using this 5 mm interval lip length. These specimens' geometric properties are all within the prequalified column cross-section limits for DSM given in Figure 3.5. Specimens have been investigated having three different column lengths with same cross-section properties which are L_1 = 500 mm, L_2 = 1000 mm, L_3 = 1500 mm. Yield strength of the material is assumed to be 235 MPa and thickness is assumed 2 mm for all column models. Elastic Modulus of steel (E) has been taken as 200000 MPa and Shear Modulus (G) has been taken as 80000 MPa. Columns are assumed to be compressed between pin supports which makes the chosen boundary conditions simply supported. Notation explanation of specimen types with three different specimen examples are given in Figure 4.2.

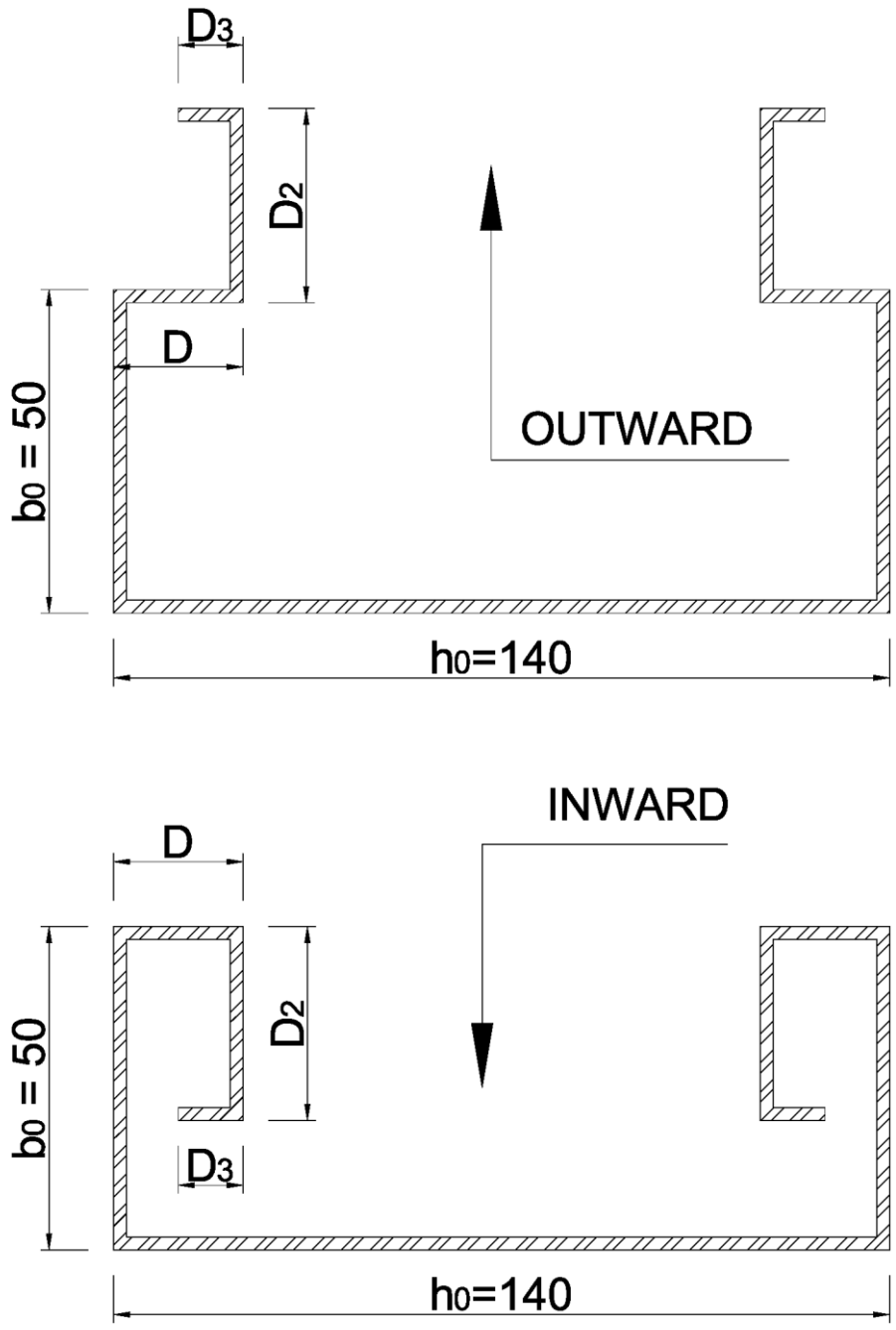

Figure 4.1 : General geometric details of specimen cross-sections.

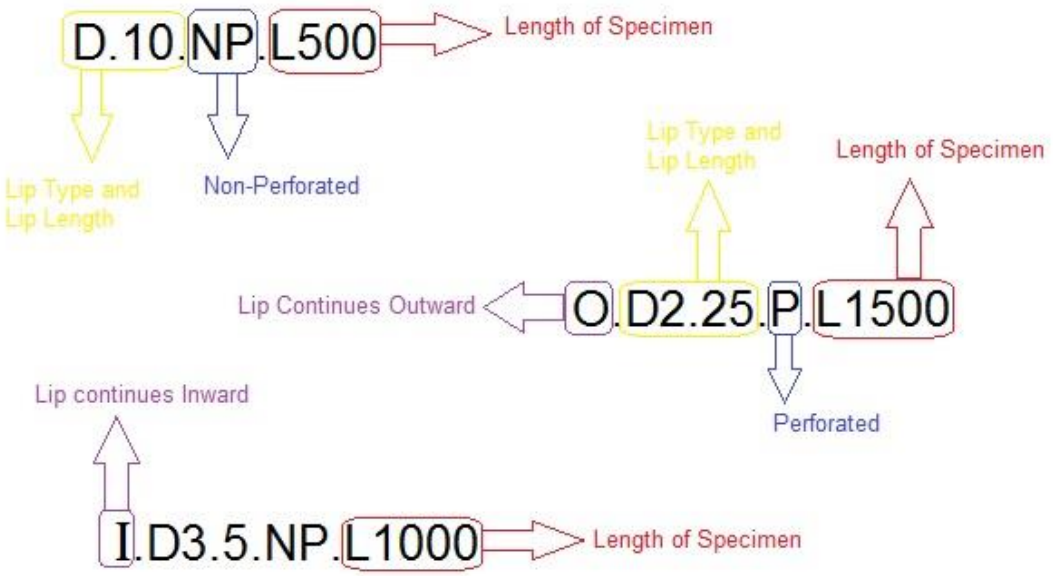

Figure 4.2 : Explanation of specimen's notation through its properties.

As a final explanation of these chosen specimens, Lip starts and continues as D with an interval of 5 mm . Then moves inwards or outwards as D_2 again in 5mm intervals. Finally after last turn, it continues as D_3 again in 5 mm interval. Maximum lip length limits have been set in accordance with manufactured sections in Turkey and also within the limits of AISI Prequalified column chart for DSM given in Figure 3.5:

Maximum limit of D is 20 mm

Maximum limit of D_2 is 30 mm

Maximum limit of D_3 is 10 mm

For instance, if a specimen has D3.10 on its notation that means its D_3 is 10 mm, D_2 is 30 mm and D is 20 mm. In total, calculations of 60 perforated and 60 unperforated column models have been done.

4.1 Analysis of Unperforated Column Models

60 unperforated column models have been analyzed in this study. Geometric details of these specimens are given in tables 4.1 to 4.3 based on the length of the columns.

Table 4.1 : Geometric properties of unperforated specimens having 500 mm column length.

Column	t (mm)	h_0 (mm)	b_0 (mm)	D (mm)	D_2 (mm)	D_3 (mm)	Section Area (mm^2)	Column Length (mm)
D.5.NP.L500	2	140	50	5	-	-	484	500
D.10.NP.L500	2	140	50	10	-	-	504	500
D.15.NP.L500	2	140	50	15	-	-	524	500
D.20.NP.L500	2	140	50	20	-	-	544	500
O.D2.5.NP.L500	2	140	50	20	5	-	556	500
O.D2.10.NP.L500	2	140	50	20	10	-	576	500
O.D2.15.NP.L500	2	140	50	20	15	-	596	500
O.D2.20.NP.L500	2	140	50	20	20	-	616	500
O.D2.25.NP.L500	2	140	50	20	25	-	636	500
O.D2.30.NP.L500	2	140	50	20	30	-	656	500
O.D3.5.NP.L500	2	140	50	20	30	5	668	500
O.D3.10.NP.L500	2	140	50	20	30	10	688	500
I.D2.5.NP.L500	2	140	50	20	5	-	556	500
I.D2.10.NP.L500	2	140	50	20	10	-	576	500
I.D2.15.NP.L500	2	140	50	20	15	-	596	500
I.D2.20.NP.L500	2	140	50	20	20	-	616	500
I.D2.25.NP.L500	2	140	50	20	25	-	636	500
I.D2.30.NP.L500	2	140	50	20	30	-	656	500
I.D3.5.NP.L500	2	140	50	20	30	5	668	500
I.D3.10.NP.L500	2	140	50	20	30	10	688	500

Table 4.2 : Geometric properties of unperforated specimens having 1000 mm column length.

Column	t (mm)	h_0 (mm)	b_0 (mm)	D (mm)	D_2 (mm)	D_3 (mm)	Section Area (mm^2)	Column Length (mm)
D.5.NP.L1000	2	140	50	5	-	-	484	1000
D.10.NP.L1000	2	140	50	10	-	-	504	1000
D.15.NP.L1000	2	140	50	15	-	-	524	1000
D.20.NP.L1000	2	140	50	20	-	-	544	1000
O.D2.5.NP.L1000	2	140	50	20	5	-	556	1000
O.D2.10.NP.L1000	2	140	50	20	10	-	576	1000
O.D2.15.NP.L1000	2	140	50	20	15	-	596	1000
O.D2.20.NP.L1000	2	140	50	20	20	-	616	1000
O.D2.25.NP.L1000	2	140	50	20	25	-	636	1000
O.D2.30.NP.L1000	2	140	50	20	30	-	656	1000
O.D3.5.NP.L1000	2	140	50	20	30	5	668	1000
O.D3.10.NP.L1000	2	140	50	20	30	10	688	1000
I.D2.5.NP.L1000	2	140	50	20	5	-	556	1000
I.D2.10.NP.L1000	2	140	50	20	10	-	576	1000
I.D2.15.NP.L1000	2	140	50	20	15	-	596	1000
I.D2.20.NP.L1000	2	140	50	20	20	-	616	1000
I.D2.25.NP.L1000	2	140	50	20	25	-	636	1000
I.D2.30.NP.L1000	2	140	50	20	30	-	656	1000
I.D3.5.NP.L1000	2	140	50	20	30	5	668	1000
I.D3.10.NP.L1000	2	140	50	20	30	10	688	1000

Table 4.3 : Geometric properties of unperforated specimens having 1500 mm column length.

Column	t (mm)	h_0 (mm)	b_0 (mm)	D (mm)	D_2 (mm)	D_3 (mm)	Section Area (mm^2)	Column Length (mm)
D.5.NP.L1500	2	140	50	5	-	-	484	1500
D.10.NP.L1500	2	140	50	10	-	-	504	1500
D.15.NP.L1500	2	140	50	15	-	-	524	1500
D.20.NP.L1500	2	140	50	20	-	-	544	1500
O.D2.5.NP.L1500	2	140	50	20	5	-	556	1500
O.D2.10.NP.L1500	2	140	50	20	10	-	576	1500
O.D2.15.NP.L1500	2	140	50	20	15	-	596	1500
O.D2.20.NP.L1500	2	140	50	20	20	-	616	1500
O.D2.25.NP.L1500	2	140	50	20	25	-	636	1500
O.D2.30.NP.L1500	2	140	50	20	30	-	656	1500
O.D3.5.NP.L1500	2	140	50	20	30	5	668	1500
O.D3.10.NP.L1500	2	140	50	20	30	10	688	1500
I.D2.5.NP.L1500	2	140	50	20	5	-	556	1500
I.D2.10.NP.L1500	2	140	50	20	10	-	576	1500
I.D2.15.NP.L1500	2	140	50	20	15	-	596	1500
I.D2.20.NP.L1500	2	140	50	20	20	-	616	1500
I.D2.25.NP.L1500	2	140	50	20	25	-	636	1500
I.D2.30.NP.L1500	2	140	50	20	30	-	656	1500
I.D3.5.NP.L1500	2	140	50	20	30	5	668	1500
I.D3.10.NP.L1500	2	140	50	20	30	10	688	1500

4.1.1 Analytical study on unperforated members using direct strength method

A study including construction of elastic buckling curves with CUFSM Software and DSM calculations has been done to calculate the nominal section strength of these specimens. Critical elastic column buckling loads of these various sections are obtained from CUFSM software. Tables 4.4, 4.5 and 4.6 include the results of critical elastic buckling loads obtained by CUFSM. For models with non-existent buckling modes; a high value of elastic critical buckling load is intentionally assumed to calculate the slenderness values. The non-existent buckling modes are indicated with N.A in relevant cells of tables 4.4 to 4.6.

Direct Strength Method is used after obtaining the critical elastic buckling loads. Nominal strengths for local, distortional and global buckling are calculated with DSM equations. Then, the nominal strength for all sections is determined. Results are given in tables 4.7, 4.8 and 4.9. Controlling mode indicates which buckling mode governs the behaviour of the member.

Table 4.4 : Critical elastic buckling loads obtained from CUFSM analysis for unperforated specimens having 500 mm column length.

Column	Yield Load (kN)	CUFSM RESULTS (LOAD FACTORS)						Critical Elastic Buckling Loads (kN)		
	P_y	$P_{cr\ell}/P_y$	hw. length (mm)	P_{crd}/P_y	hw. length (mm)	P_{cre}/P_y	hw. length (mm)	$P_{cr\ell}$	P_{crd}	P_{cre}
D.5.NP.L500	113,74	1,651	50	0,737	200	N.A.	-	187,78	83,83	N.A.
D.10.NP.L500	118,44	0,902	120	0,933	140	N.A.	-	106,83	110,50	N.A.
D.15.NP.L500	123,14	0,918	100	1,349	400	N.A.	-	113,04	166,12	N.A.
D.20.NP.L500	127,84	0,921	100	1,569	500	N.A.	-	117,74	200,58	N.A.
O.D2.5.NP.L500	131,60	0,924	100	1,616	500	N.A.	-	121,60	212,67	N.A.
O.D2.10.NP.L500	136,30	0,929	100	1,544	500	N.A.	-	126,62	210,45	N.A.
O.D2.15.NP.L500	141,00	0,930	100	1,421	500	N.A.	-	131,13	200,36	N.A.
O.D2.20.NP.L500	145,70	0,930	100	1,299	500	N.A.	-	135,50	189,26	N.A.
O.D2.25.NP.L500	150,40	0,930	100	1,203	500	N.A.	-	139,87	180,93	N.A.
O.D2.30.NP.L500	155,10	0,930	100	1,136	500	N.A.	-	144,24	176,19	N.A.
O.D3.5.NP.L500	158,86	0,930	100	1,142	500	N.A.	-	147,74	181,42	N.A.
O.D3.10.NP.L500	163,56	0,930	100	1,298	500	N.A.	-	152,11	212,30	N.A.
I.D2.5.NP.L500	131,60	0,922	100	1,699	500	N.A.	-	121,34	223,59	N.A.
I.D2.10.NP.L500	136,30	0,924	100	1,871	500	N.A.	-	125,94	255,02	N.A.
I.D2.15.NP.L500	141,00	0,926	100	2,061	500	N.A.	-	130,57	290,60	N.A.
I.D2.20.NP.L500	145,70	0,927	100	2,263	500	N.A.	-	135,06	329,72	N.A.
I.D2.25.NP.L500	150,40	0,928	100	2,463	500	N.A.	-	139,57	370,44	N.A.
I.D2.30.NP.L500	155,10	0,929	100	2,641	500	N.A.	-	144,09	409,62	N.A.
I.D3.5.NP.L500	158,86	0,929	100	2,517	400	N.A.	-	147,58	399,85	N.A.
I.D3.10.NP.L500	163,56	0,929	100	2,449	400	N.A.	-	151,95	400,56	N.A.

* hw length = halfwave length

Table 4.5 : Critical elastic buckling loads obtained from CUFSM analysis for unperforated specimens having 1000 mm column length.

Column	Yield Load (kN)	CUFSM RESULTS (LOAD FACTORS)						Critical Elastic Buckling Loads (kN)		
	P_y	$P_{cr\ell}/P_y$	hw. length (mm)	P_{crd}/P_y	hw. length (mm)	P_{cre}/P_y	hw. length (mm)	$P_{cr\ell}$	P_{crd}	P_{cre}
D.5.NP.L1000	113,74	1,651	50	0,737	200	1,843	1000	187,78	83,83	209,62
D.10.NP.L1000	118,44	0,902	120	0,933	140	2,001	1000	106,83	110,50	237,00
D.15.NP.L1000	123,14	0,918	100	1,349	400	2,031	1000	113,04	166,12	250,10
D.20.NP.L1000	127,84	0,921	100	1,569	500	1,971	1000	117,74	200,58	251,97
O.D2.5.NP.L1000	131,61	0,924	100	1,607	600	1,901	1000	121,61	211,50	250,19
O.D2.10.NP.L1000	136,31	0,929	100	1,502	600	1,817	1000	126,63	204,74	247,68
O.D2.15.NP.L1000	141,00	0,930	100	1,374	600	1,735	1000	131,13	193,73	244,64
O.D2.20.NP.L1000	145,70	0,931	100	1,255	600	N.A.	-	135,65	182,85	N.A.
O.D2.25.NP.L1000	150,40	0,931	100	1,157	600	N.A.	-	140,02	174,01	N.A.
O.D2.30.NP.L1000	155,10	0,930	100	1,084	600	N.A.	-	144,24	168,13	N.A.
O.D3.5.NP.L1000	158,86	0,930	100	1,072	600	N.A.	-	147,74	170,30	N.A.
O.D3.10.NP.L1000	163,56	0,930	100	1,155	700	N.A.	-	152,11	188,91	N.A.
I.D2.5.NP.L1000	131,60	0,922	100	1,668	600	1,895	1000	121,34	219,51	249,38
I.D2.10.NP.L1000	136,30	0,924	100	1,729	700	1,805	1000	125,94	235,66	246,02
I.D2.15.NP.L1000	141,00	0,926	100	1,778	700	1,735	1000	130,57	250,70	244,64
I.D2.20.NP.L1000	145,70	0,927	100	1,693	1000	N.A.	-	135,06	246,67	N.A.
I.D2.25.NP.L1000	150,40	0,928	100	1,678	1000	N.A.	-	139,57	252,37	N.A.
I.D2.30.NP.L1000	155,10	0,929	100	1,692	1000	N.A.	-	144,09	262,43	N.A.
I.D3.5.NP.L1000	158,86	0,929	100	1,708	1000	N.A.	-	147,58	271,33	N.A.
I.D3.10.NP.L1000	163,56	0,929	100	1,715	1000	N.A.	-	151,95	280,51	N.A.
* hw length = halfwave length										

Table 4.6 : Critical elastic buckling loads obtained from CUFSM analysis for unperforated specimens having 1500 mm column length.

Column	Yield Load (kN)	CUFSM RESULTS (LOAD FACTORS)						Critical Elastic Buckling Loads (kN)		
	P_y	$P_{cr\ell}/P_y$	hw. length (mm)	P_{crd}/P_y	hw. length (mm)	P_{cre}/P_y	hw. length (mm)	$P_{cr\ell}$	P_{crd}	P_{cre}
D.5.NP.L1500	113,74	1,651	50	0,737	200	0,909	1500	187,78	83,83	103,39
D.10.NP.L1500	118,44	0,902	120	0,933	140	1,009	1500	106,83	110,50	119,51
D.15.NP.L1500	123,14	0,918	100	1,349	400	1,119	1500	113,04	166,12	137,79
D.20.NP.L1500	127,84	0,921	100	1,569	500	1,242	1500	117,74	200,58	158,78
O.D2.5.NP.L1500	131,61	0,924	100	1,607	600	1,294	1500	121,61	211,50	170,30
O.D2.10.NP.L1500	136,31	0,929	100	1,502	600	1,369	1500	126,63	204,74	186,61
O.D2.15.NP.L1500	141,00	0,930	100	1,374	600	1,457	1500	131,13	193,73	205,44
O.D2.20.NP.L1500	145,70	0,931	100	1,255	600	1,554	1500	135,65	182,85	226,42
O.D2.25.NP.L1500	150,40	0,931	100	1,157	600	1,646	1500	140,02	174,01	247,56
O.D2.30.NP.L1500	155,10	0,930	100	1,084	600	1,670	1500	144,24	168,13	259,02
O.D3.5.NP.L1500	158,86	0,930	100	1,072	600	1,655	1500	147,74	170,30	262,91
O.D3.10.NP.L1500	163,56	0,930	100	1,155	700	1,588	1500	152,11	188,91	259,73
I.D2.5.NP.L1500	131,60	0,922	100	1,668	600	1,271	1500	121,34	219,51	167,26
I.D2.10.NP.L1500	136,30	0,924	100	1,729	700	1,269	1500	125,94	235,66	172,96
I.D2.15.NP.L1500	141,00	0,926	100	1,778	700	1,242	1500	130,57	250,70	175,12
I.D2.20.NP.L1500	145,70	0,927	100	1,693	1000	1,204	1500	135,06	246,67	175,42
I.D2.25.NP.L1500	150,40	0,928	100	1,678	1000	1,165	1500	139,57	252,37	175,22
I.D2.30.NP.L1500	155,10	0,929	100	1,692	1000	1,130	1500	144,09	262,43	175,26
I.D3.5.NP.L1500	158,86	0,929	100	1,708	1000	1,106	1500	147,58	271,33	175,70
I.D3.10.NP.L1500	163,56	0,929	100	1,715	1000	1,079	1500	151,95	280,51	176,48
* hw length = halfwave length										

Table 4.7 : Nominal axial strengths of unperforated specimens having 500 mm column length.

Column	DSM Calculations Results (kN)			Nominal Strength (kN)	
	P_{ne}	P_{nt}	P_{nd}	P_n	Controlling Mode
D.5.NP.L500	113,69	113,50	74,99	74,99	Distortional controls
D.10.NP.L500	118,39	97,30	86,40	86,40	Distortional controls
D.15.NP.L500	123,09	101,72	103,30	101,72	Local-Global controls
D.20.NP.L500	127,79	105,72	112,60	105,72	Local-Global controls
O.D2.5.NP.L500	131,55	108,94	117,00	108,94	Local-Global controls
O.D2.10.NP.L500	136,24	113,04	119,50	113,04	Local-Global controls
O.D2.15.NP.L500	140,94	116,98	120,40	116,98	Local-Global controls
O.D2.20.NP.L500	145,64	120,90	120,60	120,60	Distortional controls
O.D2.25.NP.L500	150,34	124,80	121,10	121,10	Distortional controls
O.D2.30.NP.L500	155,04	128,70	122,25	122,25	Distortional controls
O.D3.5.NP.L500	158,79	131,80	125,46	125,46	Distortional controls
O.D3.10.NP.L500	163,49	135,70	135,35	135,35	Distortional controls
I.D2.5.NP.L500	131,55	108,87	118,70	108,87	Local-Global controls
I.D2.10.NP.L500	136,24	112,83	126,20	112,83	Local-Global controls
I.D2.15.NP.L500	140,94	116,81	133,60	116,81	Local-Global controls
I.D2.20.NP.L500	145,64	120,75	140,80	120,75	Local-Global controls
I.D2.25.NP.L500	150,34	124,69	147,40	124,69	Local-Global controls
I.D2.30.NP.L500	155,04	128,63	153,40	128,63	Local-Global controls
I.D3.5.NP.L500	158,79	131,75	156,20	131,75	Local-Global controls
I.D3.10.NP.L500	163,49	135,64	160,20	135,64	Local-Global controls

Table 4.8 : Nominal axial strengths of unperforated specimens having 1000 mm column length.

Column	DSM Calculations Results (kN)			Nominal Strength (kN)	
	P_{ne}	P_{nt}	P_{nd}	P_n	Controlling Mode
D.5.NP.L1000	90,63	90,60	74,99	74,99	Distortional controls
D.10.NP.L1000	96,09	84,56	86,37	84,56	Local-Global controls
D.15.NP.L1000	100,21	88,60	103,28	88,60	Local-Global controls
D.20.NP.L1000	103,38	91,69	112,64	91,69	Local-Global controls
O.D2.5.NP.L1000	105,60	94,00	116,81	94,00	Local-Global controls
O.D2.10.NP.L1000	108,27	96,86	118,47	96,86	Local-Global controls
O.D2.15.NP.L1000	110,78	99,49	119,00	99,49	Local-Global controls
O.D2.20.NP.L1000	145,64	120,92	119,13	119,13	Distortional controls
O.D2.25.NP.L1000	150,34	124,82	119,36	119,36	Distortional controls
O.D2.30.NP.L1000	155,04	128,67	120,07	120,07	Distortional controls
O.D3.5.NP.L1000	158,79	131,79	122,46	122,46	Distortional controls
O.D3.10.NP.L1000	163,49	135,69	129,72	129,72	Distortional controls
I.D2.5.NP.L1000	105,52	93,88	118,09	93,88	Local-Global controls
I.D2.10.NP.L1000	108,09	96,58	123,58	96,58	Local-Global controls
I.D2.15.NP.L1000	110,78	99,35	128,83	99,35	Local-Global controls
I.D2.20.NP.L1000	145,64	120,75	131,31	120,75	Local-Global controls
I.D2.25.NP.L1000	150,34	124,69	135,20	124,69	Local-Global controls
I.D2.30.NP.L1000	155,04	128,63	139,76	128,63	Local-Global controls
I.D3.5.NP.L1000	158,79	131,75	143,53	131,75	Local-Global controls
I.D3.10.NP.L1000	163,49	135,64	147,95	135,64	Local-Global controls

Table 4.9 : Nominal axial strengths of unperforated specimens having 1500 mm column length.

Column	DSM Calculations Results (kN)			Nominal Strength (kN)	
	P_{ne}	P_{nt}	P_{nd}	P_n	Controlling Mode
D.5.NP.L1500	71,77	71,77	74,99	71,77	Global controls
D.10.NP.L1500	78,23	73,55	86,37	73,55	Local-Global controls
D.15.NP.L1500	84,71	79,07	103,28	79,07	Local-Global controls
D.20.NP.L1500	91,27	84,27	112,64	84,27	Local-Global controls
O.D2.5.NP.L1500	95,24	87,65	116,81	87,65	Local-Global controls
O.D2.10.NP.L1500	100,40	92,04	118,47	92,04	Local-Global controls
O.D2.15.NP.L1500	105,79	96,44	119,00	96,44	Local-Global controls
O.D2.20.NP.L1500	111,30	100,91	119,13	100,91	Local-Global controls
O.D2.25.NP.L1500	116,63	105,23	119,36	105,23	Local-Global controls
O.D2.30.NP.L1500	120,72	108,75	120,07	108,75	Local-Global controls
O.D3.5.NP.L1500	123,36	111,21	122,46	111,21	Local-Global controls
O.D3.10.NP.L1500	125,66	113,68	129,72	113,68	Local-Global controls
I.D2.5.NP.L1500	94,68	87,23	118,09	87,23	Local-Global controls
I.D2.10.NP.L1500	98,01	90,38	123,58	90,38	Local-Global controls
I.D2.15.NP.L1500	100,66	93,11	128,83	93,11	Local-Global controls
I.D2.20.NP.L1500	102,92	95,55	131,31	95,55	Local-Global controls
I.D2.25.NP.L1500	105,01	97,89	135,20	97,89	Local-Global controls
I.D2.30.NP.L1500	107,09	100,22	139,76	100,22	Local-Global controls
I.D3.5.NP.L1500	108,81	102,09	143,53	102,09	Local-Global controls
I.D3.10.NP.L1500	110,97	104,43	147,95	104,43	Local-Global controls

4.1.2 Nominal strength - lip length relationships of unperforated column models

Totally 6 different nominal strength graphs have been constructed for unperforated models for different column lengths (L=500, L=1000, L=1500) and different lip lengths and directions. Half of these graphs show the relationship for inward lip direction cases. And the other half for the outward lip direction cases as described at the begining of chapter 4. X axis of these graphs indicate the lip length and Y axis indicate the nominal strengths of the sepcimens. 5 mm - 20 mm interval of the lip length indicates the D length. D_2 length covers the margin of 20 mm – 50 mm which is also indicating the specimen's lip configuration continues inwards or outwards. D_3 length of specimen covers the final 50 mm – 60 mm interval. These regions are shown on all the following graphs. In figures 4.3 to 4.8 ; these graphs are given for unperforated specimens. Controlling buckling modes are marked as D for distortional buckling, LG for Local-global buckling and G for global buckling.

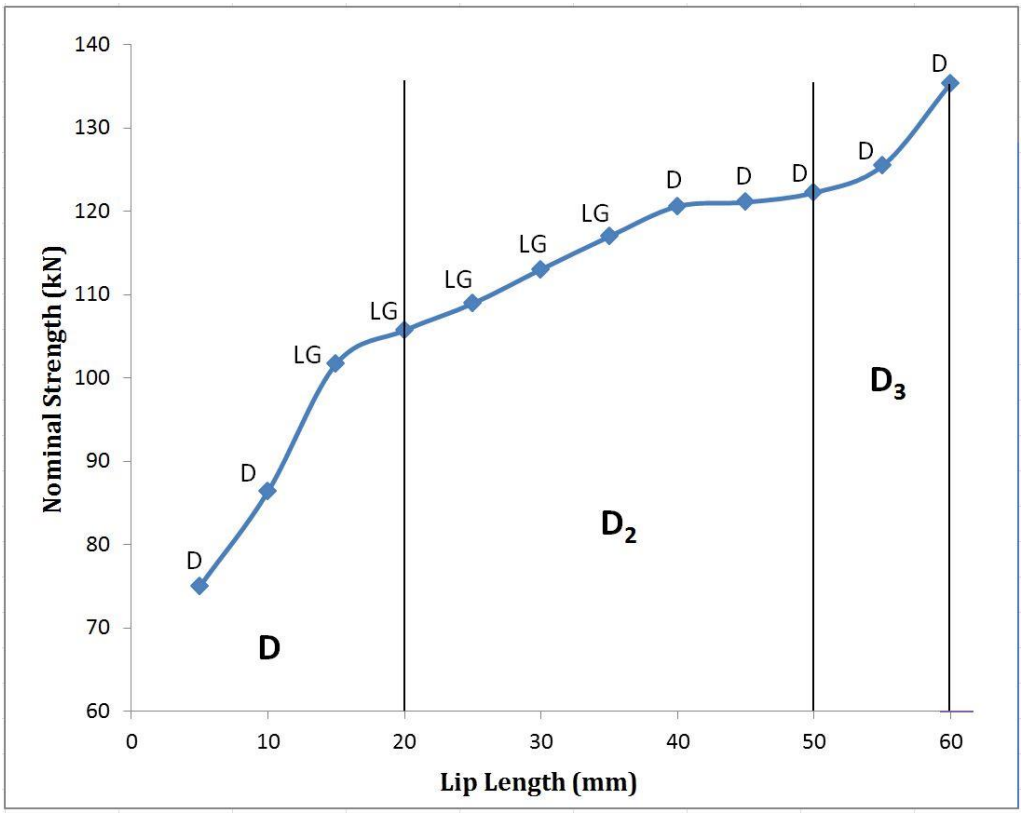

Figure 4.3 : Nominal strength – lip length relationship of the unperforated specimens having 500 mm column length (lip continues outward).

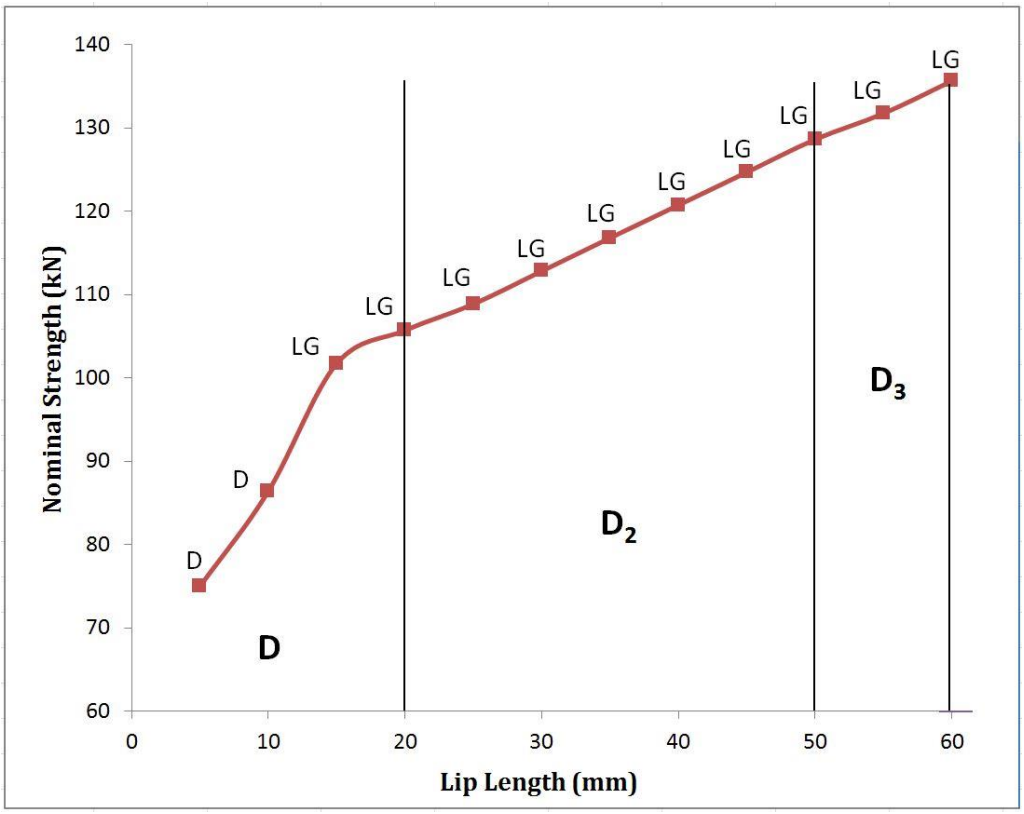

Figure 4.4 : Nominal strength – lip length relationship of the unperforated specimens having 500 mm column length (lip continues inward).

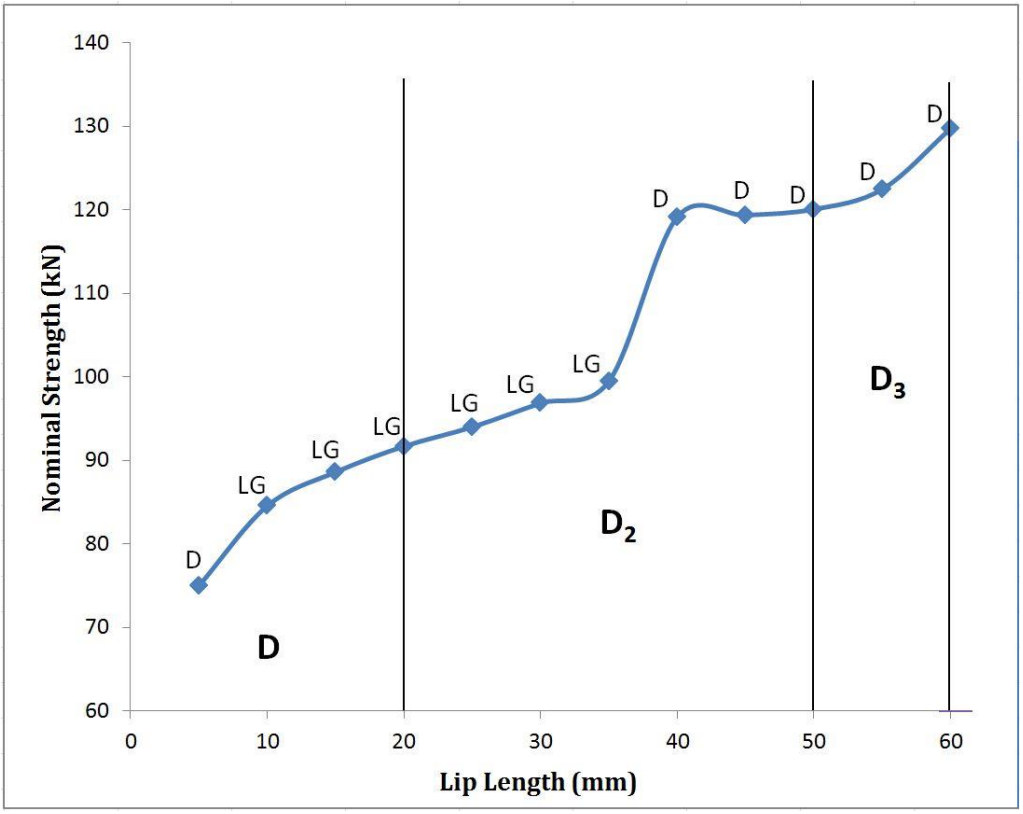
Nominal Strength (kN)
Lip Length (mm)
140
130
120
110
100
90
80
70
60
0
10
20
30
40
50
60
D
LG
D
D
D

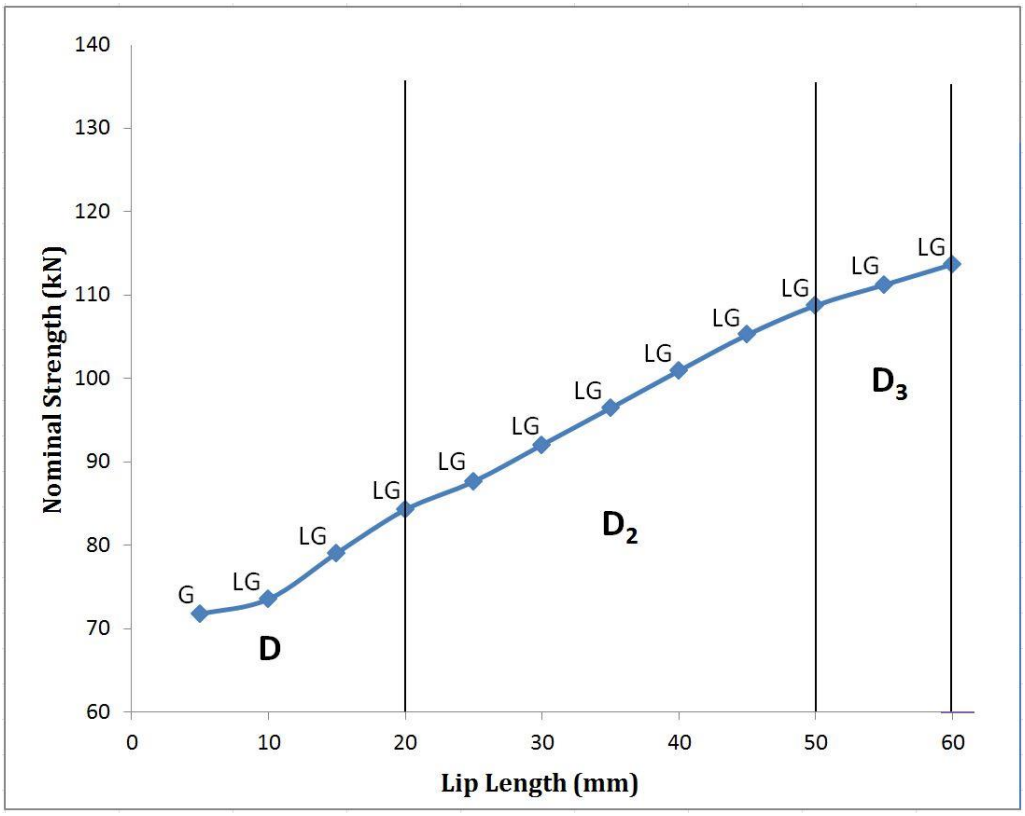

Figure 4.7 : Nominal strength – lip length relationship of the unperforated specimens having 1500 mm column length (lip continues outward).

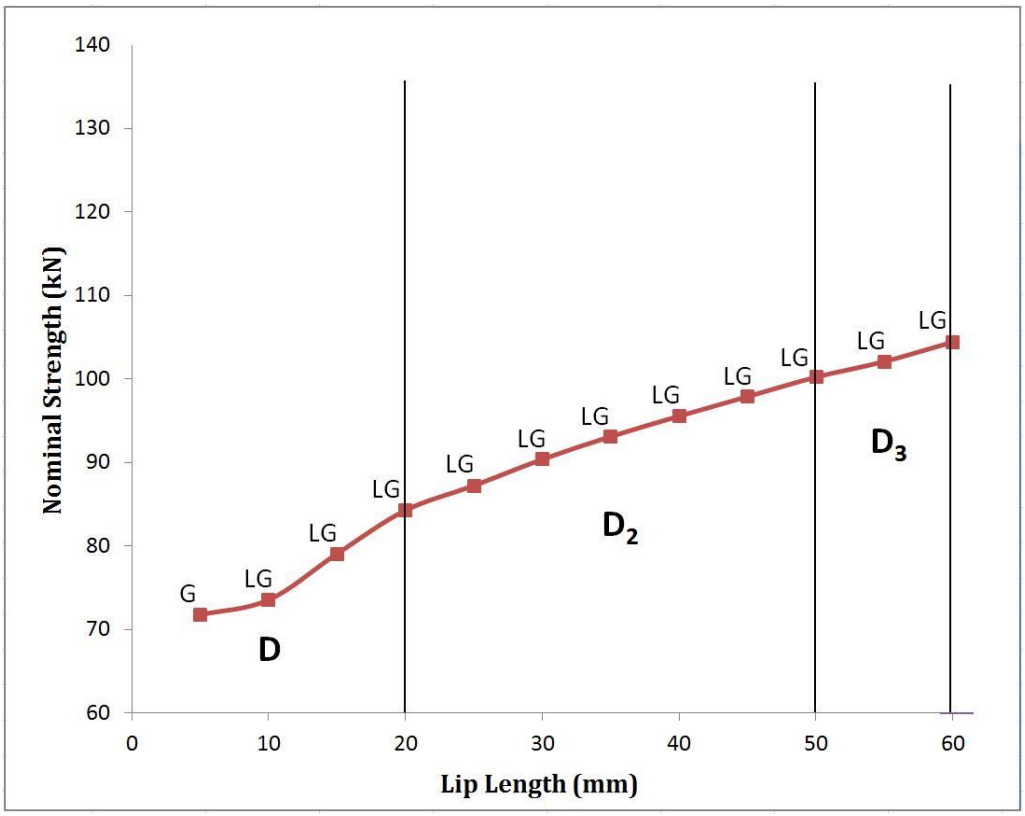

Figure 4.8 : Nominal strength – lip length relationship of the unperforated specimens having 1500 mm column length (lip continues inward).

4.1.2.1 General comparison of results for unperforated column models

Previous graphs are used to compare the nominal strengths of unperforated specimens. Five different graphs have been constructed with two major feature. First feature is the lip direction. Figures 4.9 to 4.11 include the comparison between the sections having same column length different lip directions. Figures 4.12 and 4.13 include the comparison between the sections having same lip direction different column lengths.

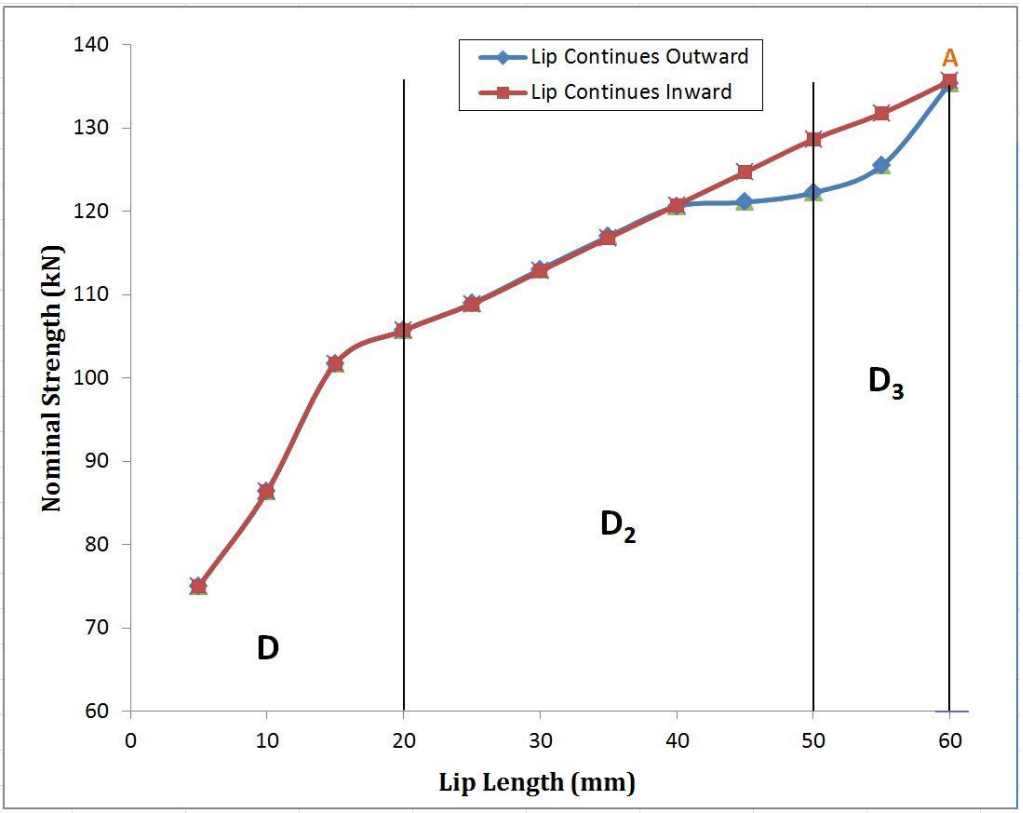

Figure 4.9 : Comparison of nominal strength – lip length relationship of the unperforated specimens having 500 mm column length.

On specimens having 500 mm and 1000 mm column lengths; lip direction starts to effect the column strength after 40 mm lip length which means D_2 lip is 20 mm long. Comparing the outward and inward lip cases, it is noted that there is a 5% strength difference the outward case being lower than the inward case. On specimens having 500 mm column length, it is observed that 2 specimens having maximum limit of lip length (60 mm) but having different lip directions have the same column capacity. This is shown by point A on Figure 4.9.

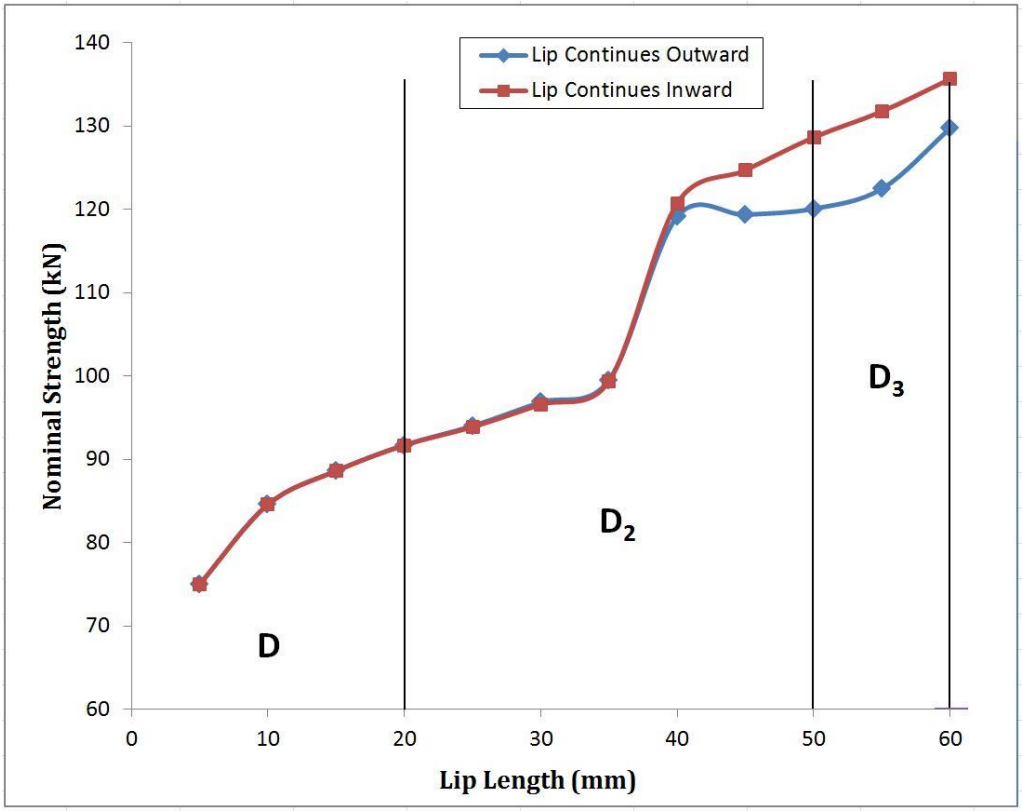

Figure 4.10 : Comparison of nominal strength – lip length relationship of the unperforated specimens having 1000 mm column length.

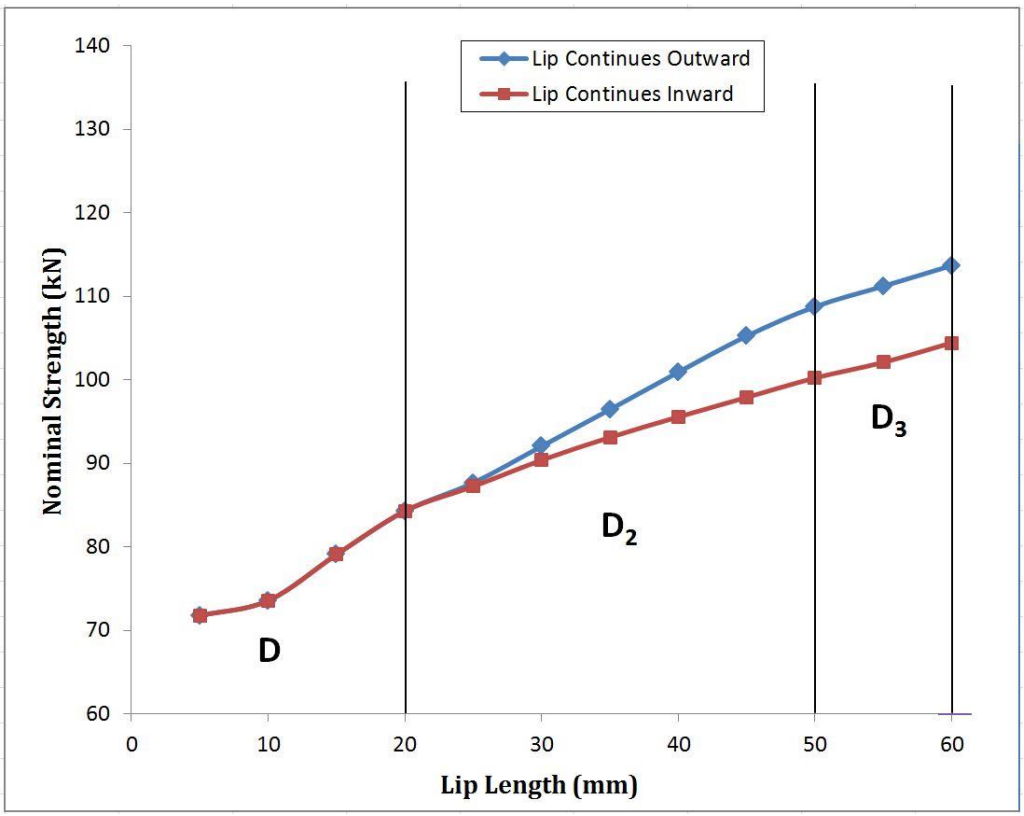

Figure 4.11 : Comparison of nominal strength – lip length relationship of the unperforated specimens having 1500 mm column length.

However, on specimens having 1000 mm column length, strength loss starts on the same lip length as in 500 mm column length but 2 specimens having maximum limit of lip length (60 mm) don't have the same strength. Similar trend is observed for 1000 column lengths as in 500 mm column lengths.Between 40mm and 60mm lip lengths (D_2 = 20-40 mm) if lip continues outwards, column strength will be less than in the situation that lip continues inwards. In this region; maximum strength difference is noted as 7.1%

On specimens having 1500 mm column length, a more or less linear relationship is observed both for outward and inward lip cases. The column strength of specimens having lips continuing outwards is greater than the column strength of the specimens having lips continuing inwards. Strength difference is up to 8.8% on sections having maximum lip length. Figures 4.12 and 4.13 include the comparison of nominal strengths for the models having same lip direction but different column lengths.

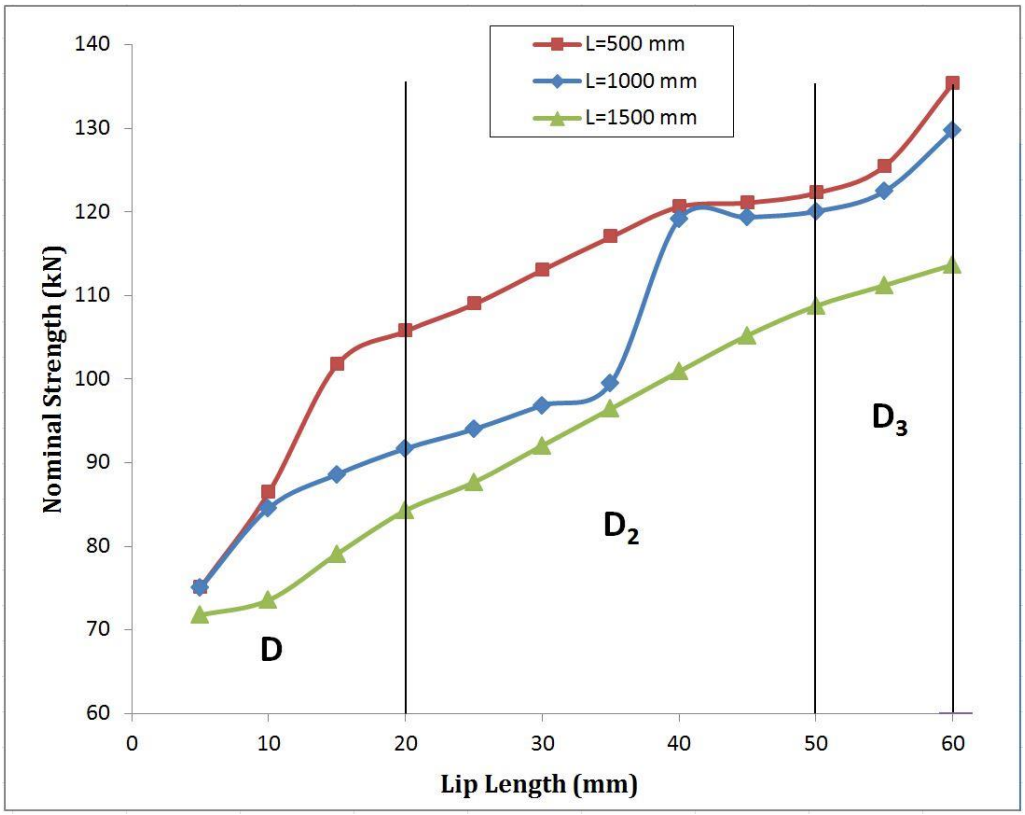

Figure 4.12 : Comparison between nominal strength – lip length relationships of the unperforated specimens having lips continuing outwards.

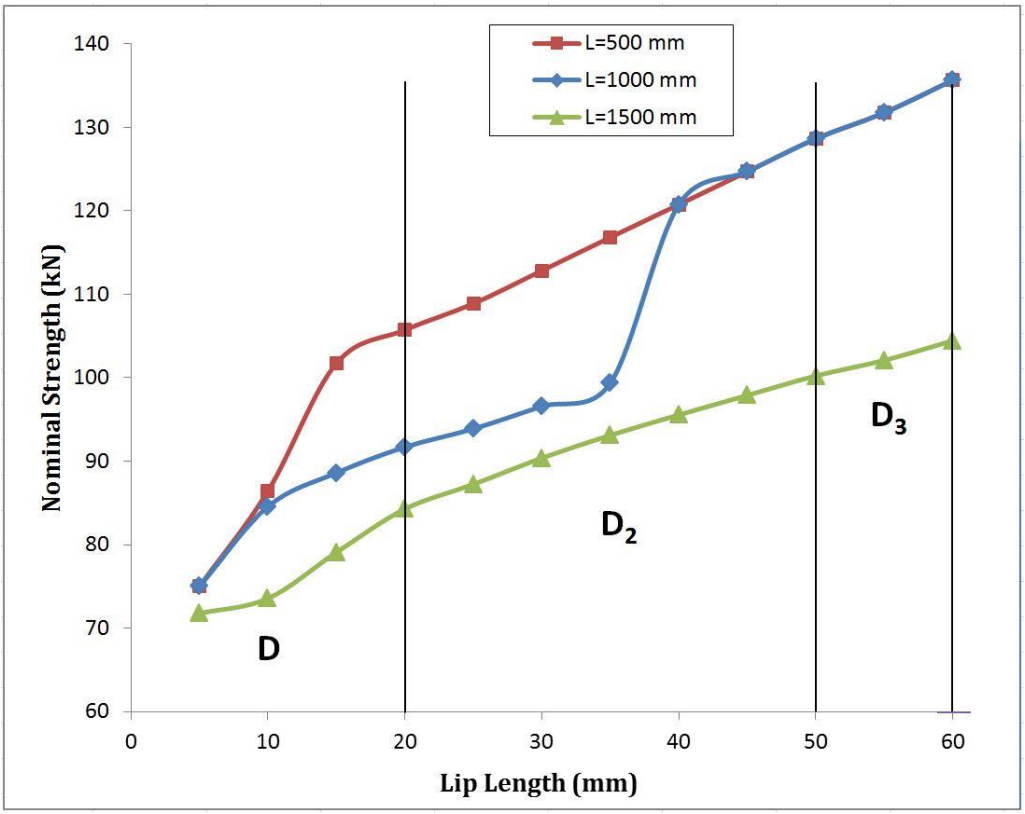

Figure 4.13 : Comparison between nominal strength – lip length relationships of the unperforated specimens having lips continuing inwards.

On specimens having lips continuing inwards; 1500 mm long specimens have the same approximate linearity on its function between column strength and lip length. An interesting point is noted on 500 mm and 1000 mm long specimens, column strengths are the same on 44 mm of lip length (D_2 lip = 24 mm). And the strength gain and the column strength are the same on increasing lip lengths. That means D_3 lip causes the same effect on both 500 mm and 1000 mm long specimens. It should be noted that for this region of lip lengths for both 500 mm and 1000 mm specimens local-global buckling is the controlling mode. On 1000 mm long specimens, between the lip length of 34-42 mm (D_2 lip = 14-22 m) there's a significant increase in column strength which is also similar with specimens with lips continuing inwards. As noted earlier; this situation seems to be related with the change in the buckling mode of corresponding cross-sections in this region (from distortional to local-global and vice versa).

4.2 Analysis of Perforated Specimens

60 perforated column models have been used in the analysis. The models have same hole configuration and different lip directions and lengths. Perforation configuration for all perforated specimens are same and given in Figure 4.14. Major concern is the effect of web perforations in rack columns. The flange perforations are not included on models, only perforations on the webs are considered. Reduced Thickness approach is used, which is previously explained in section 2.2 in the study titled "Design of Steel Storage Rack Columns via the Direct Strength Method" [61]. Chosen perforation configuration of the model is within the geometric limits of reduced thickness table given in Table 4.10.

Table 4.10 : Limits of the model of reduced thickness [61].

Parameters	Limits	Parameters	limits
B/t	24 to 88	L_{np}/L	0.33 to 0.62
H/t	26 to 83	B_{np}/B	0.51 to 0.90
H/B	0.48 to 1.87	$B_{pflange}/H$	<0.33
L	50 mm to 75 mm	$L_{pflange}/L$	<0.35
B_p/L_p	≤1.6	$(B_{pflange}\ L_{pflange})/(H \cdot L)$	<0.042

Main geometric parameters of a column having web perforations have already been given in Figure 2.26. A check based on these limits has been made for the chosen configuration of perforations on our typical model. Dimension notation in Figure 4.14 is adapted for the limits given in Table 4.10 and following calculations are related with these limits.

$B/t = 140/2 = 70$	in the limits of 24 to 88	**OK!**
$H/t = 80/2 = 40$	in the limits of 26 to 83	**OK!**
$H/B = 80/140 = 0.571$	in the limits of 0.48 to 1.87	**OK!**
$L = 60$ mm	in the limits of 50 mm to 75 mm	**OK!**
$B_p/L_p = 30/25 = 1.20$	≤ 1.6	**OK!**
$L_{np} = L - L_p = 60 - 25 = 35$	$B_{np} = B - B_p = 140 - 30 = 110$	
$L_{np}/L = 35/60 = 0.583$	in the limits of 0.33 to 0.62	**OK!**
$B_{np}/B = 110/140 = 0.786$	in the limits of 0.51 to 0.90	**OK!**

Geometric details of all perforated specimens used are given in tables 4.11 to 4.13 for different column lengths. Specimen designation is the same as previously described in Figure 4.2. In these tables, perforated section areas are calculated and given for different models.

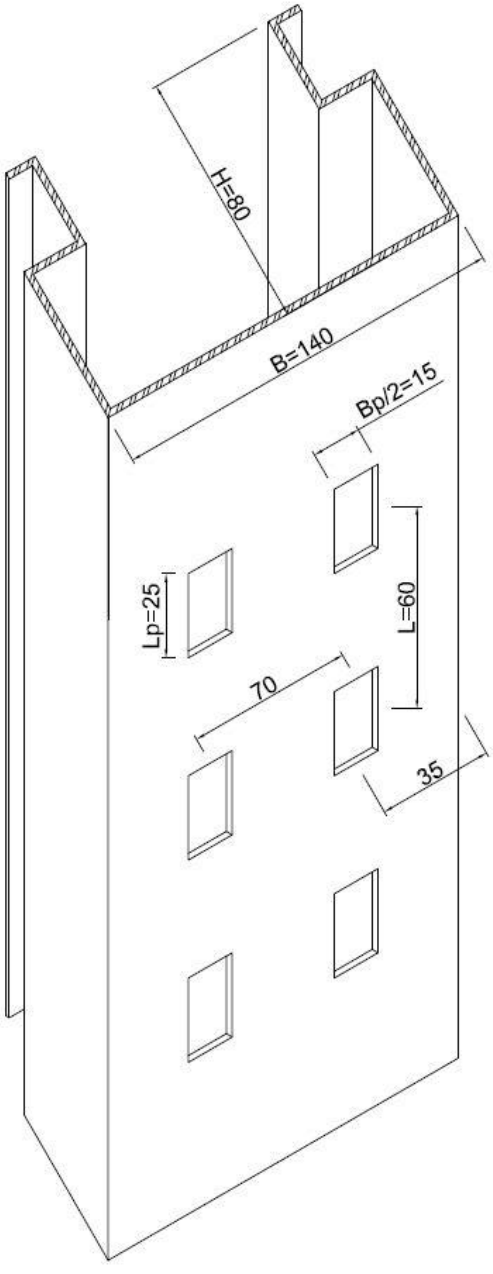

Figure 4.14 : Typical model for perforation configuration of all perforated specimens.

Table 4.11 : Geometric properties of unperforated specimens having 500 mm column length.

Column	t (mm)	h_0 (mm)	b_0 (mm)	D (mm)	D_2 (mm)	D_3 (mm)	Section Area (mm^2)	Perforated Sect. Area (mm^2)	Column Length (mm)
D.5.P.L500	2	140	50	5	-	-	484	424	500
D.10.P.L500	2	140	50	10	-	-	504	444	500
D.15.P.L500	2	140	50	15	-	-	524	464	500
D.20.P.L500	2	140	50	20	-	-	544	484	500
O.D2.5.P.L500	2	140	50	20	5	-	556	496	500
O.D2.10.P.L500	2	140	50	20	10	-	576	516	500
O.D2.15.P.L500	2	140	50	20	15	-	596	536	500
O.D2.20.P.L500	2	140	50	20	20	-	616	556	500
O.D2.25.P.L500	2	140	50	20	25	-	636	576	500
O.D2.30.P.L500	2	140	50	20	30	-	656	596	500
O.D3.5.P.L500	2	140	50	20	30	5	668	608	500
O.D3.10.P.L500	2	140	50	20	30	10	688	628	500
I.D2.5.P.L500	2	140	50	20	5	-	556	496	500
I.D2.10.P.L500	2	140	50	20	10	-	576	516	500
I.D2.15.P.L500	2	140	50	20	15	-	596	536	500
I.D2.20.P.L500	2	140	50	20	20	-	616	556	500
I.D2.25.P.L500	2	140	50	20	25	-	636	576	500
I.D2.30.P.L500	2	140	50	20	30	-	656	596	500
I.D3.5.P.L500	2	140	50	20	30	5	668	608	500
I.D3.10.P.L500	2	140	50	20	30	10	688	628	500

Table 4.12 : Geometric properties of unperforated specimens having 1000 mm column length.

Column	t (mm)	h_0 (mm)	b_0 (mm)	D (mm)	D_2 (mm)	D_3 (mm)	Section Area (mm^2)	Perforated Sect. Area (mm^2)	Column Length (mm)
D.5.P.L1000	2	140	50	5	-	-	484	424	1000
D.10.P.L1000	2	140	50	10	-	-	504	444	1000
D.15.P.L1000	2	140	50	15	-	-	524	464	1000
D.20.P.L1000	2	140	50	20	-	-	544	484	1000
O.D2.5.P.L1000	2	140	50	20	5	-	556	496	1000
O.D2.10.P.L1000	2	140	50	20	10	-	576	516	1000
O.D2.15.P.L1000	2	140	50	20	15	-	596	536	1000
O.D2.20.P.L1000	2	140	50	20	20	-	616	556	1000
O.D2.25.P.L1000	2	140	50	20	25	-	636	576	1000
O.D2.30.P.L1000	2	140	50	20	30	-	656	596	1000
O.D3.5.P.L1000	2	140	50	20	30	5	668	608	1000
O.D3.10.P.L1000	2	140	50	20	30	10	688	628	1000
I.D2.5.P.L1000	2	140	50	20	5	-	556	496	1000
I.D2.10.P.L1000	2	140	50	20	10	-	576	516	1000
I.D2.15.P.L1000	2	140	50	20	15	-	596	536	1000
I.D2.20.P.L1000	2	140	50	20	20	-	616	556	1000
I.D2.25.P.L1000	2	140	50	20	25	-	636	576	1000
I.D2.30.P.L1000	2	140	50	20	30	-	656	596	1000
I.D3.5.P.L1000	2	140	50	20	30	5	668	608	1000
I.D3.10.P.L1000	2	140	50	20	30	10	688	628	1000

Table 4.13 : Geometric properties of unperforated specimens having 1500 mm column length.

Column	t (mm)	h_0 (mm)	b_0 (mm)	D (mm)	D_2 (mm)	D_3 (mm)	Section Area (mm^2)	Perforated Sect. Area (mm^2)	Column Length (mm)
D.5.P.L1500	2	140	50	5	-	-	484	424	1500
D.10.P.L1500	2	140	50	10	-	-	504	444	1500
D.15.P.L1500	2	140	50	15	-	-	524	464	1500
D.20.P.L1500	2	140	50	20	-	-	544	484	1500
O.D2.5.P.L1500	2	140	50	20	5	-	556	496	1500
O.D2.10.P.L1500	2	140	50	20	10	-	576	516	1500
O.D2.15.P.L1500	2	140	50	20	15	-	596	536	1500
O.D2.20.P.L1500	2	140	50	20	20	-	616	556	1500
O.D2.25.P.L1500	2	140	50	20	25	-	636	576	1500
O.D2.30.P.L1500	2	140	50	20	30	-	656	596	1500
O.D3.5.P.L1500	2	140	50	20	30	5	668	608	1500
O.D3.10.P.L1500	2	140	50	20	30	10	688	628	1500
I.D2.5.P.L1500	2	140	50	20	5	-	556	496	1500
I.D2.10.P.L1500	2	140	50	20	10	-	576	516	1500
I.D2.15.P.L1500	2	140	50	20	15	-	596	536	1500
I.D2.20.P.L1500	2	140	50	20	20	-	616	556	1500
I.D2.25.P.L1500	2	140	50	20	25	-	636	576	1500
I.D2.30.P.L1500	2	140	50	20	30	-	656	596	1500
I.D3.5.P.L1500	2	140	50	20	30	5	668	608	1500
I.D3.10.P.L1500	2	140	50	20	30	10	688	628	1500

4.2.1 Analytical study on perforated members using direct strength method

A study including construction of elastic buckling curves with CUFSM Software and DSM Calculations has been done to calculate the nominal section strength of these specimens. Critical elastic column buckling loads of these various sections are obtained from CUFSM software. For the calculation of elastic buckling loads for all perforated specimens reduced thickness method was used. In section 2.3 of this thesis; reduced thickness formulas have been given. Details of this method was presented in section 2.3 under the title “Design of Steel Storage Rack Columns via the Direct Strength Method” [61].

Basically; 3 different reduced thickness values are calculated in the begining of analysis. In CUFSM, perforation locations are represented by elements having these reduced thickness values. A typical section constructed in CUFSM is given in Figure 4.16 for reduced thickness approach where reduced thickness on the section is shown. For the determination of each buckling load (local, distortional, global) a seperate calculation was made by using a different reduced thickness formula e.g. for the calculation of elastic buckling load for distortional buckling, the corresponding formula is used to calculate the reduced thickness value. Following formulas are used for determining reduced thickness values for local, distortional and global (torsional-

flexural) buckling modes for all perforated specimens. Formulas used are previously given in section 2.3:

Reduced thickness for local buckling;

$$t_{rL} = 0.61t\frac{L_{np}B_{np}}{LH} + 0.18t\frac{B_p}{L_p} + 0.11 \quad \textbf{(2.24)}$$

$$t_{rL} = 0.61 \times 2 \times \frac{35 \times 110}{60 \times 80} + 0.18 \times 2 \times \frac{30}{25} + 0.11 = 1.521 \text{ mm}$$

Reduced thickness for distortional buckling;

$$t_{rD} = 0.9t\left(\frac{L_{np}}{L}\right)^{1/3} \quad \textbf{(2.25)}$$

$$t_{rD} = 0.9 \times 2 \times \left(\frac{35}{60}\right)^{1/3} = 1.504 \text{ mm}$$

Reduced thickness for torsional-flexural buckling;

$$t_{rG} = 0.7t\left(\frac{L_{np}}{L}\right) \quad \textbf{(2.26)}$$

$$t_{rG} = 0.7 \times 2 \times \left(\frac{35}{60}\right) = 0.817 \text{ mm}$$

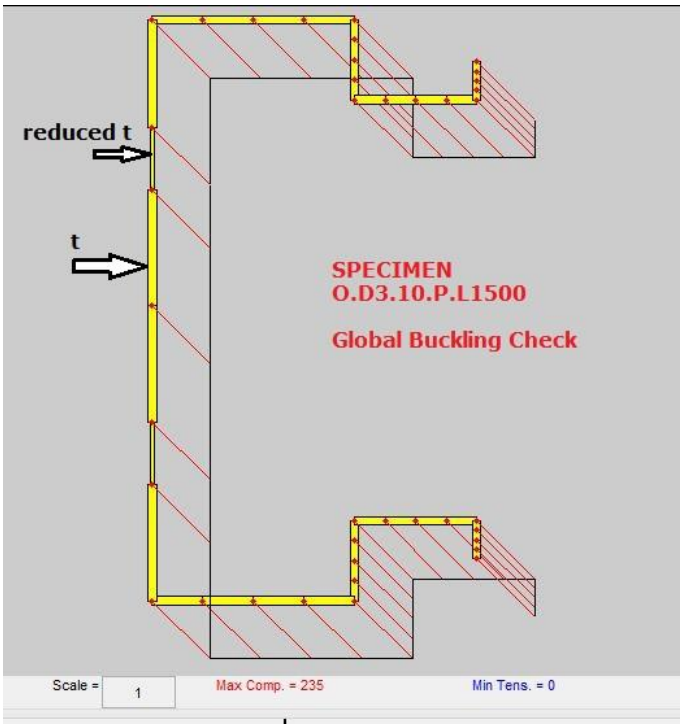

Figure 4.15 : Typical model for reduced thickness approach from CUFSM.

These thickness values are used where perforations are situated on cross-sections constructed with CUFSM software. Tables 4.14 to 4.16 include the results of critical elastic buckling loads obtained by CUFSM. Each critical elastic buckling load is found using related reduced thickness value for the effects of perforations. For models with non-existent buckling modes; a high value of elastic critical buckling load is intentionally assumed to calculate the slenderness values. The non-existent buckling modes are indicated with N.A in relevant cells of tables 4.14 to 4.16.

Direct Strength Method is used after obtaining the critical elastic buckling loads. Nominal strengths for local, distortional and global buckling are calculated with DSM equations. Then, the nominal strength for all sections are determined. Results are given in tables 4.17 to 4.19. Controlling mode indicates which buckling mode governs the behaviour of the member.

Table 4.14 : Critical elastic buckling loads obtained from CUFSM analysis for perforated specimens having 500 mm column length.

Column	Yield Load (kN)	CUFSM RESULTS (LOAD FACTORS)						Critical Elastic Buckling Loads (kN)		
	P_y	$P_{crℓ}/P_y$	hw. length (mm)	P_{crd}/P_y	hw. length (mm)	P_{cre}/P_y	hw. length (mm)	$P_{crℓ}$	P_{crd}	P_{cre}
D.5.P.L500	99,64	1,007	70	0,680	200	N.A.	-	100,34	67,76	N.A.
D.10.P.L500	104,34	0,840	100	0,960	300	N.A.	-	87,65	100,17	N.A.
D.15.P.L500	109,04	0,849	100	1,240	400	N.A.	-	92,57	135,21	N.A.
D.20.P.L500	113,74	0,852	100	1,439	500	N.A.	-	96,91	163,67	N.A.
O.D2.5.P.L500	116,56	0,856	100	1,503	500	N.A.	-	99,78	175,19	N.A.
O.D2.10.P.L500	121,26	0,860	100	1,444	500	N.A.	-	104,28	175,10	N.A.
O.D2.15.P.L500	125,96	0,861	100	1,332	500	N.A.	-	108,45	167,78	N.A.
O.D2.20.P.L500	130,66	0,862	100	1,220	500	N.A.	-	112,63	159,41	N.A.
O.D2.25.P.L500	135,36	0,862	100	1,130	500	N.A.	-	116,68	152,96	N.A.
O.D2.30.P.L500	140,06	0,862	100	1,069	500	N.A.	-	120,73	149,72	N.A.
O.D3.5.P.L500	142,88	0,862	100	1,076	500	N.A.	-	123,16	153,74	N.A.
O.D3.10.P.L500	147,58	0,862	100	1,233	500	N.A.	-	127,21	181,97	N.A.
I.D2.5.P.L500	116,56	0,853	100	1,585	500	N.A.	-	99,43	184,75	N.A.
I.D2.10.P.L500	121,26	0,856	100	1,772	500	N.A.	-	103,80	214,87	N.A.
I.D2.15.P.L500	125,96	0,858	100	1,973	500	N.A.	-	108,07	248,52	N.A.
I.D2.20.P.L500	130,66	0,859	100	2,181	500	N.A.	-	112,24	284,97	N.A.
I.D2.25.P.L500	135,36	0,860	100	2,385	500	N.A.	-	116,41	322,83	N.A.
I.D2.30.P.L500	140,06	0,860	100	2,565	500	N.A.	-	120,45	359,25	N.A.
I.D3.5.P.L500	142,88	0,861	100	2,631	500	N.A.	-	123,02	375,92	N.A.
I.D3.10.P.L500	147,58	0,861	100	2,597	500	N.A.	-	127,07	383,27	N.A.

* hw length = halfwave length

Table 4.15 : Critical elastic buckling loads obtained from CUFSM analysis for perforated specimens having 1000 mm column length.

Column	Yield Load (kN)	CUFSM RESULTS (LOAD FACTORS)						Critical Elastic Buckling Loads (kN)		
	P_y	$P_{crℓ}/P_y$	hw. length (mm)	P_{crd}/P_y	hw. length (mm)	P_{cre}/P_y	hw. length (mm)	$P_{crℓ}$	P_{crd}	P_{cre}
D.5.P.L1000	99,64	1,007	70	0,680	200	1,265	1000	100,34	67,76	126,04
D.10.P.L1000	104,34	0,840	100	0,960	300	1,199	1000	87,65	100,17	125,10
D.15.P.L1000	109,04	0,849	100	1,240	400	1,116	1000	92,57	135,21	121,69
D.20.P.L1000	113,74	0,852	100	1,439	500	1,051	1000	96,91	163,67	119,54
O.D2.5.P.L1000	116,56	0,856	100	1,456	600	1,001	1000	99,78	169,71	116,68
O.D2.10.P.L1000	121,26	0,860	100	1,368	600	0,927	1000	104,28	165,88	112,41
O.D2.15.P.L1000	125,96	0,861	100	1,254	600	0,854	1000	108,45	157,95	107,57
O.D2.20.P.L1000	130,66	0,862	100	1,146	600	N.A.	-	112,63	149,74	N.A.
O.D2.25.P.L1000	135,36	0,862	100	1,056	600	N.A.	-	116,68	142,94	N.A.
O.D2.30.P.L1000	140,06	0,862	100	0,999	600	N.A.	-	120,73	139,92	N.A.
O.D3.5.P.L1000	142,88	0,862	100	0,982	700	N.A.	-	123,16	140,31	N.A.
O.D3.10.P.L1000	147,58	0,862	100	1,047	700	N.A.	-	127,21	154,52	N.A.
I.D2.5.P.L1000	116,56	0,853	100	1,518	600	1,020	1000	99,43	176,94	118,89
I.D2.10.P.L1000	121,26	0,856	100	1,571	700	1,007	1000	103,80	190,50	122,11
I.D2.15.P.L1000	125,96	0,858	100	1,584	1000	1,020	1000	108,07	199,52	128,48
I.D2.20.P.L1000	130,66	0,859	100	1,557	1000	N.A.	-	112,24	203,44	N.A.
I.D2.25.P.L1000	135,36	0,860	100	1,559	1000	N.A.	-	116,41	211,03	N.A.
I.D2.30.P.L1000	140,06	0,860	100	1,589	1000	N.A.	-	120,45	222,56	N.A.
I.D3.5.P.L1000	142,88	0,861	100	1,617	1000	N.A.	-	123,02	231,04	N.A.
I.D3.10.P.L1000	147,58	0,861	100	1,633	1000	N.A.	-	127,07	241,00	N.A.
* hw length = halfwave length										

Table 4.16 : Critical elastic buckling loads obtained from CUFSM analysis for perforated specimens having 1500 mm column length.

Column	Yield Load (kN)	CUFSM RESULTS (LOAD FACTORS)						Critical Elastic Buckling Loads (kN)		
	P_y	$P_{crℓ}/P_y$	hw. length (mm)	P_{crd}/P_y	hw. length (mm)	P_{cre}/P_y	hw. length (mm)	$P_{crℓ}$	P_{crd}	P_{cre}
D.5.P.L1500	99,64	1,007	70	0,680	200	0,887	1500	100,34	67,76	88,38
D.10.P.L1500	104,34	0,840	100	0,960	300	0,984	1500	87,65	100,17	102,67
D.15.P.L1500	109,04	0,849	100	1,240	400	1,049	1500	92,57	135,21	114,38
D.20.P.L1500	113,74	0,852	100	1,439	500	1,047	1500	96,91	163,67	119,09
O.D2.5.P.L1500	116,56	0,856	100	1,456	600	1,031	1500	99,78	169,71	120,17
O.D2.10.P.L1500	121,26	0,860	100	1,368	600	1,015	1500	104,28	165,88	123,08
O.D2.15.P.L1500	125,96	0,861	100	1,254	600	0,999	1500	108,45	157,95	125,83
O.D2.20.P.L1500	130,66	0,862	100	1,146	600	0,981	1500	112,63	149,74	128,18
O.D2.25.P.L1500	135,36	0,862	100	1,056	600	0,958	1500	116,68	142,94	129,67
O.D2.30.P.L1500	140,06	0,862	100	0,999	600	N.A.	-	120,73	139,92	N.A.
O.D3.5.P.L1500	142,88	0,862	100	0,982	700	N.A.	-	123,16	140,31	N.A.
O.D3.10.P.L1500	147,58	0,862	100	1,047	700	N.A.	-	127,21	154,52	N.A.
I.D2.5.P.L1500	116,56	0,853	100	1,518	600	1,022	1500	99,43	176,94	119,12
I.D2.10.P.L1500	121,26	0,856	100	1,571	700	0,981	1500	103,80	190,50	118,96
I.D2.15.P.L1500	125,96	0,858	100	1,584	1000	0,942	1500	108,07	199,52	118,65
I.D2.20.P.L1500	130,66	0,859	100	1,557	1000	0,912	1500	112,24	203,44	119,16
I.D2.25.P.L1500	135,36	0,860	100	1,559	1000	0,889	1500	116,41	211,03	120,34
I.D2.30.P.L1500	140,06	0,860	100	1,589	1000	0,882	1500	120,45	222,56	123,53
I.D3.5.P.L1500	142,88	0,861	100	1,617	1000	0,879	1500	123,02	231,04	125,59
I.D3.10.P.L1500	147,58	0,861	100	1,633	1000	0,873	1500	127,07	241,00	128,84
* hw length = halfwave length										

Table 4.17 : Nominal axial strengths of perforated specimens having 500 mm column length.

Column	DSM Calculations Results (kN)			Nominal Strength (kN)	
	P_{ne}	P_{nt}	P_{nd}	P_n	Controlling Mode
D.5.P.L500	99,60	84,86	63,38	63,38	Distortional controls
D.10.P.L500	104,30	83,67	76,98	76,98	Distortional controls
D.15.P.L500	108,99	87,76	88,77	87,76	Local-Global controls
D.20.P.L500	113,69	91,65	97,49	91,65	Local-Global controls
O.D2.5.P.L500	116,51	94,07	101,33	94,07	Local-Global controls
O.D2.10.P.L500	121,21	98,01	104,05	98,01	Local-Global controls
O.D2.15.P.L500	125,91	101,85	105,18	101,85	Local-Global controls
O.D2.20.P.L500	130,61	105,69	105,75	105,69	Local-Global controls
O.D2.25.P.L500	135,30	109,49	106,47	106,47	Distortional controls
O.D2.30.P.L500	140,00	113,30	107,85	107,85	Distortional controls
O.D3.5.P.L500	142,82	115,58	110,30	110,30	Distortional controls
O.D3.10.P.L500	147,52	119,38	119,90	119,38	Local-Global controls
I.D2.5.P.L500	116,51	93,96	103,02	93,96	Local-Global controls
I.D2.10.P.L500	121,21	97,86	110,69	97,86	Local-Global controls
I.D2.15.P.L500	125,91	101,73	118,19	101,73	Local-Global controls
I.D2.20.P.L500	130,61	105,57	125,34	105,57	Local-Global controls
I.D2.25.P.L500	135,30	109,41	131,99	109,41	Local-Global controls
I.D2.30.P.L500	140,00	113,21	138,04	113,21	Local-Global controls
I.D3.5.P.L500	142,82	115,53	141,26	115,53	Local-Global controls
I.D3.10.P.L500	147,52	119,33	145,68	119,33	Local-Global controls

Table 4.18 : Nominal axial strengths of perforated specimens having 1000 mm column length.

Column	DSM Calculations Results (kN)			Nominal Strength (kN)	
	P_{ne}	P_{nt}	P_{nd}	P_n	Controlling Mode
D.5.P.L1000	71,57	67,86	63,38	63,38	Distortional controls
D.10.P.L1000	73,59	66,23	76,98	66,23	Local-Global controls
D.15.P.L1000	74,94	68,24	88,77	68,24	Local-Global controls
D.20.P.L1000	76,38	70,15	97,49	70,15	Local-Global controls
O.D2.5.P.L1000	76,73	71,03	100,29	71,03	Local-Global controls
O.D2.10.P.L1000	77,20	72,34	102,19	72,34	Local-Global controls
O.D2.15.P.L1000	77,16	73,22	102,96	73,22	Local-Global controls
O.D2.20.P.L1000	130,61	105,69	103,32	103,32	Distortional controls
O.D2.25.P.L1000	135,30	109,49	103,73	103,73	Distortional controls
O.D2.30.P.L1000	140,00	113,30	105,00	105,00	Distortional controls
O.D3.5.P.L1000	142,82	115,58	106,38	106,38	Distortional controls
O.D3.10.P.L1000	147,52	119,38	112,72	112,72	Distortional controls
I.D2.5.P.L1000	77,33	71,32	101,65	71,32	Local-Global controls
I.D2.10.P.L1000	80,02	74,02	106,88	74,02	Local-Global controls
I.D2.15.P.L1000	83,56	77,22	111,31	77,22	Local-Global controls
I.D2.20.P.L1000	130,61	105,57	114,85	105,57	Local-Global controls
I.D2.25.P.L1000	135,30	109,41	119,03	109,41	Local-Global controls
I.D2.30.P.L1000	140,00	113,21	123,88	113,21	Local-Global controls
I.D3.5.P.L1000	142,82	115,53	127,05	115,53	Local-Global controls
I.D3.10.P.L1000	147,52	119,33	131,61	119,33	Local-Global controls

Table 4.19 : Nominal axial strengths of perforated specimens having 1500 mm column length.

Column	DSM Calculations Results (kN)			Nominal Strength (kN)	
	P_{ne}	$P_{n\ell}$	P_{nd}	P_n	Controlling Mode
D.5.P.L1500	62,16	61,61	63,38	61,61	Local-Global controls
D.10.P.L1500	68,19	62,89	76,98	62,89	Local-Global controls
D.15.P.L1500	73,16	67,14	88,77	67,14	Local-Global controls
D.20.P.L1500	76,26	70,07	97,49	70,07	Local-Global controls
O.D2.5.P.L1500	77,67	71,62	100,29	71,62	Local-Global controls
O.D2.10.P.L1500	80,28	74,29	102,19	74,29	Local-Global controls
O.D2.15.P.L1500	82,85	76,86	102,96	76,86	Local-Global controls
O.D2.20.P.L1500	85,28	79,34	103,32	79,34	Local-Global controls
O.D2.25.P.L1500	87,45	81,62	103,73	81,62	Local-Global controls
O.D2.30.P.L1500	140,00	113,30	106,97	106,97	Distortional controls
O.D3.5.P.L1500	142,82	115,58	106,38	106,38	Distortional controls
O.D3.10.P.L1500	147,52	119,38	112,72	112,72	Distortional controls
I.D2.5.P.L1500	77,39	71,36	101,65	71,36	Local-Global controls
I.D2.10.P.L1500	79,14	73,46	106,88	73,46	Local-Global controls
I.D2.15.P.L1500	80,77	75,46	111,31	75,46	Local-Global controls
I.D2.20.P.L1500	82,57	77,52	114,85	77,52	Local-Global controls
I.D2.25.P.L1500	84,53	79,70	119,03	79,70	Local-Global controls
I.D2.30.P.L1500	87,14	82,25	123,88	82,25	Local-Global controls
I.D3.5.P.L1500	88,75	83,85	127,05	83,85	Local-Global controls
I.D3.10.P.L1500	91,37	86,41	131,61	86,41	Local-Global controls

4.2.2 Nominal strength - lip length relationships of perforated column models

Totally 6 different nominal strength graphs have been constructed for perforated models for different column lengths (L=500, L=1000, L=1500) and different lip lengths and directions. Half of these graphs show the relationship for inward lip direction cases. And the other half for the outward lip direction cases as described at the begining of chapter 4. X axis of these graphs indicate the lip length and Y axis indicate the nominal strengths of the sepcimens. 5 mm - 20 mm interval of the lip length indicates the D length. D_2 length covers the margin of 20 mm – 50 mm which is also indicating the specimen's lip configuration continues inwards or outwards. D_3 length of specimen covers 50 mm – 60 mm interval. These regions are shown on all the following graphs. In figures 4.16 to 4.21 ; these graphs are given for perforated specimens. Controlling buckling modes are marked as D for distortional buckling, LG for Local-global buckling and G for global buckling.

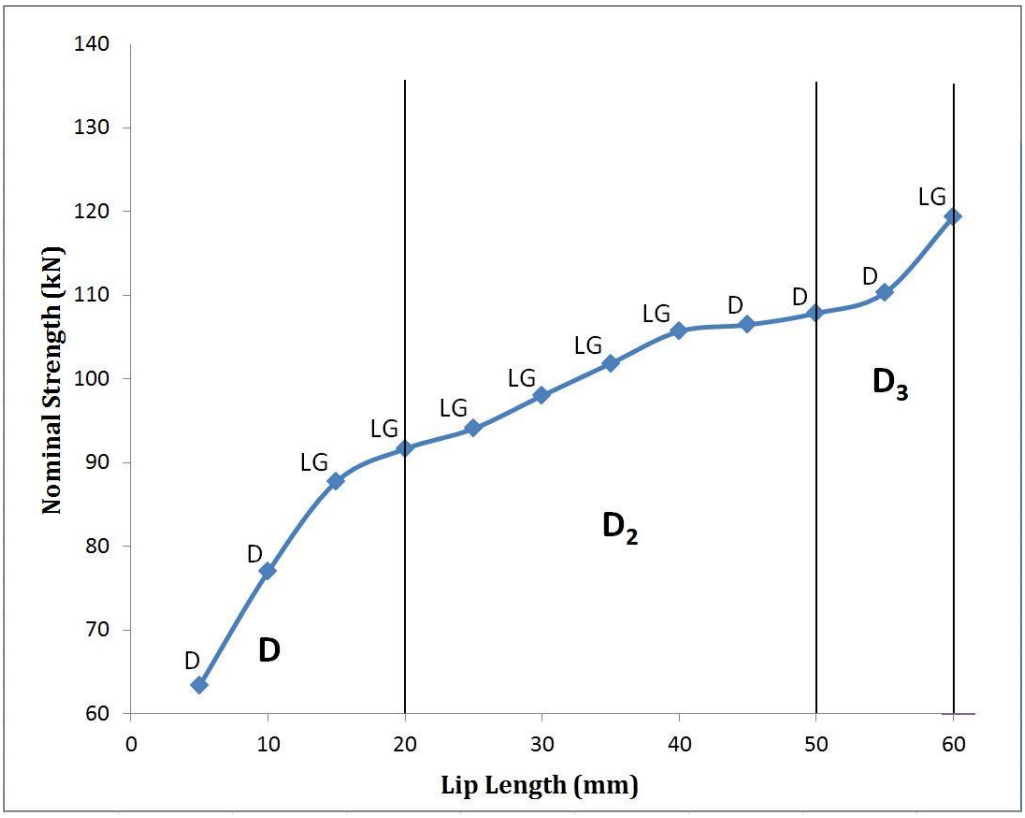

Figure 4.16 : Nominal strength – lip length relationship of the perforated specimens having 500 mm column length (lip continues outward).

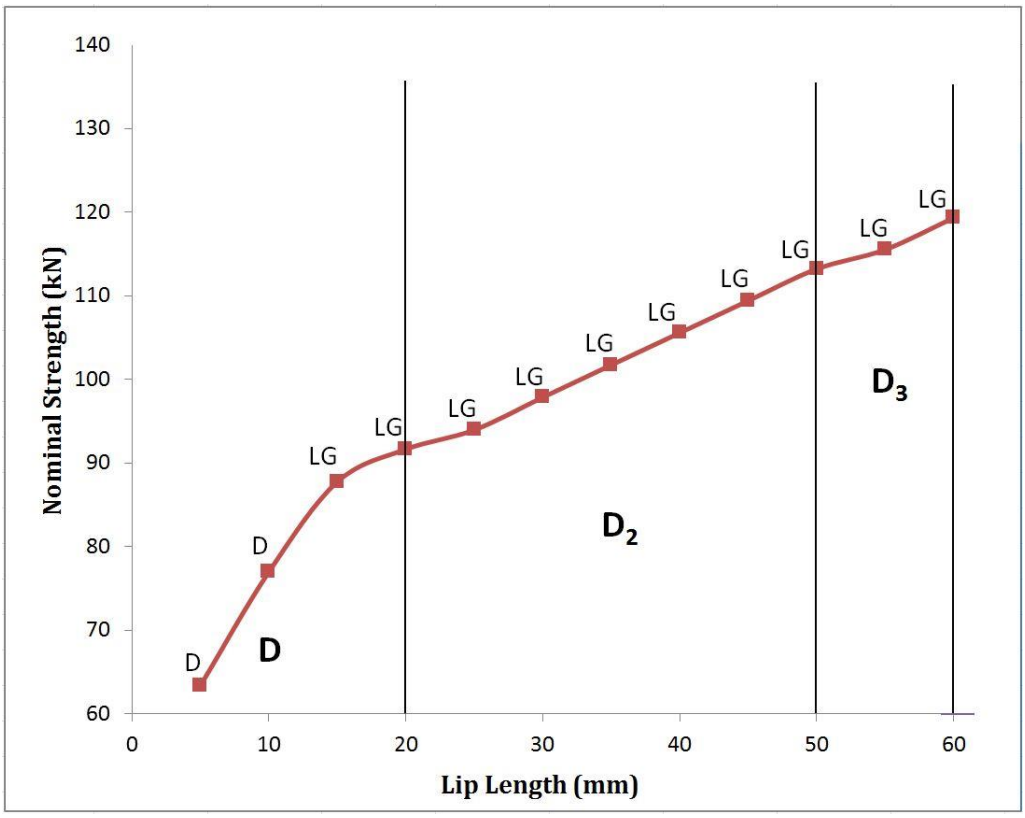

Figure 4.17 : Nominal strength – lip length relationship of the perforated specimens having 500 mm column length (lip continues inward).

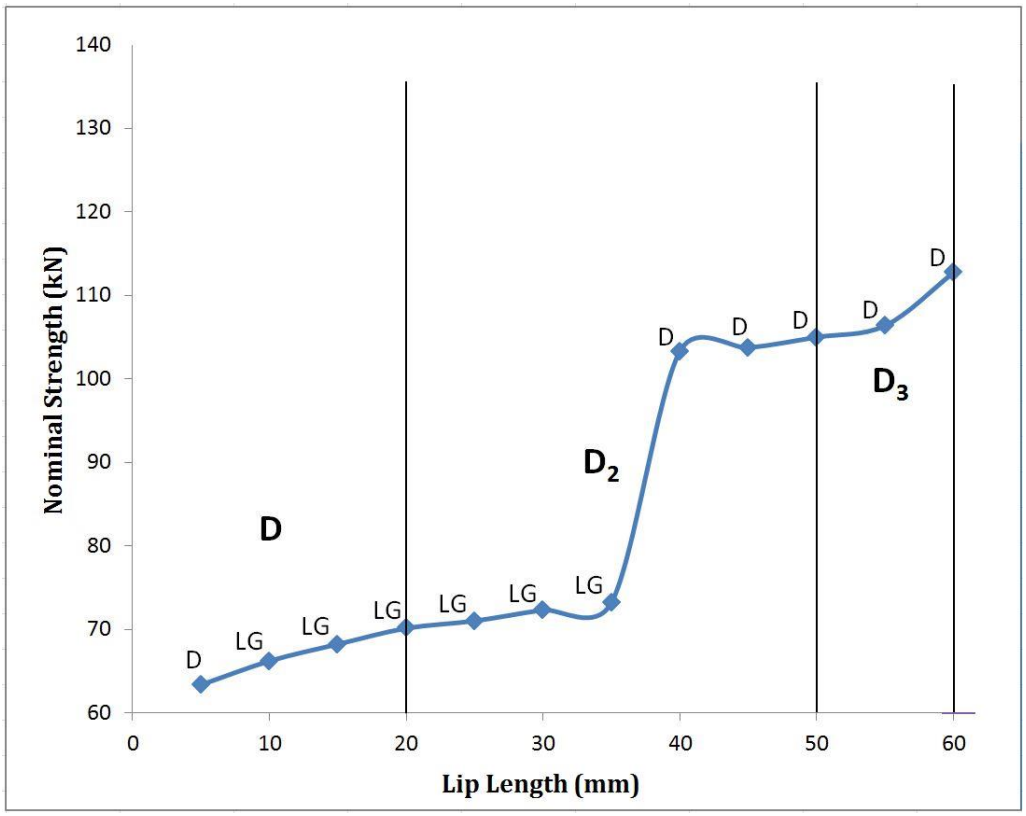

Figure 4.18 : Nominal strength – lip length relationship of the perforated specimens having 1000 mm column length (lip continues outward).

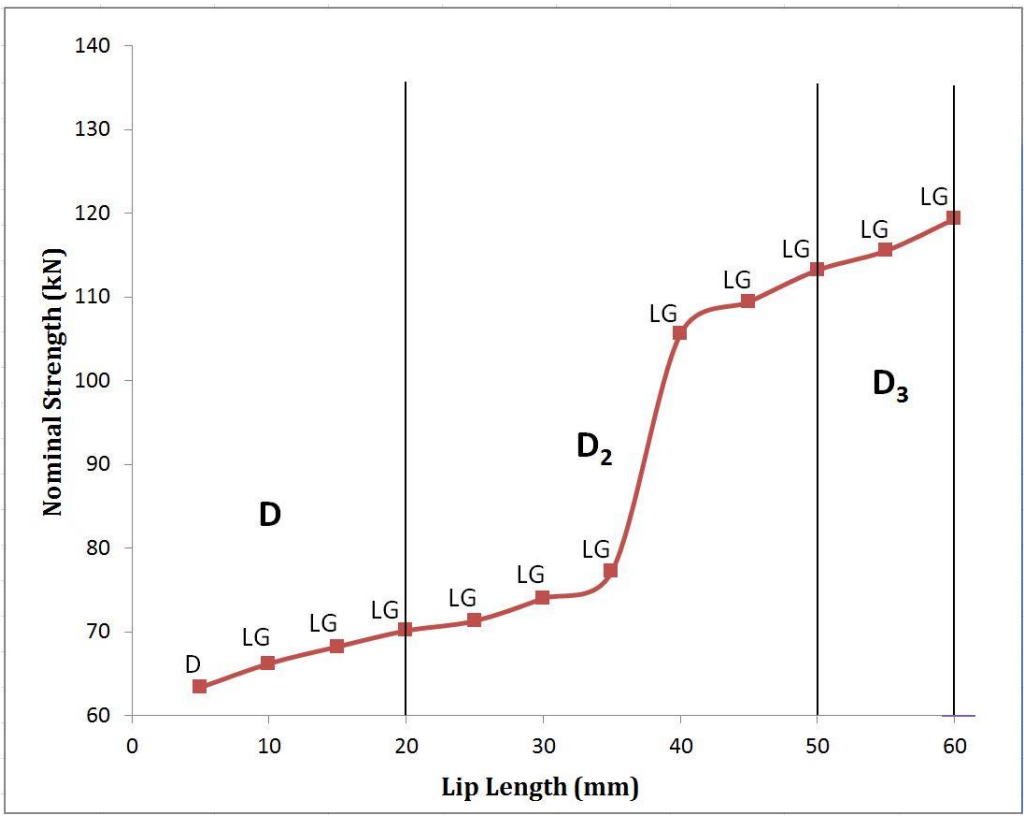

Figure 4.19 : Nominal strength – lip length relationship of the perforated specimens having 1000 mm column length (lip continues inward).

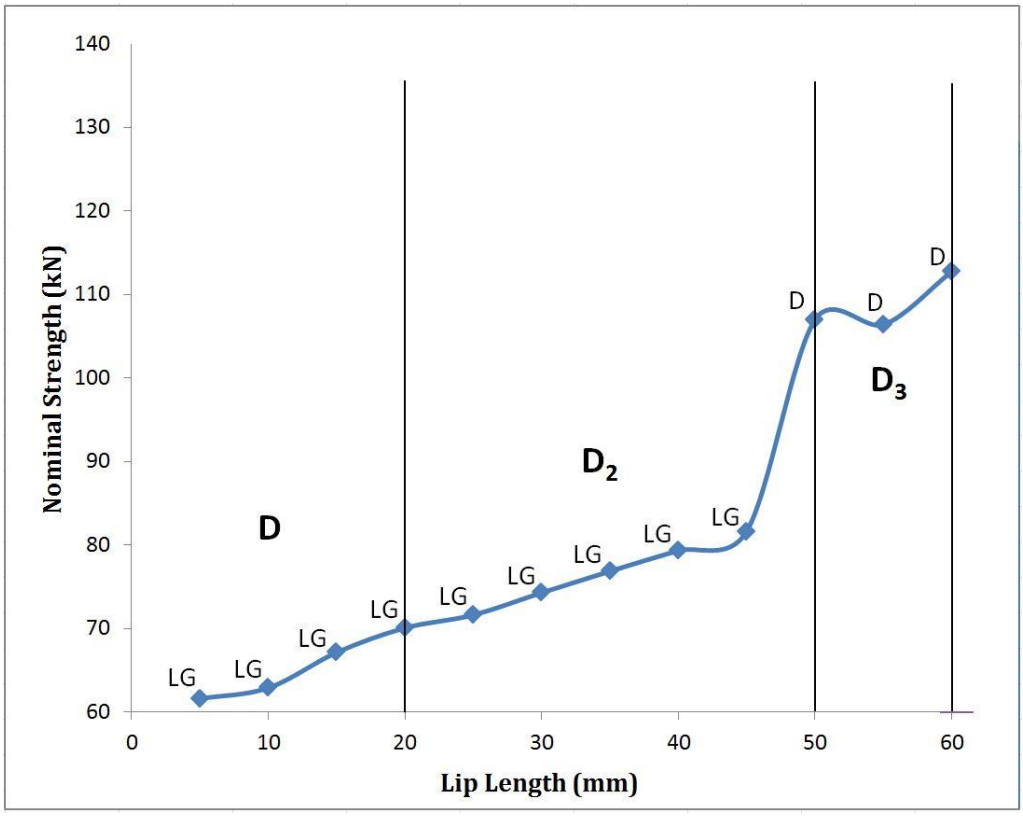

Figure 4.20 : Nominal strength – lip length relationship of the perforated specimens having 1500 mm column length (lip continues outward).

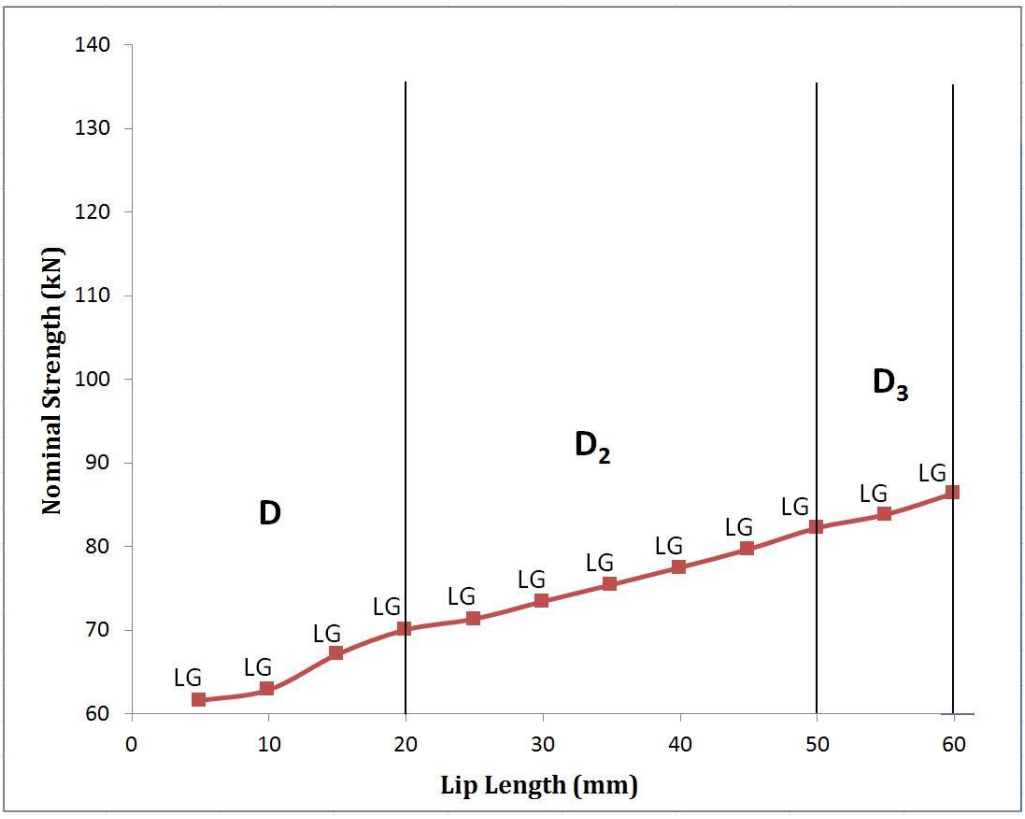

Figure 4.21 : Nominal strength – lip length relationship of the perforated specimens having 1500 mm column length (lip continues inward).

4.2.2.1 General comparison of results for perforated column models

Previous graphs are used to compare the nominal strengths of perforated specimens. Five different graphs have been constructed with two major feature. First feature is the lip direction. Figures 4.22 to 4.24 include the comparison between the sections having the same column length with different lip directions. Figures 4.26 and 4.27 include the comparison between the sections having same lip direction different column lengths.

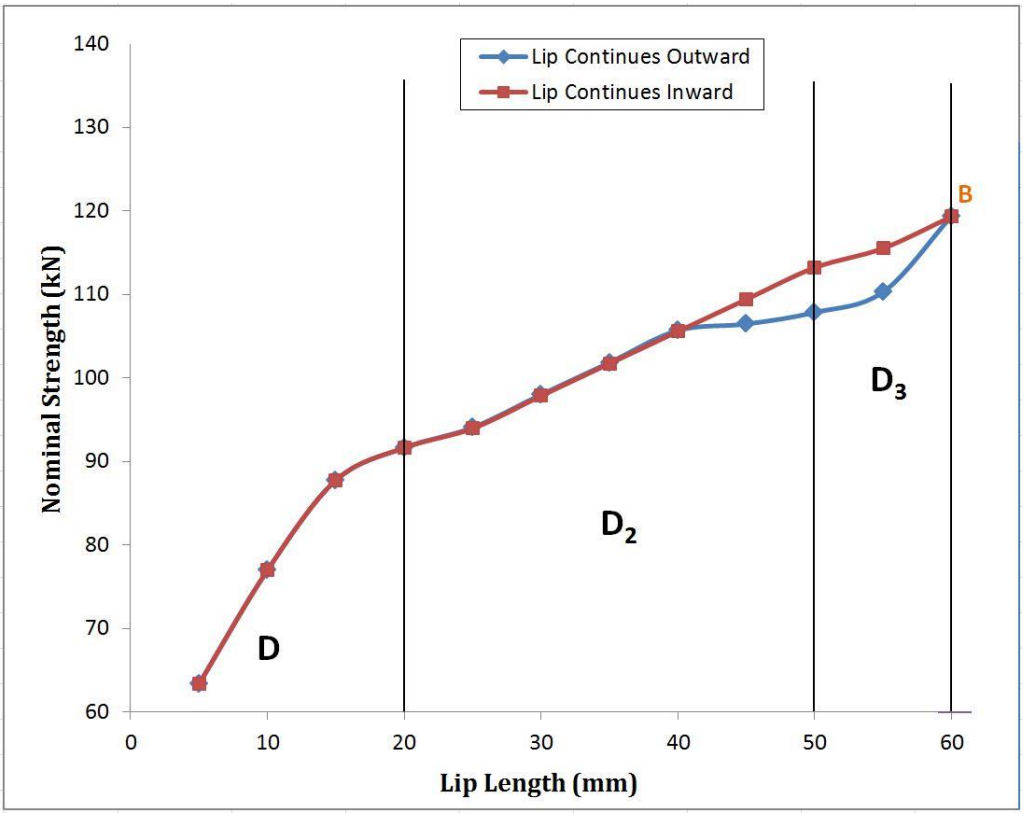

Figure 4.22 : Comparison of nominal strength – lip length relationship of the perforated specimens having 500 mm column length.

On specimens having 500 mm and 1000 mm column lengths; lip direction starts to effect the column strength after 40 mm lip length which means D_2 lip is 20 mm long, similar as unperforated specimens. Comparing the outward and inward lip cases, it is noted that there is a 4.7% strength difference the outward case being lower than the inward case. On specimens having 500 mm column length, it is observed that 2 specimens having maximum limit of lip length but having different lip directions have approximately the same column capacity. This is shown by point B on Figure 4.22.

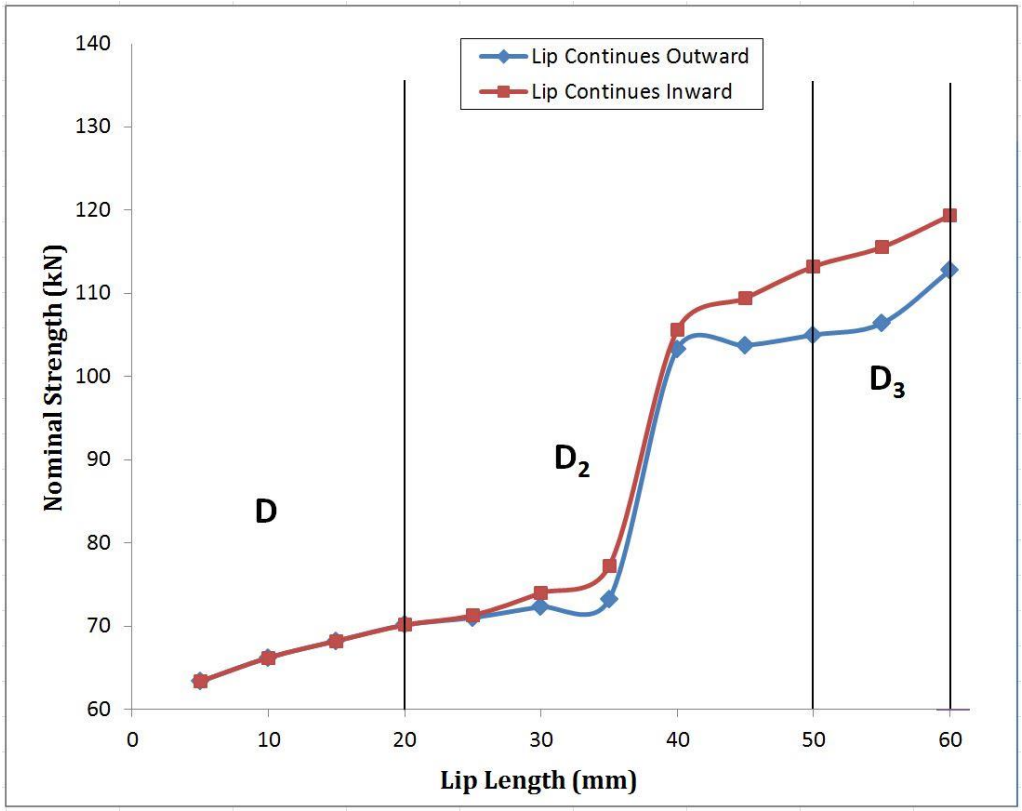

Figure 4.23 : Comparison of nominal strength – lip length relationship of the perforated specimens having 1000 mm column length.

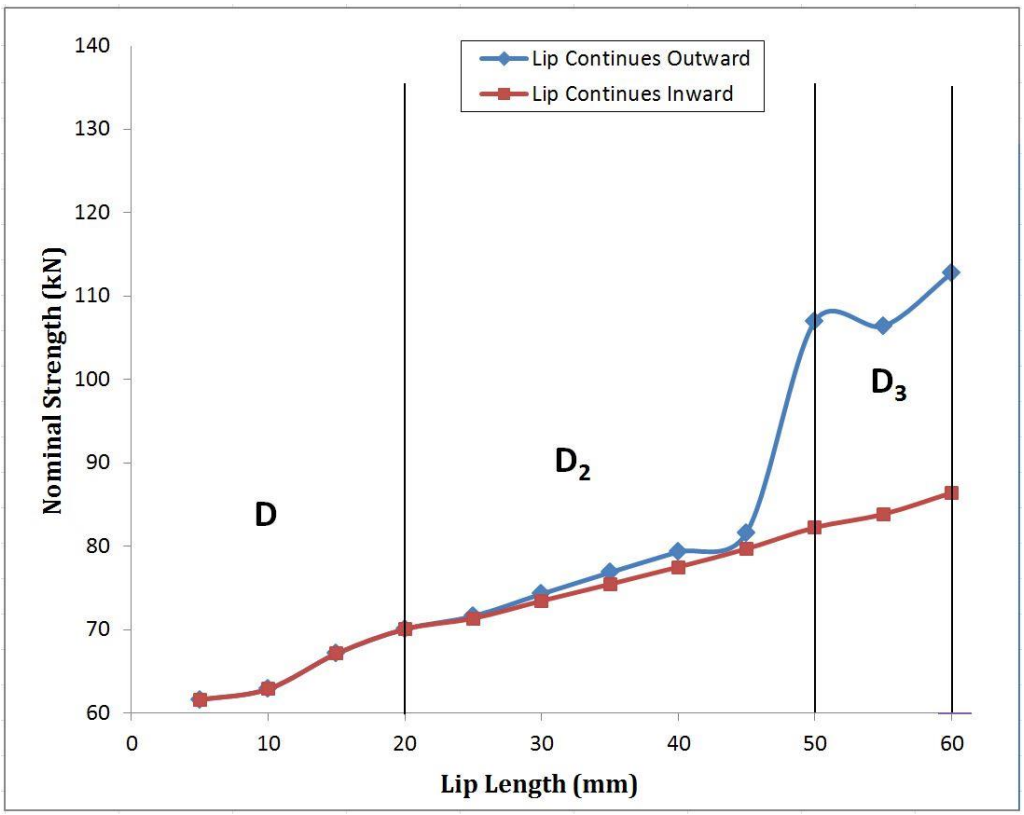

Figure 4.24 : Comparison of nominal strength – lip length relationship of the perforated specimens having 1500 mm column length.

However, on specimens having 1000 mm column length, strength loss starts on the 30 mm lip length (D_2 = 10 mm) and two specimens having maximum limit of lip length (60mm) don't have the same strength. Similar trend is observed for specimens having lips continuing outward and inward. If lip continues outwards, column strength will be less than in the situation that lip continues inwards. This strength difference increases after 40 mm of lip length (D_2 = 20 mm). Maximum strength difference is noted as 8.6%.

On specimens having 1500 mm column length, the specimens having lips continuing inwards has a linear relationship up to 45 mm of lip length (D_2 = 25mm). The column strength of specimens having lips continuing outwards are greater than the specimens having lips continuing inwards. This strength difference begins after 45 mm of lip length (D_2 = 25mm) and is up to 30.4% on sections having maximum lip length. It is interesting to note here that in this region, where there is high strength difference controlling buckling modes are also different. Inward cases are dominated by local-global buckling mode whereas the corresponding outward cases in this region are dominated by distortional buckling (As shown in Figure 4.25). This behaviour of buckling mode difference was not observed for unperforated cases although there was still a strength difference between outward and inward cases (8.8% more for outward).

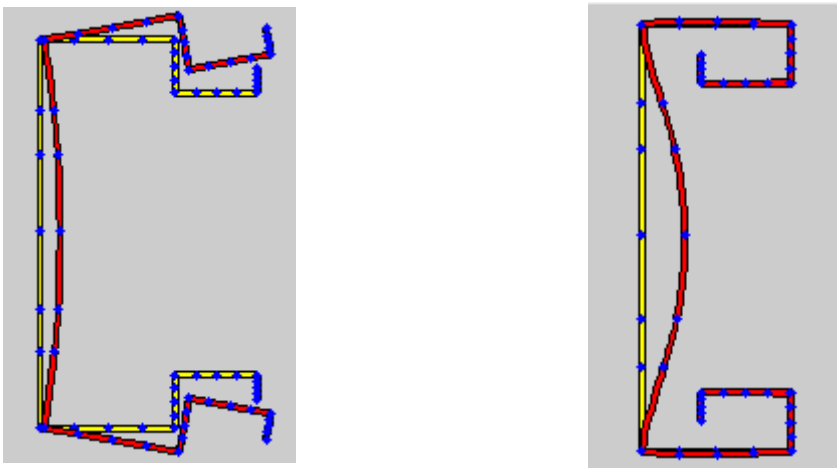

Figure 4.25 : Controlling buckling modes for inward and outward cases of perforated 1500 mm long columns with maximum lip length configuration.

As a result of these comparisons, lip direction effects the same specimens differently with respect to their column length. Especially, on sections having 1500 mm column length, the strength difference is significantly considerable on sections having more

complicated lips. The column lengths between 1000 mm and 1500 mm are distinctive for the effects of inward or outward direction of rack column specimens.

Figures 4.26 and 4.27 include the comparison of nominal strengths for the models having same lip direction, different column lengths.

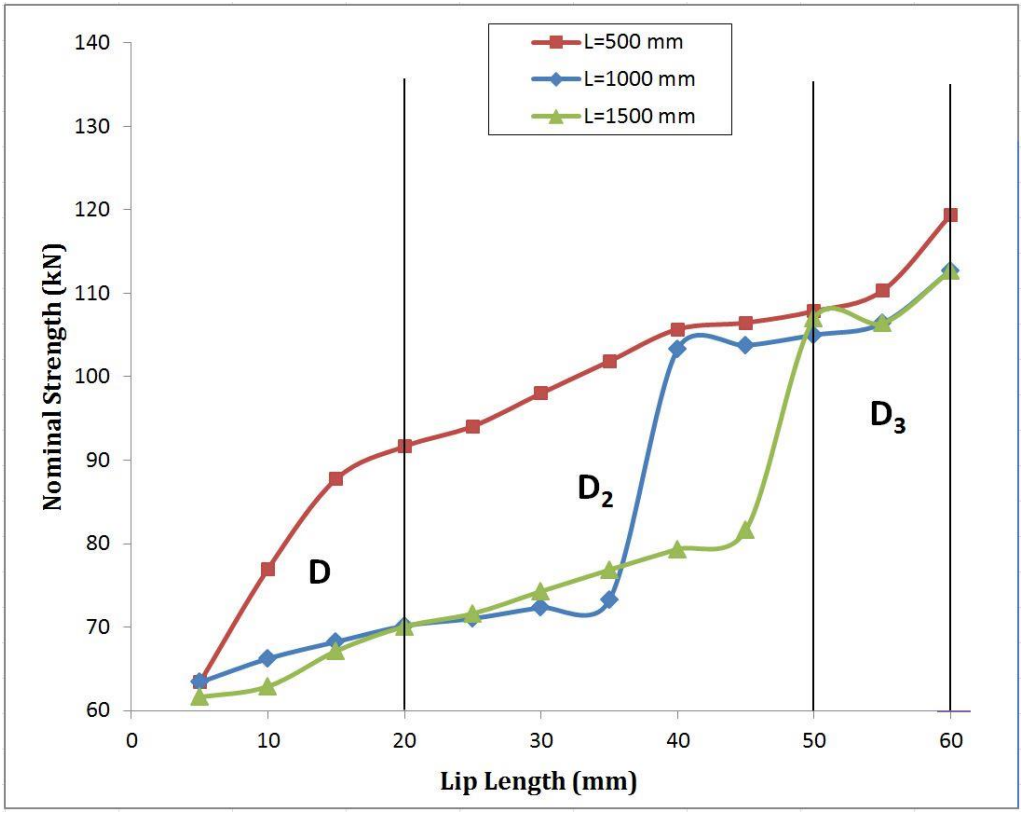

Figure 4.26 : Comparison between nominal strength – lip length relationships of the perforated specimens having lips continuing outwards.

On specimens having lips continuing outwards; in general, strength of 500 mm long specimens are greater than strength of 1000mm long specimens. The strength of 1000 mm long specimens are generally greater than strength of 1500mm long specimens except 25-35 mm (D2 = 5-15 mm) and 50-55mm (D3 = 0-5 mm) of lip length intervals. Specimens having 40 mm lip length (D2 lip = 20 mm) with 500 and 1000 mm column lengths have the same strength. On 1000 mm long specimens, between the lip length of 35-40 mm (D2 lip = 15-20 m) there's a significant increase in strength. This situation seems to be related with the change in the buckling mode of corresponding cross-sections in this region (from distortional to local-global and vice versa).

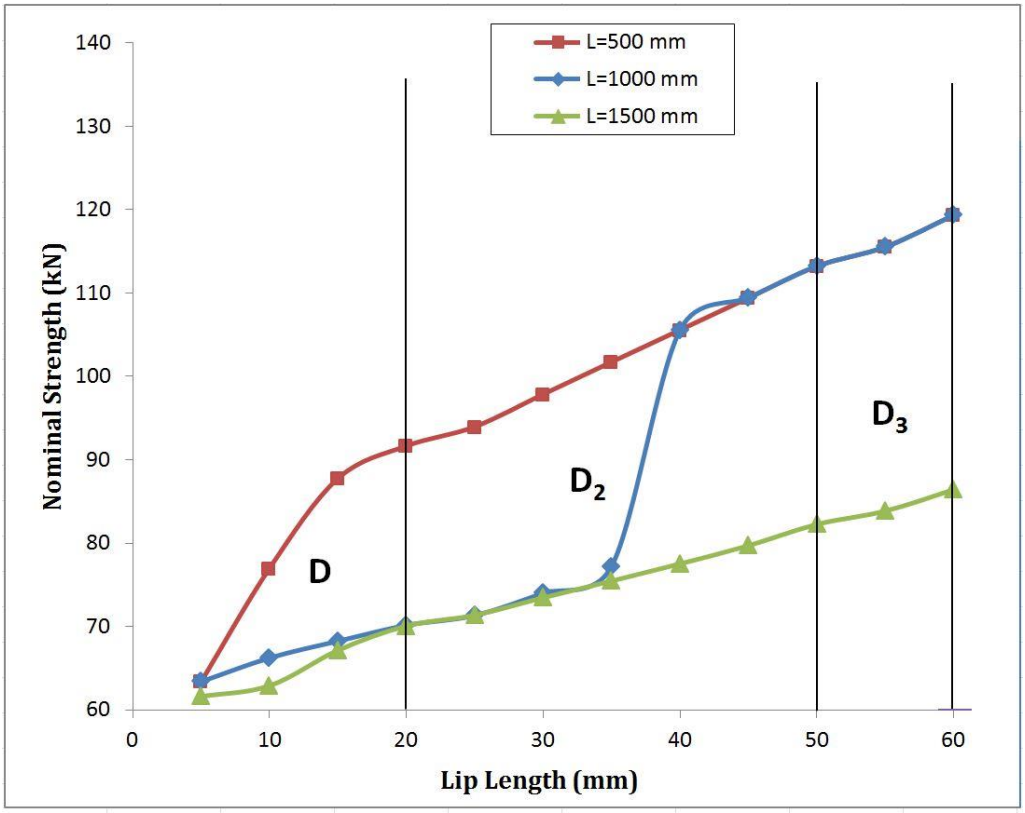

Figure 4.27 : Comparison between nominal strength – lip length relationships of the perforated specimens having lips continuing inwards.

On 500 and 1000 mm long specimens, between 40 – 50 mm of lip length (D_2 lip = 20-30 m) not a major strength gain is seen but after 50 mm of lip length (start of D_3 lip) , there is a sudden increase in strength which shows the importance of D_3 lip on column strength. On 1500 mm long specimens, there is also a sudden increase in strength between 45 – 50 mm of lip length (D_2 lip = 25-30 m). This situation seems to be also related with the change in the buckling mode of corresponding cross-sections in this region (from local-global to distortional).

On specimens having lips continuing inwards; 1500 mm long specimens have approximate linearity on its function between column strength and lip length. An interesting point is noted on 500 mm and 1000 mm long specimens, column strengths are the same on 44 mm of lip length (D_2 lip = 24 m). And the strength gain and the column strength are the same on increasing lip lengths. That means D_3 lip causes the same effect on both 500 mm and 1000 mm long specimens. On 1500 mm and 1000 mm long specimens, between 18-34 mm of lip length (begining of D_2 lip until 14 mm length) the strength values is approximately same. In this region; buckling modes for both cases are also same (local-global controlling modes). On

1000 mm long specimens, between the lip length of 34-42 mm (D_2 lip = 14-22 m) there's a significant increase in column strength which is also similar with specimens having lips continuing outwards. As noted earlier this situation seems to be related with the change in the buckling mode of corresponding cross-sections in this region (from distortional to local-global and vice versa).

4.3 Comparison Between the Strength of Unperforated Rack Column Models with Perforated Column Models

Comparison of relationships between nominal strength and lip length for unperforated and perforated members is given on 6 different graphs for 3 different lengths. X axis of these graphs indicate the lip length and Y axis indicate the nominal strengths of the specimens. 5 mm - 20 mm interval of the lip length indicates the D length. D_2 length covers the margin of 20 mm – 50 mm which is also indicating the specimen's lip configuration continuing inwards or outwards. D_3 length of specimen covers 50 mm – 60 mm interval. In figures 4.28 to 4.33 ; these graphs are given including comparisons for various column lengths and lip directions.

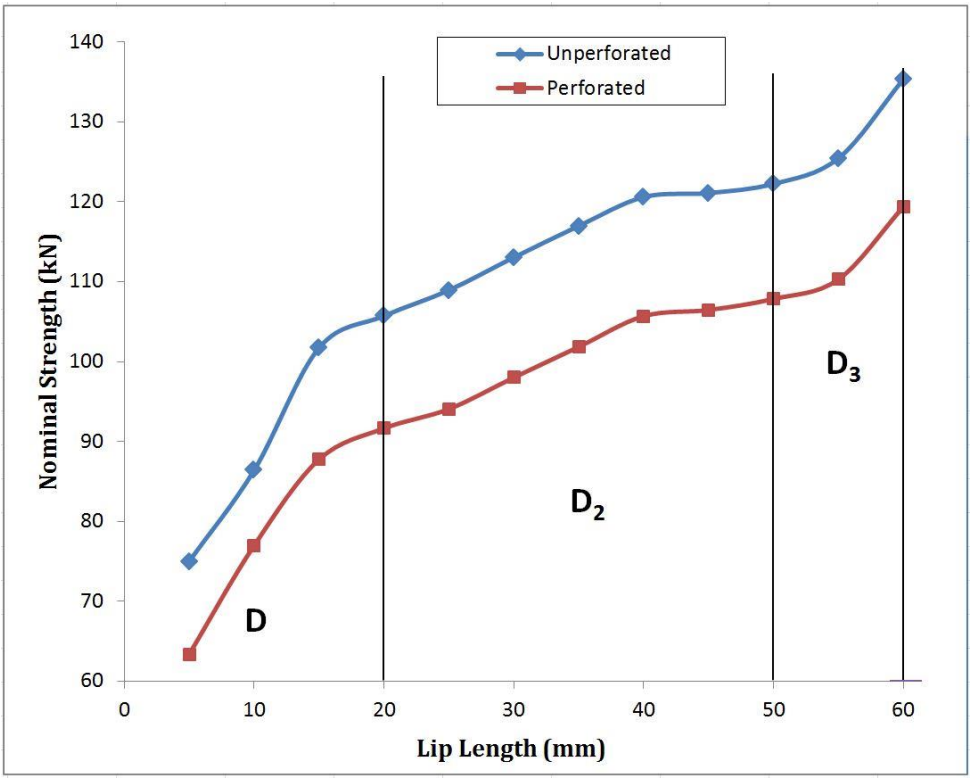

Figure 4.28 : Comparison between nominal strength – lip length relationships of the perforated and unperforated specimens having lips continuing outward and column length 500 mm.

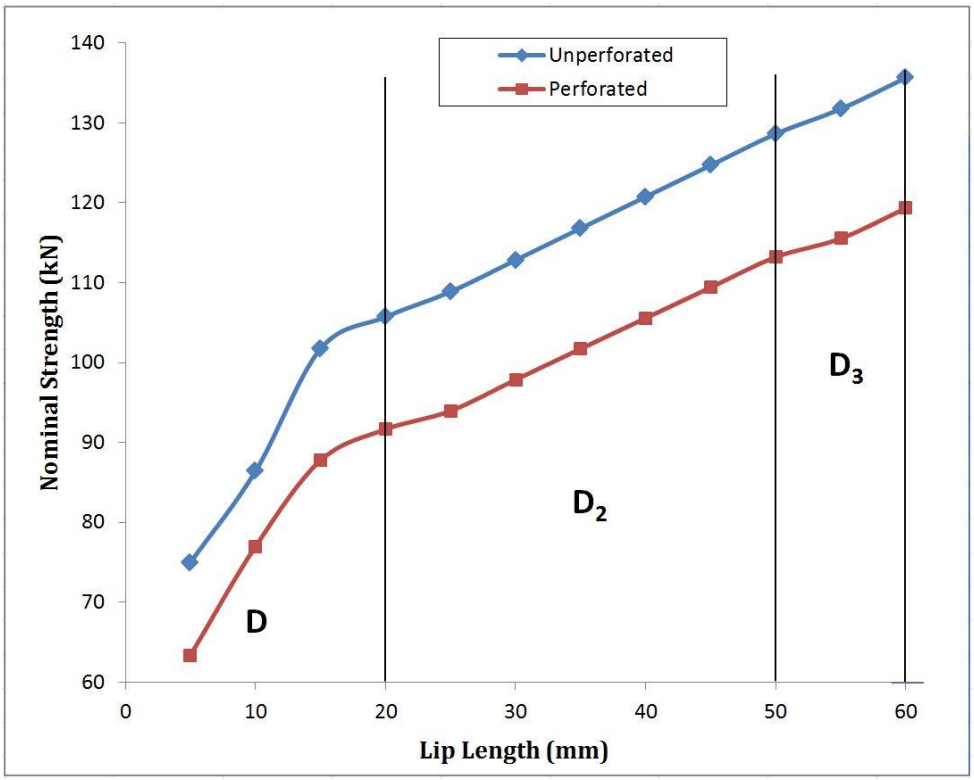

Figure 4.29 : Comparison between nominal strength – lip length relationships of the perforated and unperforated specimens having lips continuing inward and column length 500 mm.

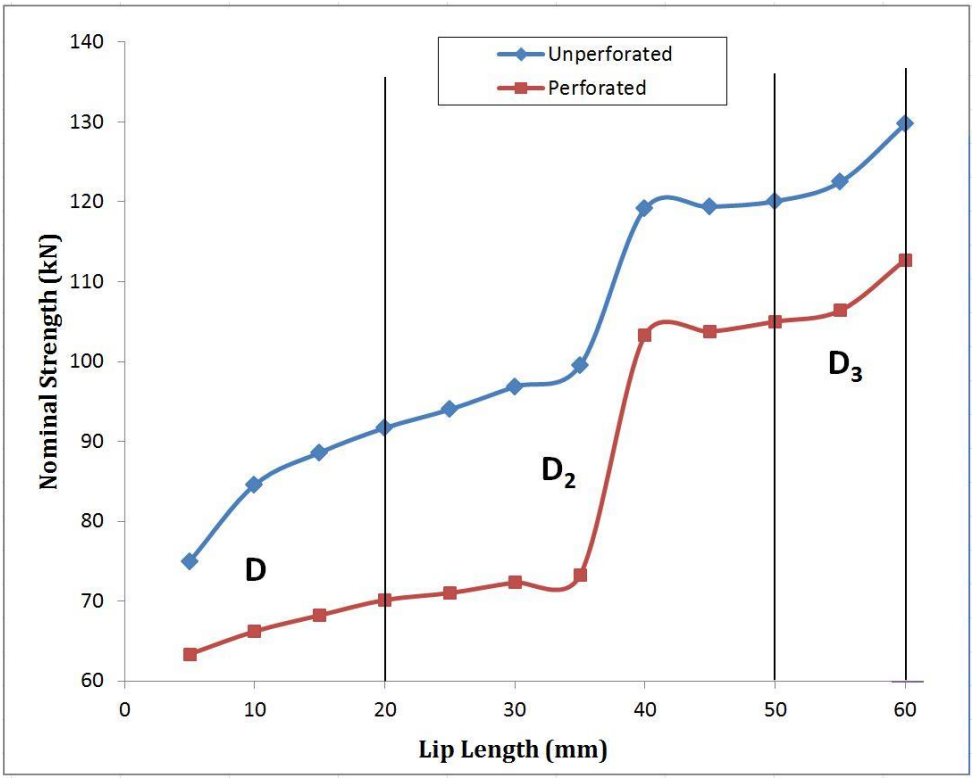

Figure 4.30 : Comparison between nominal strength – lip length relationships of the perforated and unperforated specimens having lips continuing outward and column length 1000 mm.

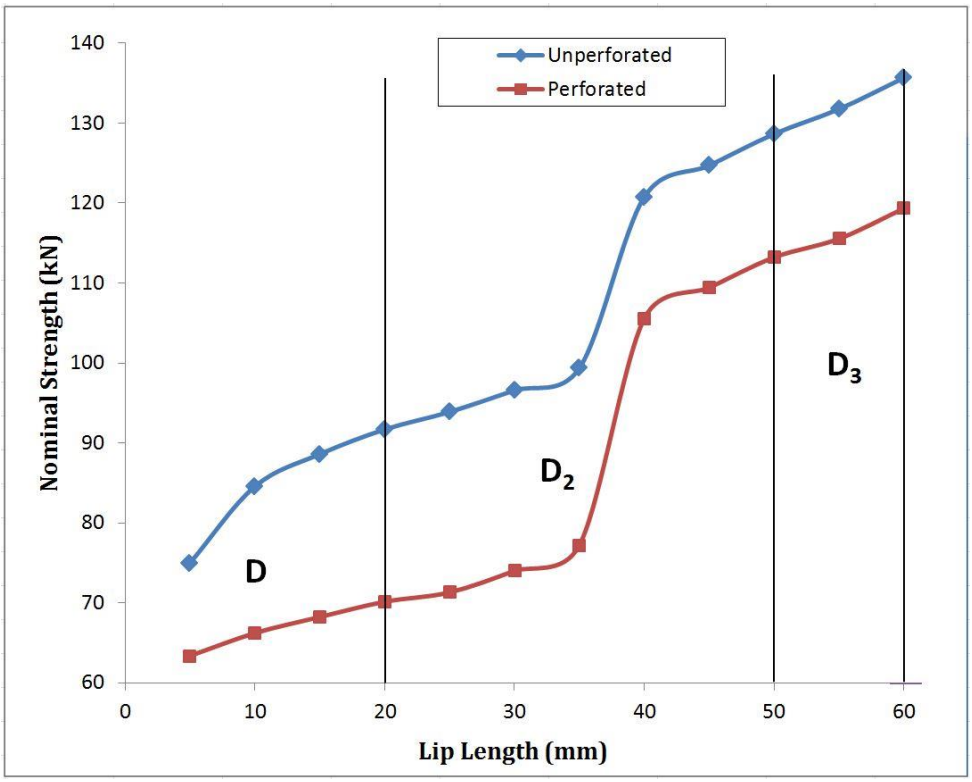

Figure 4.31 : Comparison between nominal strength – lip length relationships of the perforated and unperforated specimens having lips continuing inward and column length 1000 mm.

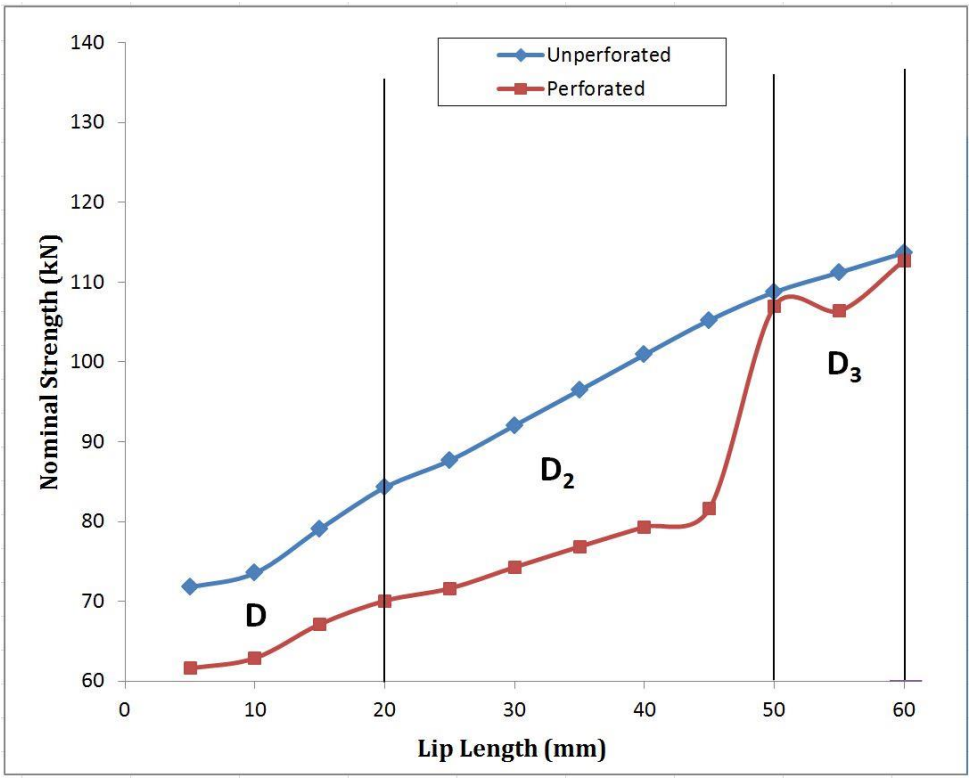

Figure 4.32 : Comparison between nominal strength – lip length relationships of the perforated and unperforated specimens having lips continuing outward and column length 1500 mm.

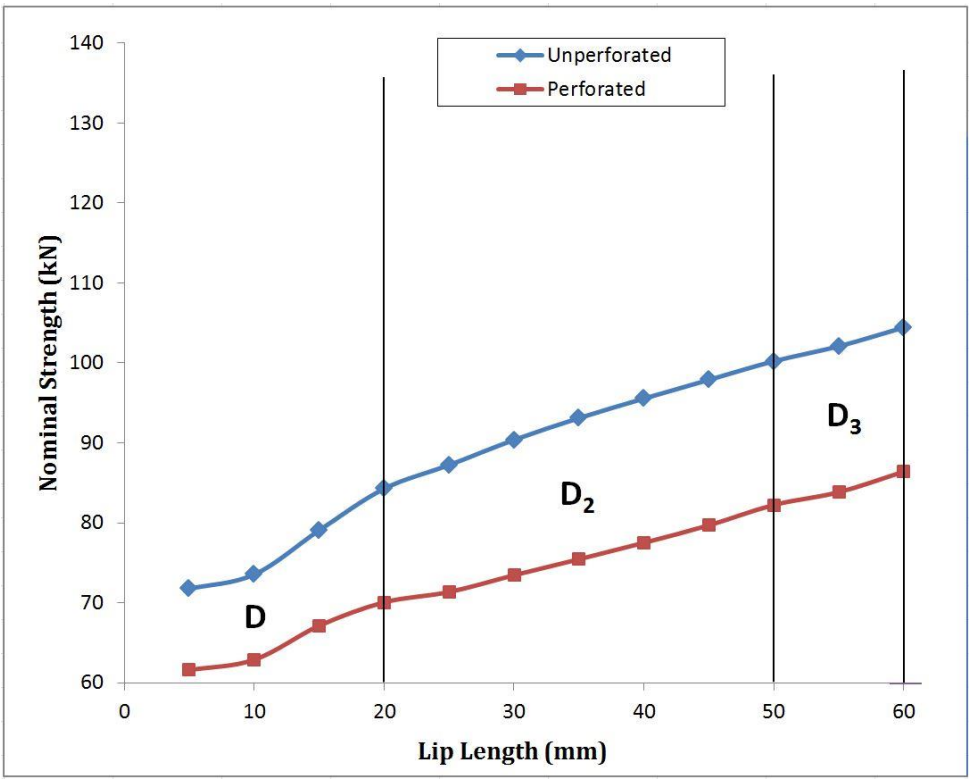

Figure 4.33 : Comparison between nominal strength – lip length relationships of the perforated and unperforated specimens having lips continuing inward and column length 1500 mm.

On specimens having lips continuing outward and column length 500 mm, perforated and unperforated curves follow a similar trend for increasing lip length. However, as expected perforated specimens' strength values are less than unperforated specimens. This strength difference is calculated as minimum 12.2% maximum 14.1% . On specimens having lips continuing inward and column length 500 mm, again similar trend is observed for the curves of perforated and unperforated specimens. Strength difference is calculated as minimum 12% maximum 14%.

On specimens having lips continuing outward and column length 1000 mm, perforated and unperforated curves have similarity in shapes but differ in severeal intervals of lip length. Between 35 and 40 mm of lip length (D_2 = 15-20 mm) there is a significant increase in strength on both perforated and unperforated specimens. The amount of increase on perforated specimens is calculated as 30 kN however the increase seen on unperforated specimens is calculated as 20 kN in related interval. This situation shows D_2 lip length affects perforated sections more than unperforated sections on corresponding column length and lip direction. Generally, perforated

specimens' strength values are less than unperforated specimens. This strength difference is calculated as minimum 14.2% maximum 36.9% . On specimens having lips continuing inward and column length 1000 mm, similar situation in same interval is also observed. The amount of increase on perforated specimens is calculated as 28 kN however the increase seen on unperforated specimens is calculated as 20 kN in related interval. In general, perforated specimens' strength values are less than unperforated specimens and this strength difference is calculated as minimum 14.3% maximum 29.8% . It has been noted that maximum strength difference calculated between perforated and unperforated sections on specimens having lips continuing outwards are 7.1% greater than specimens having lips continuing inward.

On specimens having lips continuing outward and column length 1500 mm, perforated and unperforated curves follow similar trend up to 40 mm of lip length (D_2=20 mm). After 40 mm of lip length, there is a significant increase on strength of perforated specimens and on 50 mm of lip length (end of D_2 lip) perforated specimens' strength is approximately same as unperforated specimens. On continuing lip lengths there is a drop on perforated specimens' strength and at the end of D_3 lip, the strength values of perforated and unperforated specimens are approximately same again. This situation might be related to the change in the controlling mode of related perforated specimens within those lip length intervals. Perforated specimens on related interval have distortional controlling buckling mode and unperforated specimens have local-global controlling buckling mode. Maximum strength difference calculated between perforated and unperforated specimens is 29.6% and minimum is 0%. On specimens having lips continuing inward and column length 1500 mm, similar situation is not observed. A parallel trend is noted for the curves of perforated and unperforated specimens. Generally, perforated specimens' strength values are less than unperforated specimens and maximum strength difference is calculated as 20.9% and minimum strength difference is calculated as 17.9%. It has been noted that maximum strength difference calculated between perforated and unperforated sections on specimens having lips continuing outwards are 8.7% greater than specimens having lips continuing inwards.

5. CONCLUSION

Steel Storage Rack Systems play a vital role in logistics and storing goods.This has particularly increased the importance of these systems over the last decade. In our country, importance of these systems is increasing through the demand of insufficient space to storage goods from various industries and fields. The structural strength and stability of steel storage rack structures have an increasing significance since the usage of these structures and value of the goods carried by these structures have increased.

Determining the structural capacity of steel storage rack columns has currently been regulated by several standarts and methods. American Iron and Steel Institute S100-2007 Standart is one of these few standarts to regulate the method of calculation to determine the strength of cold formed steel columns. The standart presents Effective Width Method and Direct Strength Method for calculations.

Direct Strength Method, presented in Appendix 1 part of AISI S100-2007 standart has newly been developed method for determination of the strength of concentrically axially loaded cold formed steel members. DSM calculations include finite strip method which is previously summarized in detail.

Steel Storage Rack Columns can be assumed to be a specific type of the general Cold formed steel columns. However, the behaviour of steel storage rack columns differs from the general behaviour of the CFS columns due to their thickness, lip configuration and the presence of perforations. Steel storage rack columns may consist of various lip types, lengths and perforations for the intended use. These two major variables affect the capacity of rack columns and hence the stability and strength of whole rack structure. In this study, the effects of lip configuration and perforations on the strength of steel storage rack columns is investigated using Direct Strength Method.

The main parts of the present study can be summarized as follows;

- Review of previous studies conducted on steel storage rack columns and direct strength method.
- Assessment of current practise (AISI S100-700 provisions) with respect to calculation of cold formed steel column capacity with Effective Width Method and Direct Strength method.
- The analytical study carried out on 120 column models having different column lengths, lip directions, lip lengths and perforated and unperforated cases.

In AISI S100-700 standart, currently the effect of perforations on column strength is accounted for by physical testing. No design rules are given to consider the effect of perforations on the three major buckling modes including local, distortional and global. In this study, a recently developed analytical approach which integrates the Direct Strength Method by a method called "Reduced Thickness Approach" was used. Comparisons were made between nominal strength values of columns with varying cross-section geometries (lip configuration) for both unperforated and perforated cases. Also three different column lengths were considered. The results were given in tables and graphs showing the effect of changing the above mentioned variables. In these tables and graphs, it was shown that changing the lip direction (inward or outward) effected the column strength. Significant differences were observed for specific ranges of lip lengths and column lengths. For example, sudden increases in strength were observed particularly for 1000 mm long columns with having both inward and outward lip configurations within a specific range of lip lengths. In this range, it was observed that buckling modes were also changing. As expected, the presence of perforations resulted in strength reductions of up to 36.9%. By using the reduced thickness approach, it was possible to calculate these differences in strength due to presence of perforations. The details of these findings were given within the thesis. It is recommended as a future study to support these findings by experimental testing.

REFERENCES

[1] **Yu, W. W., and LaBoube, R. A.** (2010). Cold Formed Steel Design. Fourth Ed., John Wiley & Sons, Inc., Missouri University of Science and Technology

[2] **Cold-formed steel**. (n.d.). In *Wikipedia.* Date retrieved: 20.03.2013, adress: http://en.wikipedia.org/wiki/Cold_formed_steel

[3] **Cold-formed steel sections**. (n.d.). In *Ruukki.* Date retrieved: 20.03.2013, adress: http://www.ruukki.com/~/media/Images/Steel-products/Cold-rolled-steels/cold-formed-steel-sections.ashx

[4] **Chen, H**. (n.d.). An Overview of Cold-Formed Steel Structures, *American Iron and Steel Institute*, AIA HSW, Washington DC.

[5] **Roll forming**. (n.d.). In *Cmrp.* Date retrieved: 20.03.2013, adress: http://www.cmrp.com/blog/wp-content/uploads/2014/02/Roll-Forming-with-a-Series-of-Progessive-Forming-Dies.jpg

[6] **CFS building**. (n.d.). In *Alphaturn.* Date retrieved: 20.03.2013, adress: www.alphaturn.grlight_construction.aspx

[7] **Three adjacent building blocks, Boulogne**. (n.d.). In *Nemetscheck-scia.* Date retrieved: 20.03.2013, adress: http://nemetschek-scia.com/sites/nemetschek-scia.com/files/references/profil-du-future_billancourt.jpg

[8] **CFS hangar**. (n.d.). In *Elast.* Date retrieved: 20.03.2013, adress: http://www.elast.com.au/images/thiess%207.jpg

[9] **CFS roof deck sheet**. (n.d.). In *D-macindustries.* Date retrieved: 20.03.2013, adress: http://www.d-macindustries.com/images/type%20b%20roof%20deck.jpg

[10] **CFS roof deck**. (n.d.). In *Structuremag.* Date retrieved: 20.03.2013, adress: http://www.structuremag.org/images/0108-is-1.jpg

[11] **CFS wall panel**. (n.d.). In *Chinasteelstructure.* Date retrieved: 20.03.2013, adress: http://www.chinasteelstructure.en.made-in-china.com/

[12] **Freitas, A. M. S., Freitas, M. S. R., Souza F. T.** (2005). Analysis of steel storage rack columns. *Journal of Constructional Steel Research, **61***, 1136-1137.

[13] **CFS storage rack structure**. (n.d.). In *Weiku.* Date retrieved: 20.03.2013, adress: http://www.weiku.com/

[14] **Pallet Racking**. (n.d.). In *Wikipedia.* Date retrieved: 20.03.2013, adress: http://en.wikipedia.org/wiki/File:Drive-In-Rack.jpg

[15] **Pallet Racking Hull**. (n.d.). In *Premier-storage.* Date retrieved: 20.03.2013, adress: http://www.premier-storage.co.uk/projects/wp-content/uploads/2011/08/pallet_racking_std_mainpic_large.jpg

[16] **AISI S100-2007** (2007). North American Specification for the Design of Cold-Formed Steel Structural Members, *American Iron and Steel Institute,* USA.

[17] **Winter, G.** (1970). Commentary on the 1968 Edition of the Specification for the Design of Cold-Formed Steel Structural Members, *American Iron and Steel Institute,* Washington, DC.

[18] **Chajes, A., and Winter, G.** (1965). Torsional-Flexural Buckling of Thin Walled Members. *Journal of the Structural Division, ASCE Proceedings, vol.* ***91***.

[19] **Chajes, A., Fang, P. J., and Winter, G.** (1966). Torsional-Flexural Buckling, Elastic and Inelastic, of Cold-Formed Thin-Walled Columns, *Engineering Research Bulletin, 66-1,* Cornell University, Ithaca, NY.

[20] **Peköz, T. B.** (1986). Development of a Unified Approach to the Design of Cold-Formed Steel Members. *AISI Report SG-86-4, American Iron and Steel Institute,* Washington, DC.

[21] **Shanley, F. R.** (1947). Inelastic Column Theory. *Journal of Aeronautical Science,* ***14***.

[22] **Galambos, T. V.** (1968). Structural Members and Frames. Prentice-Hall, Englewood Cliffs, NJ.

[23] **Goodier, J. N.** (1941). The Buckling of Compressed Bars by Torsion and Flexure. *Cornell University Experiment Station,* Ithaca, NY.

[24] **Timoshenko, S. P.** (1945). Theory of Bending, Torsion and Buckling of Thin-Walled Members of Open Cross Section. *Journal of the Franklin Institute,* **4,5**.

[25] **Bleich, F.** (1952). Buckling Strength of Metal Structures. McGraw-Hill, NY.

[26] **Flexural-torsional column buckling**. (n.d.). In *Emeraldinsight.* Date retrieved: 22.04.2013, adress: http://www.emeraldinsight.com/content_images/fig/1820250204024.png

[27] **Flexural-torsional column buckling of I beam**. (n.d.). In *Fhwa.* Date retrieved: 22.04.2013, adress: http://www.fhwa.dot.gov/bridge/lrfd/images/us_ds3_img22785.gif

[28] **Maljaars, J**. (2008). Local Buckling of Slender Alminium Sections Exposed to Fire, *PhD Thesis,* Eindhoven Technical University, Netherlands.

[29] **Gerard, G**., **and Becker. H.** (1957). Handbook of Structural Stability, Part –I Buckling of Flat Plates. *NACA Technical Note* ***3781***, Washington, DC.

[30] **Timoshenko, S. P., Gere, J. M.** (1961). Theory of Elastic Stability. McGraw-Hill, NY.

[31] **Rasmussen, K. J. R., Hancock, G. J.** (1992). Nonlinear Analyses of Thin-Walled Channel Section Columns. *Thin-Walled Structures,* ***13***, 1-2

[32] **Rasmussen, K. J. R.** (1994). Design of Thin-Walled Column with Unstiffened Flanges. *Engineering Structures*, ***13***, 5.

[33] **Nagahama, K., Camotim, D., Batista, E.** (2002). Local Buckling, Post-Buckling and Mode Interaction Finite Element Analyses in Cold-Formed Steel Members. *Proceedings of the sixth conference on Computational structures technology*, 235-236.

[34] **Hancock, G. J.** (1998). Design of Cold-Formed Steel Structures. Third Ed. Australian Institute of Steel Construction, Sydney.

[35] **Schafer, B. W.** (2012). In *John Hopkins University Civil Engineering.* Professor's personal web page Date retrieved: 05.05.2013, adress: http://www.ce.jhu.edu/bschafer/cufsm/

[36] **Young, B., Jintang Y.** (2004). Column Tests of Cold-Formed Steel Channels with Complex Stiffeners by Direct Strength Method. *Journal of Structural Engineering, **130***, 1756-1763.

[37] **Jintang Y., Young, B.** (2002). Column Tests of Cold-Formed Steel Channels with Complex Stiffeners. *Journal of Structural Engineering, **128**,* 737–745.

[38] **Hancock, G. J., Cook, D., Moisy, R. E., Yen A.** (2005). Direct Strength Design of Hot Rolled and Cold-Formed Steel Compression Members. *Advances in Steel Structures*, **I**, 13-20.

[39] **Papengelis, J. P. and Hancock, G. J.** (1995), Computer Analysis of Thin-Walled Structural Members. *Computers and Structures*, ***56(1)***, 157-176.

[40] **Schafer, B. W., Ádány, S.** (2006). Buckling analysis of cold-formed steel members using CUFSM: conventional and constrained finite strip methods. *18th International Specialty Conference on Cold-Formed Steel Structures*, Orlando.

[41] **Schafer, B. W.** (2008). Review: The Direct Strength Method of cold-formed steel member design. *Journal of Constructional Steel Research, **64**,* 766–778.

[42] **Lau, S. C. W., Hancock, G. J.** (1987). Distortional buckling formulas for channel columns. *Journal of Structural Engineering*, ***113(5)***.

[43] **Kwon, Y. B., Hancock, G. J.** (1992). Strength tests of cold-formed channel sections undergoing local and distortional buckling. *Journal of Structural Engineering, **117(2),*** 803-1786.

[44] **Hancock, G. J., Kwon, Y. B., Bernard, E.S.** (1994). Strength design curves for thin-walled sections undergoing distortional buckling. *Journal of Constructional Steel Research*, ***31***, 2-3.

[45] **Schafer, B. W.** (2000). Distortional buckling of cold-formed steel columns. *Final Report to the American Iron and Steel Institute*, Washington DC

[46] **Schafer, B. W.** (2002). Local, distortional, and Euler buckling in thin-walled columns. *Journal of Structural Engineering, **128(3)***, 289–99.

[47] **Yang, D., Hancock, G. J.** (2004). Compression tests of high strength steel channel columns with interaction between local and distortional buckling. *Journal of Structural Engineering*, ***130(12),*** 1954–63.

[48] **Silvestre, N., Camotim, D.** (2006). Direct Strength Method for lipped channel columns and beams affected by local-plate/distortional interaction. *Proceedings of the eighteenth international specialty conference on cold formed steel structures*, 17–37.

[49] **Kumar, M. V. A., Kalyanaraman, V.** (2010). Evaluation of Direct Strength Method for CFS Compression Members without Stiffeners. *Journal of Structural Engineering*, ***136(7)*** , 879–885.

[50] **Mulligan, G. P., and Peköz, T. B.** (1984). Local buckling interaction in cold formed columns. *Journal of Structural Engineering, **110(11)**,* 2635-2654.

[51] **Talja, A.** (1990). Design of the buckling resistance of compressed HSS channels. *Research Note No*. **1163**, Technical Research Centre of Finland.

[52] **Young, B.** (1998). The behaviour and design of the cold formed channel columns, *Ph.D. thesis*, Univ. of Sydney, Australia.

[53] **Key, P. W., Hasan, S. W., Hancock, G. J.** (1988). Column behaviour of cold formed hollow sections. *Journal of Structural Engineering, **1142***, 309-407.

[54] **Wilkinson, T., and Hancock, G. J.** (1997). Test for the compact web slenderness of cold formed rectangular hollow section. *Res. Rep. No.R744,* Dept. of Civil Engineering, Univ. of Sydney.

[55] **Niemi, E., and Rinnevalli, J.** (1990). Buckling tests on cold formed square hollow sections of steel Fe510. *J. Constr. Steel Res., **16(3)***, 221-230.

[56] **Kalyanaraman, V., Pekoz, T. B., and Winter, G.** (1979). Unstiffened compression elements. *ASCE Annual Convention and Exposition*. 1-38.

[57] **Landesmann, A. and Camotim, D.** (2013). On the Direct Strength Method (DSM) design of cold-formed steel columns against distortional failure. *Thin-walled Structures, **67***, 1.

[58] **Roure, F., Pastor, M. M., Casafont, M., Somalo, M. R.** (2010). Stub column tests for racking design: Experimental testing, FE analysis and EC3. *Thin-walled Structures, **49***, 167-184.

[59] **European Standard EN1993-1-3** (2009). Eurocode 3 - Design of Steel Structures, *European Committee for Standardization,* Brussels.

[60] **Casafont, M., Pastor, M. M., M., Roure, F., Peköz, T. B.** (2011). An experimental investigation of distortional buckling of steel storage rack columns. *Thin-walled Structures, **49***, 933-946.

[61] **Casafont, M., Pastor, M. M. M., Roure, F., Bonada, J., Peköz, T. B.** (2013). Design of Steel Storage Rack Columns via the Direct Strength Method. *Journal of Structural Engineering*, ***139***, 669-679.

[62] **Casafont, M., Pastor, M. M., M., Bonada, J., Roure, F., Peköz, T. B.** (2012). Linear buckling of perforated steel storage rack columns with the finite strip method. *Thin-walled Structures*, ***61***, 71-85.

[63] **Moen, C. D., Schafer, B. W.** (2009). Direct Strength Design of Cold-Formed Steel Members With Perforations. *Research Report, AISI Committee on Specifications for the Design of Cold-Formed Steel Structural Members*, Washington, DC.

CURRICULUM VITAE

Name Surname:

Atakan MANGIR

Place and Date of Birth:

Istanbul – 09.04.1989

Address:

Seyitnizam mah. Akevler Sitesi, C-1 Blok, Kat:7, D:25, Zeytinburnu / İST.

E-Mail:

atakanmangir@gmail.com

B.Sc.:

Civil Engineering - İstanbul Kültür University (100% Sch.)

M.Sc.:

Structural Engineering - Istanbul Technical University (2011-2014)

Professional Experience and Rewards:

(2011) Istanbul Kültür University
1st Degree Reward in Hall of Fame between graduates of Civil Engineering Dept.

(2011-2012) DEMARS Construction
Maintenance and restoration of structures and facilities owned by Istanbul Metropolitan Municipality
Project Engineer

(2012 -) Fatih University
Civil Engineering Dept. – Research Assistant.

(2013-2014) Istanbul Development Agency
Establishment of Industrial Storage Rack Systems (ISRS) Design and Test Centre, Project Assistant - *Fatih University.*